

Two-Product Make-to-Stock System: Strategic Joining and Optimal Inventory Levels

Odysseas Kanavetas*

Ekaterina Kosarevskaia†

Abstract

This paper analyzes a two-product make-to-stock queueing system where a single production facility serves two customer classes with independent Poisson arrivals. Customers make strategic join-or-balk decisions without observing current inventory levels. The analysis establishes the existence and uniqueness of Nash equilibria in customer joining strategies for various inventory scenarios. Optimal base-stock levels are characterized from both profit-maximizing and welfare-maximizing perspectives, with closed-form expressions for key performance measures.

Keywords: Make-to-stock, Multi-class queues, Strategic customers, Capacity allocation, Queueing-game equilibrium, Optimal inventory

1 Introduction

Make-to-stock systems aim to hold inventory in anticipation of uncertain demand, yet the moment customers arrive, their individual choices can reshape the entire operation. In multi-product settings, where a shared production facility must manufacture different product types, these dynamics become particularly complex. Producers must determine appropriate target inventory levels for each distinct product while balancing holding costs against stockout risks. When customers strategically decide whether to purchase specific products, their collective behavior significantly impacts overall system performance. This resource-sharing challenge appears across industries — from manufacturing facilities producing both premium and economy variants to cloud computing systems allocating capacity between interactive and batch processing services.

– *Classical inventory models.* Inventory management research dates to Harris [16] economic order quantity model. Subsequent work incorporated stochastic demand and dynamic decisions: Arrow et al. [3] on optimal inventory policies, Scarf [27] on (S, s) policies, and Karlin [21] on dynamic inventory control. Multi-product and nonstationary extensions followed [30], with comprehensive treatments in Zipkin [35], Silver et al. [28], and Graves et al. [14]. Multi-item models with shared capacity include Federgruen and Katalan [13].

– *Inventory models with queues and make-to-stock systems.* Queueing formulations of make-to-stock systems model the inventory shortfall as a single-server queue. Buzacott and Shanthikumar [7] develop this representation systematically; the non-strategic version of our two-product system corresponds to one of the standard make-to-stock queues in their framework. Veatch and Wein [29]

*Mathematical Institute, Leiden University, Einsteinweg 55, Leiden 2333CC, Netherlands. Email: o.kanavetas@math.leidenuniv.nl

†Mathematical Institute, Leiden University, Einsteinweg 55, Leiden 2333CC, Netherlands. Email: e.kosarevskaia@math.leidenuniv.nl

use the same representation to derive optimal dynamic control in a tandem production–inventory system. Closer to our setting, Ha [15] and de Véricourt et al. [11] study single-item make-to-stock systems with multiple demand classes sharing a production resource, showing that optimal policies take the form of inventory-rationing or stock-allocation rules. Benjaafar and ElHafsi [5], Abouee-Mehrizi et al. [2], and Zhao and Lian [34] likewise analyze multiclass or multistage queueing–inventory systems under target inventory and rationing policies.

– *Strategic queues without inventory.* In parallel, another stream models customers as strategic agents deciding whether to join a queue. Naor [25] analyzes joining behavior in an M/M/1 queue and shows how tolls align individual and social objectives. Edelson and Hilderbrand [12] study congestion pricing for Poisson queues. Extensions include Hassin [17], Mendelson [24] on computer service pricing, Burnetas and Economou [6], and the monographs of Hassin and Haviv [19] and Hassin [18]. Hassin and Roet-Green [20] consider an unobservable queue where customers may pay to inspect queue length before joining, characterizing equilibrium inspection and joining behavior.

– *Make-to-stock queues with demand responsiveness.* Within the make-to-stock framework, several papers incorporate demand responsiveness to prices or congestion at an aggregate level. Caldentey and Wein [10] analyze a single-product system with two selling channels, using dynamic pricing and admission control. Ata and Shneorson [4] study dynamic control and quantify the value of demand information. Cachon and Swinney [8] consider strategic consumers who may delay purchases in anticipation of markdowns.

Most closely related to our work is the literature on single-product make-to-stock queues with strategic joining decisions. Öz and Karaesmen [26] study a single-product queue with unobservable inventory, where customers choose equilibrium joining probabilities based on stationary performance measures; their comparison of decentralized and centralized objectives makes this the closest single-product analogue to our work. Closely related extensions retain strategic joining but differ mainly in the producer’s control lever: Li et al. [22] consider an unobservable finite-capacity system with setup times, characterizing optimal two-threshold production policies. Zhang and Wang [33] analyze dynamic-service make-to-stock systems, identifying optimal inventory thresholds in a Stackelberg game. Other variants modify the customer-flow dynamics or add additional instruments: Wang and Cai [31] extend the framework to retrial customers. Cai et al. [9] study pricing and information disclosure under different observability structures. Finally, Zare et al. [32] incorporate strategic customers in a two-echelon supply chain, focusing on vertical manufacturer–distributor interactions rather than horizontal product competition.

Building on the above make-to-stock queueing-inventory and strategic-joining literature, we study a two-product setting where both product classes share a single production server under target inventory (base-stock) policies, and customers make joining decisions without observing inventory or backlog levels. The analysis explores how target inventory levels and price/waiting trade-offs influence customer joining strategies and system performance. Different inventory targets for each product affect equilibrium joining probabilities, which in turn determine stockouts and waiting times. We examine both a profit-maximizing producer’s perspective and a social planner’s view of overall welfare, highlighting the externalities that arise when products share production capacity but face distinct customer segments. These findings also apply to settings beyond conventional manufacturing and retail. Shared resources in healthcare (e.g., diagnostic equipment), cloud computing (e.g., server allocation), or transportation (e.g., electric vehicle charging) all involve users who make decisions under imperfect information. Modern computing environments must balance capacity across multiple service tiers while accommodating strategic users; see Abhishek et al. [1], Lin et al. [23]. Accounting for strategic behavior is thus critical for coordinating resource

allocation and managing costs.

The remainder of the paper is organized as follows. Section 2 introduces our two-product make-to-stock system, defining the key parameters and interactions. Section 3 establishes the analytical foundation by deriving closed-form expressions for critical performance measures — expected waiting times, inventory levels, and backlogs. Sections 4 and 5 analyze the system from a decentralized perspective, where decisions are made independently by participants. Section 4 explores how customers strategically decide whether to join the system, characterizing the structure of Nash equilibria under different inventory configurations. Section 5 shifts to the producer’s viewpoint in a Stackelberg game framework, where the producer acts as a leader by setting optimal inventory targets while anticipating customer responses. In contrast, Section 6 examines a centralized approach where a social planner coordinates both inventory and customer participation decisions simultaneously to maximize overall welfare rather than individual objectives. Section 7 presents our numerical findings on how asymmetry in customer waiting costs affects system performance when products compete for limited production capacity.

2 Model Description

2.1 Single-Product Make-to-Stock System

We begin with the single-product make-to-stock system, following Buzacott and Shanthikumar [7] and Öz and Karaesmen [26], which serves as the foundation for our two-product extension.

A single production facility maintains a target inventory level (base-stock level) $S \in \mathbb{Z}_+$. Customers arrive as a Poisson process with rate Λ and, without observing the current inventory or queue length, decide whether to join or balk. A joining customer pays p and either receives a unit immediately or, if inventory is zero, waits in the backlog. In either case, their arrival triggers exactly one production job added to the queue.

The facility processes jobs first-come-first-served (FCFS) with exponential service times at rate μ . Crucially, the job created by an arrival is not tied to that customer’s unit. For example, let $S = 2$ and suppose inventory is zero, no customer is backlogged, and two jobs are in the queue (both currently destined to rebuild inventory). A customer who joins is backlogged; the next completion serves this customer, while the job their arrival created later rebuilds inventory (provided no additional customers arrive before it completes).

2.2 Two-Product Extension

We now extend to two products sharing a single production line, with target inventory levels S_1 and S_2 . Customers requesting product i arrive as independent Poisson processes with rate Λ_i , and do not observe current inventories or queue lengths when deciding whether to join.

The production mechanics extend directly: a joining type- i customer pays p_i and triggers one type- i job appended to a single FCFS queue shared by both products. The customer receives the product immediately if in stock, or waits in the backlog otherwise. The production line processes all jobs at rate μ ; a completed type- i job serves the oldest waiting type- i customer if one exists, otherwise replenishes on-hand inventory. Holding cost is h_i per unit of on-hand inventory per unit time.

While FCFS is natural in the single-product model (all jobs identical), it need not be optimal with two products sharing capacity: production capacity may be spent on type-1 replenishment even while type-2 customers are waiting. Studying alternative service disciplines is an interesting

direction for future research; we keep FCFS as a tractable baseline that still captures competition for shared capacity.

Figure 1 illustrates this system. Key parameters include prices p_i , rewards $R_i > p_i$, waiting costs c_i per unit time, and holding costs h_i . While Λ_i denotes the arrival rate, λ_i denotes the effective arrival rate of customers who actually join. In the decentralized setting, $\lambda_i = \Lambda_i q_i$, where q_i is the joining probability; under the social planner, λ_i is directly chosen as the optimal participation rate.

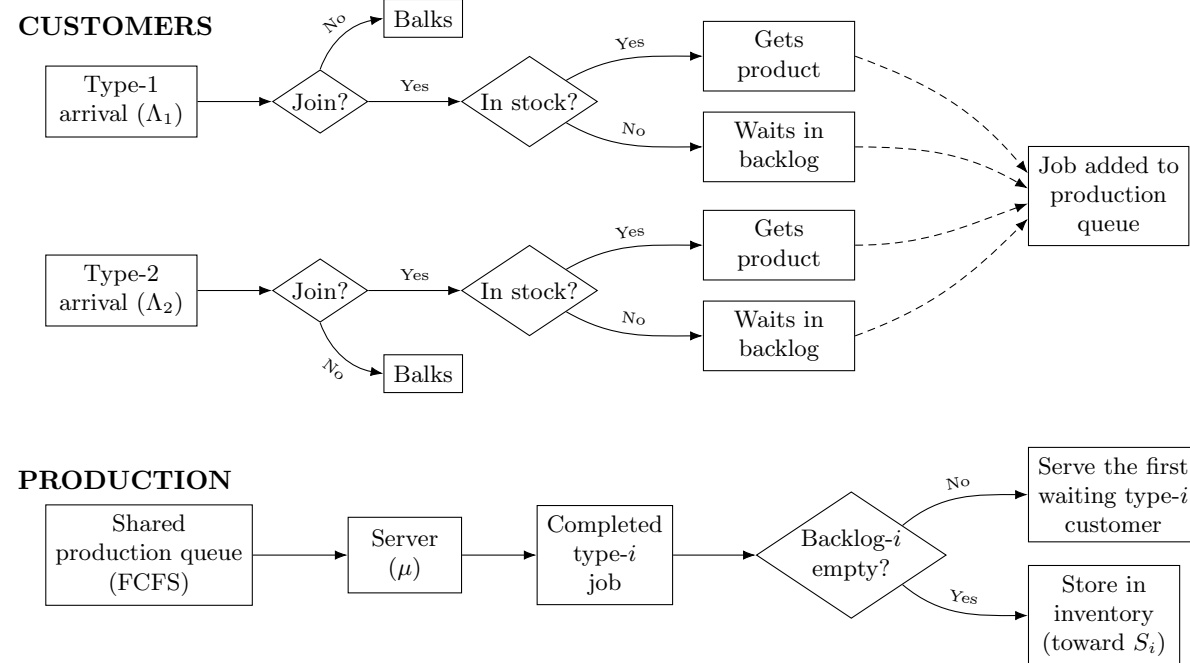


Figure 1: Two-Product Make-to-Stock System: Customer Flow and Production Process

This system shows a key tradeoff: higher inventory reduces customer waiting times but increases holding costs. Because customers cannot see current inventory levels, they must make joining decisions based on expected rather than actual waiting times, similar to how retail shoppers decide whether to visit a store without knowing its current stock levels.

3 Queueing Analysis and Performance Measures

We now derive closed-form expressions for waiting times, inventory levels, and backlogs. These formulas support our later strategic analysis while also providing practical insights for non-strategic settings (where $\lambda_i = \Lambda_i$). The expressions reveal how waiting times, inventory levels, and backlogs respond to system parameters, demonstrating the inherent tradeoffs when two products share production capacity.

3.1 Stationary Distributions

3.1.1 Baseline Results

This subsection summarizes stationary distributions established by Buzacott and Shanthikumar [7, Section 4.4] for two-product make-to-stock systems, which serve as the foundation for our analysis. In this setting, a single production server processes both product types at rate μ , and the system

maintains a target inventory level of S_i units for each product i . If $N_i(t)$, the number of product- i jobs in the production queue, exceeds S_i , the difference $B_i(t) = N_i(t) - S_i$ is interpreted as a backlog of customers who arrived to find no finished inventory available.

Conversely, $I_i(t) = [S_i - N_i(t)]^+$ gives the on-hand inventory of product i whenever $N_i(t)$ falls below S_i . Hence, N_i , I_i , and B_i capture the state of the system from different angles:

- $N_i(t)$: the number of type- i jobs in the production queue (either waiting or in service),
- $I_i(t)$: the on-hand inventory: units of product i available to immediately serve arrivals,
- $B_i(t)$: the backlog of type- i customers still waiting for a unit to be produced.

These three variables provide a complete picture of the system's state. When inventory level is positive, customers receive products immediately upon arrival. As inventory level depletes and jobs accumulate in the queue, $N_i(t)$ increases. Once number of jobs exceeds inventory level, the backlog grows, indicating customers who must wait for production to complete. The balance between these measures directly impacts customer satisfaction and operational costs — high inventory reduces waiting but increases holding costs, while high backlog indicates poor service quality.

Across products, $N(t) = N_1(t) + N_2(t)$ is simply the total number of jobs in the queue. Although the processes $\{N_1(t)\}$ and $\{N_2(t)\}$ are not Markov individually, their sum $N(t)$ behaves as an M/M/1 queue with total arrival rate $\lambda_1 + \lambda_2$ and service rate μ . In the long run, the system reaches a steady state where the probability distribution of queue length no longer changes with time. This stationary distribution is:

$$\mathbb{P}\{N = n\} = \left(1 - \frac{\lambda_1 + \lambda_2}{\mu}\right) \left(\frac{\lambda_1 + \lambda_2}{\mu}\right)^n, \quad n = 0, 1, 2, \dots \quad (3.1)$$

Since arrivals of types 1 and 2 are independent Poisson processes with rates λ_1 and λ_2 , each job in N is of type i with probability $\lambda_i/(\lambda_1 + \lambda_2)$. By multinomial thinning, conditional on $N = n$, the vector (N_1, N_2) follows a multinomial distribution:

$$\mathbb{P}\{N_1 = n_1, N_2 = n_2 \mid N = n\} = \binom{n}{n_1} \left(\frac{\lambda_1}{\lambda_1 + \lambda_2}\right)^{n_1} \left(\frac{\lambda_2}{\lambda_1 + \lambda_2}\right)^{n_2}, \quad n_1 + n_2 = n.$$

Combining this with (3.1) yields the joint distribution

$$\begin{aligned} \mathbb{P}\{N_1 = n_1, N_2 = n_2\} \\ = \left(1 - \frac{\lambda_1 + \lambda_2}{\mu}\right) \left(\frac{\lambda_1 + \lambda_2}{\mu}\right)^{n_1+n_2} \binom{n_1+n_2}{n_1} \left(\frac{\lambda_1}{\lambda_1 + \lambda_2}\right)^{n_1} \left(\frac{\lambda_2}{\lambda_1 + \lambda_2}\right)^{n_2}. \end{aligned}$$

Summing over n_j and applying standard geometric series identities, the marginal distribution of N_i takes a geometric form:

$$\mathbb{P}\{N_i = n_i\} = \left(1 - \frac{\lambda_i}{\mu - \lambda_j}\right) \left(\frac{\lambda_i}{\mu - \lambda_j}\right)^{n_i}, \quad \text{for } i, j \in \{1, 2\}, j \neq i.$$

The stationary distribution of on-hand inventory I_i follows by applying the transformation $I_i = [S_i - N_i]^+$ to the geometric distribution of N_i . Since $I_i = 0$ corresponds to $N_i \geq S_i$ and $I_i = k \in \{1, \dots, S_i\}$ corresponds to $N_i = S_i - k$, we obtain:

$$\mathbb{P}\{I_i = k\} = \begin{cases} \left(\frac{\lambda_i}{\mu - \lambda_j}\right)^{S_i}, & k = 0, \\ \left(1 - \frac{\lambda_i}{\mu - \lambda_j}\right) \left(\frac{\lambda_i}{\mu - \lambda_j}\right)^{S_i-k}, & k = 1, \dots, S_i, \end{cases} \quad j \neq i. \quad (3.2)$$

The probability that I_i is zero captures a stockout situation, meaning all S_i target units are in the production queue. When the queue has fewer than S_i jobs, some finished inventory remains available.

The stationary distribution of backlog B_i is obtained similarly via $B_i = [N_i - S_i]^+$. The event $B_i = 0$ corresponds to $N_i \leq S_i$, whereas $B_i = k \geq 1$ corresponds to $N_i = S_i + k$, yielding the piecewise geometric form:

$$\mathbb{P}\{B_i = k\} = \begin{cases} 1 - \left(\frac{\lambda_i}{\mu - \lambda_j}\right)^{S_i+1}, & k = 0, \\ \left(1 - \frac{\lambda_i}{\mu - \lambda_j}\right) \left(\frac{\lambda_i}{\mu - \lambda_j}\right)^{S_i+k}, & k = 1, 2, \dots. \end{cases} \quad (3.3)$$

The event $B_i = 0$ means the system has sufficient inventory to prevent backlog, while $B_i > 0$ indicates customers are waiting for products to be manufactured.

The next parts of this section leverage these results to derive closed-form expressions for waiting times and expected on-hand inventories, then expand to backlog expectations as well.

3.1.2 Queue Position of Arriving Customer

To derive the expected waiting time, we identify how many jobs must complete before a newly arriving type- i customer receives a unit. Since the arrival triggers a new type- i job at the tail of the queue, one might assume the customer must wait for that job. The situation is more subtle.

Throughout this subsection, we use two state-dependent labels for jobs in the production queue: backlog-serving (completions allocated to currently waiting customers) and replenishment (completions that rebuild inventory toward S_i once backlog is cleared). These labels may shift with the next arriving customer; they do not affect production and are used only for the waiting-time derivation. Under a target inventory level $S_i > 0$ and a stockout event ($I_i = 0$), the queue contains S_i type- i replenishment jobs (possibly preceded by type- i backlog-serving jobs). A new type- i customer who joins is served by the completion of the job that, immediately before the arrival, was the oldest replenishment type- i job already in the queue. The newly triggered job enters at the tail as the newest replenishment job. Figure 2 illustrates this mechanism for the case where $i = 1$ and shows how type-2 jobs may be interspersed throughout.

Let $N_i^a(t)$ be the number of jobs ahead of, and including the serving type- i job (i.e., the job whose completion supplies a newly arriving type- i backorder at time t , after any earlier backorders). Let $N_i^b(t)$ be the number of jobs strictly behind it. Hence, at time t , before any potential arrival,

$$N(t) = N_i^a(t) + N_i^b(t),$$

where (see Section 3.1.1) $N(t)$ follows an M/M/1-type stationary distribution under effective arrival rates λ_1, λ_2 , and service rate μ .

The joint stationary distribution of $(N_i^a(t), N_i^b(t))$ is:

$$\mathbb{P}\{N_i^a = n^a, N_i^b = n^b\} = \binom{n^b}{S_i - 1} \frac{(\lambda_1 + \lambda_2)^{n^a-1} \lambda_i^{S_i} \lambda_j^{n^b-S_i+1} (\mu - \lambda_1 - \lambda_2)}{\mu^{n^a+n^b+1}}, \quad j \neq i, \quad (3.4)$$

valid for $n^a \geq 1$ and $n^b \geq S_i - 1$, and zero otherwise. The binomial coefficient arises because exactly $S_i - 1$ of the n^b jobs behind the customer's position must be type- i replenishment jobs, with the

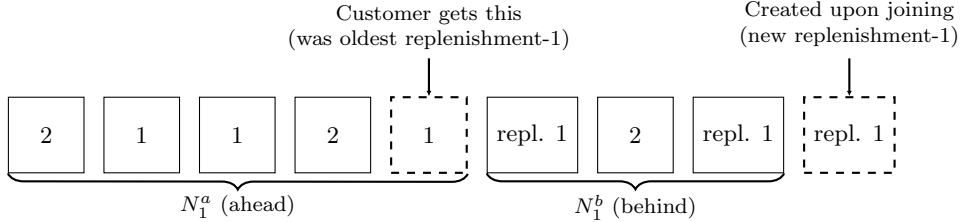


Figure 2: Queue Position for Backlogged Arrival

remaining jobs assigned types through standard thinning of the Poisson process. For the detailed proof, see Appendix A.1.

This distribution specifies the 'position in queue' N_i^a for an arriving type- i backlog under the condition of out-of-stock. The next subsection uses $\mathbb{E}[N_i^a]$ to derive an explicit formula for the expected waiting time of that newly arrived customer.

3.2 Waiting Times

When a customer arrives to find no inventory available, their expected waiting time depends on the system's congestion level, the inventory policy, and the interaction between products sharing service capacity.

For a newly arrived type- i customer, the expected waiting time $\mathbb{E}W_i(\lambda_1, \lambda_2)$ equals the expected number of jobs ahead of it N_i^a multiplied by the mean service time $1/\mu$. By analyzing the queue structure and applying appropriate summation techniques on the joint distribution (see Appendix A.2 for details), we obtain:

Proposition 3.1. *The expected waiting time for a newly arriving type- i customer is*

$$\mathbb{E}[W_i(\lambda_1, \lambda_2)] = \left(\frac{\lambda_i}{\mu - \lambda_j} \right)^{S_i} \cdot \frac{1}{\mu - \lambda_1 - \lambda_2}, \quad j \neq i. \quad (3.5)$$

This formula reveals several key operational insights. First, waiting time decreases as S_i increases, since $\lambda_i < \mu - \lambda_j$ for stability, making $(\frac{\lambda_i}{\mu - \lambda_j})^{S_i}$ smaller with larger inventory targets. The fraction $\frac{\lambda_i}{\mu - \lambda_j}$ represents a product-specific congestion measure — the ratio between product i 's demand and its effective service capacity (after accounting for capacity consumed by product j). The power S_i shows how inventory buffers against this congestion. The term $(\mu - \lambda_1 - \lambda_2)$ in the denominator reflects overall system utilization — as total arrival rates approach service capacity, waiting times increase for all products.

Notably, this expression depends on the other product only through its arrival rate λ_j , not its inventory level S_j . This happens because each arriving customer of type j adds exactly one job to the production queue, regardless of whether it is a replenishment job or a backlog-serving job. From the perspective of a type- i customer, the distinction between these job types for product j is irrelevant — what matters is only how many total jobs from product j are ahead in the queue, which is determined solely by λ_j .

3.3 Inventory Levels

Using the stationary distribution (3.2) of on-hand inventory $I_i(\lambda_1, \lambda_2)$, we compute the expected inventory for each product. Through appropriate summation and application of geometric series identities, we obtain:

$$\mathbb{E}[I_i(\lambda_1, \lambda_2)] = S_i - \frac{\lambda_i}{\mu - \lambda_1 - \lambda_2} \left[1 - \left(\frac{\lambda_i}{\mu - \lambda_j} \right)^{S_i} \right], \quad j \neq i. \quad (3.6)$$

This expression reveals how expected inventory balances target levels against system dynamics. The starting point S_i represents the target inventory level, which is then reduced by the expected depletion term. This depletion depends on two congestion measures: $\frac{\lambda_i}{\mu - \lambda_1 - \lambda_2}$ captures overall system congestion, while $(\frac{\lambda_i}{\mu - \lambda_j})^{S_i}$ reflects product-specific stockout probability. As S_i increases, this stockout probability decreases (since $\frac{\lambda_i}{\mu - \lambda_j} < 1$ for stability), meaning the bracketed term approaches 1. This creates a diminishing returns effect — each additional unit of target inventory contributes less to the expected on-hand inventory. Under high arrival rates approaching capacity limits, this effect strengthens, as both congestion measures increase and depletion accelerates.

3.4 Backlog Levels

For the backlog $B_i(\lambda_1, \lambda_2)$, we derive the expected value using the distribution from (3.3).

Summing over all possible backlog values and applying the identity for infinite geometric series, we obtain:

$$\mathbb{E}[B_i(\lambda_1, \lambda_2)] = \left(\frac{\lambda_i}{\mu - \lambda_j} \right)^{S_i} \cdot \frac{\lambda_i}{(\mu - \lambda_1 - \lambda_2)}.$$

This expression reveals how expected backlog decreases with higher inventory targets, sharing structural similarities with the waiting time formula. The term $\frac{\lambda_i^{S_i+1}}{(\mu - \lambda_j)^{S_i}}$ incorporates the same product-specific congestion measure raised to power S_i , showing how inventory buffers against stockouts. The additional λ_i factor reflects that backlog only occurs for customers who actually join the system. The denominator term $(\mu - \lambda_1 - \lambda_2)$ again captures overall system utilization — as total demand approaches capacity, backlog grows regardless of inventory levels. Higher S_i values reduce expected backlog by decreasing the probability of stockout events, though this protection becomes less effective as congestion increases.

4 Strategic Customer Behavior

Using the performance measures from Section 3, we now begin our examination of the decentralized decision-making approach. In this framework, customers and producers act independently to maximize their own objectives rather than coordinating decisions. This section focuses on the first stage of decentralization: how customers strategically decide whether to join the system based on their expected utilities, considering both the producer's inventory choices and the anticipated behavior of other customers. Section 5 will complete this decentralized perspective by examining how the producer optimizes inventory targets while anticipating these customer responses.

4.1 Utility Functions and Best Response

Consider a type- i customer ($i = 1, 2$) who observes strategies q_1, q_2 being played by other customers in the system. These joining probabilities determine the effective arrival rates $\lambda_i = q_i \Lambda_i$ used in

our earlier performance measures. The customer's expected utility from joining is:

$$U_i(\text{join}; q_1, q_2) = R_i - p_i - c_i \mathbb{E}[W_i(q_1 \Lambda_1, q_2 \Lambda_2)],$$

where R_i is the reward, p_i is the price, c_i is the waiting-cost rate, and $\mathbb{E}[W_i(\Lambda_1 q_1, \Lambda_2 q_2)]$ is the expected waiting time given others' strategies (Section 3.2).

If the customer balks, the utility $U_i(\text{balk}; q_1, q_2)$ is zero.

If the customer joins with probability p , the expected utility becomes

$$U_i(p; q_1, q_2) = p \cdot U_i(\text{join}; q_1, q_2) + (1 - p) \cdot 0 = p \cdot U_i(\text{join}; q_1, q_2).$$

This linear relationship between p and expected utility means that the customer's optimal decision will depend only on the sign of $U_i(\text{join}; q_1, q_2)$. For notational simplicity, throughout the remainder of this paper, we will use $U_i(q_1, q_2)$ to denote $U_i(\text{join}; q_1, q_2)$.

A customer's decision process mirrors what shoppers intuitively do every day: weigh the value of a product against its price and the hassle of potentially waiting. When many customers adopt joining strategy q_i , they collectively influence the system's congestion level, creating a feedback loop where individual decisions affect everyone's experience.

The utility function has several important properties that shape the strategic interactions in this system:

Lemma 4.1 (Continuity and Monotonicity of U_i). *For each $i = 1, 2$, the function*

$$U_i(q_1, q_2) = R_i - p_i - c_i \mathbb{E}[W_i(q_1 \Lambda_1, q_2 \Lambda_2)]$$

is continuous in (q_1, q_2) over $[0, 1]^2$. Moreover, U_i is strictly decreasing in both q_1 and q_2 .

The proof is provided in Appendix B.1. It follows by standard calculus arguments, examining partial derivatives of the utility function in both the $S_i = 0$ and $S_i > 0$ cases to establish strict monotonicity.

Then, we define the best response for type i as

$$\text{BR}_i(q_1, q_2) = \arg \max_{p \in [0, 1]} p \cdot U_i(q_1, q_2).$$

From linearity, the best response is:

$$\text{BR}_i(q_1, q_2) = \begin{cases} 1 & \text{if } U_i(q_1, q_2) > 0 \\ 0 & \text{if } U_i(q_1, q_2) < 0, \\ [0, 1] & \text{if } U_i(q_1, q_2) = 0 \end{cases}$$

where the value 1 corresponds to the pure action 'always join' and 0 to 'always balk.' In particular, away from indifference points where $U_i(q_1, q_2) = 0$, the unique best response is pure; mixing (i.e., any probability in $[0, 1]$) is optimal only when the customer is indifferent between joining and balking. The next lemma studies the structure of these best responses when one type's joining probability is fixed.

Lemma 4.2 (Unique Fixed Points in One Variable). *Fix any $q_2 \in [0, 1]$. As a function of $q_1 \in [0, 1]$, the mapping $\text{BR}_1(\cdot, q_2)$ admits exactly one fixed point q_1^* in $[0, 1]$. Concretely:*

1. $q_1^* = 0$ if and only if $U_1(0, q_2) \leq 0$.
2. $q_1^* = 1$ if and only if $U_1(1, q_2) \geq 0$.
3. Otherwise, exactly one point $q_1^* \in (0, 1)$ satisfies $U_1(q_1^*, q_2) = 0$, and that q_1^* is the unique fixed point.

The same holds for type 2 by fixing q_1 and considering $\text{BR}_2(q_1, q_2)$ in q_2 .

The proof is provided in Appendix B.2. It relies on the strict monotonicity established in Lemma 4.1 and applies the Intermediate Value Theorem to guarantee a unique crossing point.

The strict decrease of U_i in both q_1 and q_2 established in Lemma 4.1 is a standard avoid-the-crowd property in congestion games: when more customers join, the incentive to join decreases. In one-dimensional queueing models, such avoid-the-crowd behavior directly yields existence and uniqueness of a symmetric equilibrium joining probability; see, for example, the discussion in Hassin and Roet-Green [20, Section 1.1] and the references therein. A fixed point q_1^* represents a self-consistent strategy where, given the strategy q_2 of type-2 customers, q_1^* is the best response for type-1 customers. This means that when all type-1 customers adopt probability q_1^* and type-2 customers use q_2 , no individual type-1 customer has an incentive to deviate from q_1^* . Despite the set-valued nature of best responses at indifference points, the lemma guarantees that such a fixed point is always unique for any fixed strategy of the other customer type.

4.2 Nash Equilibrium Characterization

4.2.1 Classification

In the previous analysis, the best-response functions BR_1 and BR_2 have been studied for each customer type separately. When customers of both types make their decisions simultaneously, we search for stable strategies where no individual would benefit by unilaterally changing their decision. This concept of Nash equilibrium (NE) characterizes the likely long-term behavior in the system.

While best responses may be set-valued at indifference points (where $U_i = 0$), in equilibrium each customer type adopts a specific joining probability. A pair $(q_1^*, q_2^*) \in [0, 1]^2$ is a Nash equilibrium if each probability is consistent with the best response to the other:

$$q_1^* \in \text{BR}_1(q_1^*, q_2^*), \quad q_2^* \in \text{BR}_2(q_1^*, q_2^*).$$

Equivalently, if each best-response is single-valued at (q_1^*, q_2^*) , it is possible (by Lemma 4.2) to write

$$(q_1^*, q_2^*) = (\text{BR}_1(q_1^*, q_2^*), \text{BR}_2(q_1^*, q_2^*)),$$

meaning (q_1^*, q_2^*) is the fixed point of $(\text{BR}_1, \text{BR}_2)$.

These equations capture the self-enforcing nature of equilibrium — given that all customers join with probability (q_1^*, q_2^*) , a tagged type-1 customer finds q_1^* optimal, and a tagged type-2 customer finds q_2^* optimal.

Because, by Lemma 4.2, each equilibrium joining probability for type i must be either 0, 1, or a unique interior value in $(0, 1)$, there are nine possible ways to form (q_1^*, q_2^*) . The proposition below compiles these nine patterns and summarizes each one's utility-based conditions.

Proposition 4.1 (Nash Equilibrium Classification). *Any Nash equilibrium (q_1^*, q_2^*) must lie in exactly one of the nine cases shown in Table 1. Each case corresponds to a fixed point of (BR_1, BR_2) , with the relevant utility inequalities (or equalities) determining when that fixed point occurs.*

Table 1: Possible Equilibrium Conditions

(0,0) - NE: $U_1(0, 0) \leq 0$ $U_2(0, 0) \leq 0$	(0, q_2^*) , $q_2^* \in (0, 1)$ - NE: $U_1(0, q_2^*) \leq 0$ $U_2(0, q_2^*) = 0$	(0,1) - NE: $U_1(0, 1) \leq 0$ $U_2(0, 1) \geq 0$
(q_1^*,0), $q_1^* \in (0, 1)$ - NE: $U_1(q_1^*, 0) = 0$ $U_2(q_1^*, 0) \leq 0$	(q_1^*,q_2^*), $q_1^*, q_2^* \in (0, 1)$ - NE: $U_1(q_1^*, q_2^*) = 0$ $U_2(q_1^*, q_2^*) = 0$	(q_1^*,1), $q_1^* \in (0, 1)$ - NE: $U_1(q_1^*, 1) = 0$ $U_2(q_1^*, 1) \geq 0$
(1,0) - NE: $U_1(1, 0) \geq 0$ $U_2(1, 0) \leq 0$	(1,q_2^*), $q_2^* \in (0, 1)$ - NE: $U_1(1, q_2^*) \geq 0$ $U_2(1, q_2^*) = 0$	(1,1) - NE: $U_1(1, 1) \geq 0$ $U_2(1, 1) \geq 0$

The proof is provided in Appendix B.3. It proceeds by systematically applying Lemma 4.2 to each type, showing that the fixed points of the best response must satisfy certain utility conditions.

4.2.2 Existence of a Nash Equilibrium

Before investigating the uniqueness properties of equilibria under different inventory scenarios, we first establish that at least one equilibrium always exists in our setting, ensuring the model's predictions are well-defined.

Proposition 4.2 (Existence of Nash Equilibrium). *A Nash equilibrium (q_1^*, q_2^*) exists in this model.*

Proof sketch. The existence of a Nash equilibrium follows from Brouwer's Fixed Point Theorem. Although the best-response mappings BR_1 and BR_2 are set-valued correspondences, Lemma 4.2 allows us to construct a continuous function $f(q_1, q_2) = (f_1(q_2), f_2(q_1))$ mapping $[0, 1]^2$ to itself, where $f_1(q_2)$ is the unique fixed point of $BR_1(q_1, q_2)$ for fixed q_2 , and similarly for $f_2(q_1)$.

The continuity of f_1 and f_2 follows from the continuity of utility functions and the uniqueness of fixed points. By Brouwer's theorem, f has a fixed point (q_1^*, q_2^*) where $q_1^* = f_1(q_2^*)$ and $q_2^* = f_2(q_1^*)$, which by construction satisfies the Nash equilibrium conditions. See Appendix B.4 for the complete proof. \square

The challenge encountered here is closely related to that in Hassin and Roet-Green [20], who study a queueing game in which customers choose among join, inspect, and balk. In their model, as in ours, individual utilities satisfy an avoid-the-crowd property in each dimension, but the symmetric strategy is two-dimensional and the standard one-dimensional avoid-the-crowd uniqueness arguments do not apply. They resolve this by analyzing the geometry of an expected-utility set in two dimensions. Both models illustrate how avoid-the-crowd analysis extends to multidimensional strategy spaces. It is natural, after establishing the existence of a Nash equilibrium, to ask whether that equilibrium is unique. This question is easier to address by considering different scenarios for the target inventory levels S_i .

4.2.3 Zero Inventory Scenario: Continuum or Unique Equilibrium

When both product types maintain zero inventory targets, the customer equilibrium structure depends critically on the relationship between cost-to-margin ratios and service capacity. This serves as the baseline case for understanding more complex inventory policies.

Proposition 4.3. *Let $S_1 = S_2 = 0$. The Nash equilibrium for the joining probabilities (q_1^*, q_2^*) can be described as follows:*

1. If

$$\frac{c_1}{R_1 - p_1} = \frac{c_2}{R_2 - p_2} \quad \text{and} \quad \frac{c_1}{R_1 - p_1} < \mu < \frac{c_1}{R_1 - p_1} + \Lambda_1 + \Lambda_2,$$

there is a continuum of Nash equilibria satisfying

$$q_1^* \Lambda_1 + q_2^* \Lambda_2 = \mu - \frac{c_1}{R_1 - p_1}, \quad 0 \leq q_1^*, q_2^* \leq 1.$$

2. Otherwise, there is a unique Nash equilibrium that can be explicitly determined from Table 2.

Table 2: Equilibrium Outcomes for $S_1 = 0, S_2 = 0$

$(0,0)$:	$(0, q_2^*)$:	$(0,1)$:
$\mu \leq \frac{c_1}{R_1 - p_1}$ $\mu \leq \frac{c_2}{R_2 - p_2}$ $\frac{c_1}{R_1 - p_1} \geq \frac{c_2}{R_2 - p_2}$	$q_2^* = \frac{1}{\Lambda_2} (\mu - \frac{c_2}{R_2 - p_2})$ $\mu > \frac{c_2}{R_2 - p_2}$ $\mu < \frac{c_2}{R_2 - p_2} + \Lambda_2$ $\frac{c_1}{R_1 - p_1} \geq \frac{c_2}{R_2 - p_2}$	$\mu \geq \frac{c_2}{R_2 - p_2} + \Lambda_2$ $\mu \leq \frac{c_1}{R_1 - p_1} + \Lambda_2$
$(q_1^*, 0)$, $q_1^* = \frac{1}{\Lambda_1} (\mu - \frac{c_1}{R_1 - p_1})$: $\mu > \frac{c_1}{R_1 - p_1}$ $\mu < \frac{c_1}{R_1 - p_1} + \Lambda_1$ $\frac{c_1}{R_1 - p_1} \leq \frac{c_2}{R_2 - p_2}$	(q_1^*, q_2^*) , $q_1^* \Lambda_1 + q_2^* \Lambda_2 = \mu - \frac{c_1}{R_1 - p_1}$, $0 < q_1^*, q_2^* < 1$: $\mu > \frac{c_1}{R_1 - p_1}$ $\mu < \frac{c_1}{R_1 - p_1} + \Lambda_1 + \Lambda_2$ $\frac{c_1}{R_1 - p_1} = \frac{c_2}{R_2 - p_2}$	$(q_1^*, 1)$, $q_1^* = \frac{1}{\Lambda_1} (\mu - \Lambda_2 - \frac{c_1}{R_1 - p_1})$: $\mu > \frac{c_1}{R_1 - p_1} + \Lambda_2$ $\mu < \frac{c_1}{R_1 - p_1} + \Lambda_1 + \Lambda_2$ $\frac{c_1}{R_1 - p_1} \geq \frac{c_2}{R_2 - p_2}$
$(1,0)$: $\mu \geq \frac{c_1}{R_1 - p_1} + \Lambda_1$ $\mu \leq \frac{c_2}{R_2 - p_2} + \Lambda_1$	$(1, q_2^*)$, $q_2^* = \frac{1}{\Lambda_2} (\mu - \Lambda_1 - \frac{c_2}{R_2 - p_2})$: $\mu > \frac{c_2}{R_2 - p_2} + \Lambda_1$ $\mu < \frac{c_2}{R_2 - p_2} + \Lambda_1 + \Lambda_2$ $\frac{c_1}{R_1 - p_1} \leq \frac{c_2}{R_2 - p_2}$	$(1,1)$: $\mu \geq \frac{c_1}{R_1 - p_1} + \Lambda_1 + \Lambda_2$ $\mu \geq \frac{c_2}{R_2 - p_2} + \Lambda_1 + \Lambda_2$

Proof sketch. The key to this analysis is examining how the utility functions simplify when $S_1 = S_2 = 0$:

$$U_i(q_1, q_2) = R_i - p_i - c_i \frac{1}{\mu - q_1 \Lambda_1 - q_2 \Lambda_2}.$$

This enables explicit computation of all possible equilibrium configurations. When $\frac{c_1}{R_1 - p_1} = \frac{c_2}{R_2 - p_2}$, the condition $U_1 = U_2 = 0$ yields a line segment of equilibria. In all other cases, a unique equilibrium exists. The complete case analysis appears in Appendix B.5. \square

This result reveals that even for zero inventories scenario the system can support multiple equilibria only when both customer types have identical patience ratios (the ratio of waiting cost to potential surplus, $\frac{c_i}{R_i - p_i}$). In this special case, customers of both types respond identically to waiting time relative to their product's value, creating a line of equilibrium points that represents different ways

to allocate the same total service utilization. Each point on this line maintains the critical balance where total effective arrivals equal μ minus the patience threshold.

When patience ratios differ, however, a unique equilibrium emerges that typically favors the more patient customer type (lower $\frac{c_i}{R_i - p_i}$ ratio). This uniqueness highlights how even small differences in customer waiting sensitivity create predictable service patterns without requiring external coordination.

4.2.4 Positive Inventory Scenario: Unique Equilibrium

When at least one product maintains a positive inventory level, the strategic landscape changes significantly compared to the zero inventory scenario.

Proposition 4.4. *When at least one product maintains a positive inventory level:*

1. *If $S_i > 0$ for some product i , then $q_i^* \in (0, 1]$ in any Nash equilibrium (i.e., complete balking is impossible).*
2. *If $S_1 > 0$ and $S_2 > 0$, there exists a unique Nash equilibrium for the customers' joining probabilities (q_1^*, q_2^*) .*
3. *If exactly one target inventory level is positive (either $S_1 > 0, S_2 = 0$ or $S_1 = 0, S_2 > 0$), there still exists a unique Nash equilibrium.*

Unlike in the zero inventory case, where we derived explicit expressions for equilibrium strategies, the equilibria in positive-inventory scenarios must generally be found numerically. The utility functions become more complex, involving higher powers of the joining probabilities, which precludes simple closed-form solutions.

Proof sketch. The proof proceeds in three steps:

Step 1: Proving that $S_i > 0$ implies $q_i > 0$. When $S_i > 0$, a customer who arrives to find the system empty of other type- i customers would receive immediate service with probability 1, yielding utility $R_i - p_i > 0$. This makes joining strictly preferable to balking, ruling out $q_i = 0$ as an equilibrium.

Step 2: Uniqueness when both $S_1, S_2 > 0$. For interior equilibria where both types partially join $(q_1, q_2) \in (0, 1)^2$, we analyze the implicit functions $q_1(q_2)$ and $q_2(q_1)$ defined by $U_1(q_1, q_2) = 0$ and $U_2(q_1, q_2) = 0$. The composition of these functions creates a contractive mapping with derivative strictly between 0 and 1, ensuring at most one fixed point.

For boundary equilibria where at least one type fully joins (e.g., $q_1 = 1$), we show that no such equilibrium can coexist with any other equilibrium by analyzing the behavior best responses at the boundaries.

Step 3: Uniqueness with asymmetric inventory. When exactly one product has positive inventory, similar monotonicity arguments apply with appropriate modifications to handle the possibility of $q_i = 0$ for the zero inventory product.

The complete proof with detailed analysis appears in Appendix B.6. \square

The intuition behind this uniqueness result lies in how positive inventory transforms the mathematical structure of customer responses. When $S_i > 0$, the utility function involves higher powers

of joining probabilities through terms like $(q_i \Lambda_i)^{S_i}$, creating a more complex but well-behaved relationship between strategies. This structure ensures that customers' best responses interact in a way that admits only one fixed point. Unlike the zero inventory case where multiple equilibria can emerge under symmetric patience ratios, the positive-inventory scenario always yields a unique, predictable outcome regardless of whether customer types have similar or different preferences.

5 Producer's Decision Problem

Having characterized how customers strategically respond to inventory levels through Nash equilibria, we now examine the producer's perspective. The interaction between producer and customers naturally forms a Stackelberg game — a sequential decision model where one player (the leader) commits to a strategy before others (the followers) respond. In our context, the producer acts as the leader by setting inventory targets, while customers follow by determining their joining strategies. Unlike simultaneous-move games, the leader anticipates the followers' responses and incorporates this knowledge into its decision, making this a particularly suitable framework for analyzing producer-customer interactions where commitment to inventory levels precedes customer decisions.

5.1 Profit Function

The producer's profit can be written as

$$\Pi(S) = p_1 \Lambda_1 q_1^{(S_1, S_2)} + p_2 \Lambda_2 q_2^{(S_1, S_2)} - h_1 \mathbb{E}[I_1(S)] - h_2 \mathbb{E}[I_2(S)],$$

where $S = (S_1, S_2)$ denotes the target inventory vector, p_i is the price charged for product type i , and $\Lambda_i q_i^{(S_1, S_2)}$ is the effective arrival rate of type- i customers given their equilibrium joining probability $q_i^{(S_1, S_2)}$ at inventory S . The term h_i is the holding cost per unit of inventory for product i , while $\mathbb{E}[I_i(S)]$ is the expected inventory level derived in Section 3.3:

$$\mathbb{E}[I_i(S)] = S_i - \frac{\Lambda_i q_i^{(S_1, S_2)}}{\mu - \Lambda_1 q_1^{(S_1, S_2)} - \Lambda_2 q_2^{(S_1, S_2)}} \left(1 - \left(\frac{\Lambda_i q_i^{(S_1, S_2)}}{\mu - \Lambda_j q_j^{(S_1, S_2)}} \right)^{S_i} \right), \quad j \neq i.$$

The Stackelberg game structure appears in how the profit function is evaluated. The producer first selects inventory levels (S_1, S_2) , then customers determine their joining probabilities by reaching a Nash equilibrium among themselves, resulting in $(q_1^{(S_1, S_2)}, q_2^{(S_1, S_2)})$. Only after this sequential process is the producer's profit actually realized. The notation $q_i^{(S_1, S_2)}$ emphasizes that these probabilities are not independent variables but functions determined by the inventory choice.

This sequential decision process creates a fundamental tradeoff: higher inventory levels improve customer experience and increase joining probabilities $q_i^{(S_1, S_2)}$ (thus boosting revenue), but also raise holding costs. The optimization challenge is intensified because the equilibrium joining probabilities $q_i^{(S_1, S_2)}$ generally lack closed-form expressions except in special cases like $S_1 = S_2 = 0$. Instead, they must be computed numerically for each inventory pair through the methods described in Section 4, making the producer's optimization problem analytically intricate.

Unless $(S_1, S_2) = (0, 0)$ and the ratio conditions specified in Proposition 4.3 hold (which allows multiple equilibria), each inventory pair (S_1, S_2) determines a unique customer equilibrium

$(q_1^{(S_1, S_2)}, q_2^{(S_1, S_2)})$. In the exceptional scenario with multiple equilibria, we adopt the convention of selecting the equilibrium that yields the lowest profit to ensure robust performance guarantees.

5.2 Target Inventory Thresholds

To solve this Stackelberg game efficiently, we establish natural bounds on the producer's inventory decisions.

Proposition 5.1. *There exist thresholds \bar{S}_1 and \bar{S}_2 such that for all $S_1 \geq \bar{S}_1$ and $S_2 \geq \bar{S}_2$, customers of both types always join the system*

$$\left(q_1^{(S_1, S_2)} = q_2^{(S_1, S_2)} = 1 \right),$$

and the producer's profit does not exceed

$$\Pi(S) \leq \Pi(\bar{S}_1, \bar{S}_2) \quad \text{for all } S_1 \geq \bar{S}_1, S_2 \geq \bar{S}_2.$$

Moreover, these thresholds can be chosen as

$$\bar{S}_1 = \min\{S_1 \mid U_1^{S_1}(1, 1) \geq 0\}, \quad \bar{S}_2 = \min\{S_2 \mid U_2^{S_2}(1, 1) \geq 0\}. \quad (5.1)$$

The proof appears in Appendix C.1. Once inventory exceeds these thresholds, adding more units increases costs without attracting more customers. Once sufficient inventory is available to make all potential customers willing to join, further increases merely raise costs without attracting new demand.

In the context of the Stackelberg game, this result identifies bounds on the leader's rational strategy space. The first-mover advantage of the producer is effectively limited — beyond the thresholds \bar{S}_1 and \bar{S}_2 , the followers' responses remain unchanged at full participation, rendering additional inventory strategically irrelevant. This property significantly simplifies the optimization problem by restricting the search to a finite set of candidate inventory levels.

5.3 Profit-Maximizing Policy

The producer's strategy involves determining the optimal inventory pair (S_1^*, S_2^*) that maximizes profit, considering how customers will respond to each possible inventory configuration. By Proposition 5.1, searching within $S_1 \in [0, \bar{S}_1]$ and $S_2 \in [0, \bar{S}_2]$ is sufficient for finding the optimal target inventory levels.

The complete solution procedure involves:

1. Calculate the upper bounds \bar{S}_1 and \bar{S}_2 using (5.1).
2. For each inventory pair (s_1, s_2) within these bounds:
 - (a) Determine the resulting Nash equilibrium joining probabilities $(q_1^{(S_1, S_2)}, q_2^{(S_1, S_2)})$.
 - (b) Evaluate the producer's profit under these equilibrium responses.
3. Select the inventory pair that yields the highest profit.

6 Social Planner's Problem

The previous two sections examined decentralized decision-making where the producer optimizes profit while customers independently maximize their individual utilities. We now consider a centralized perspective — how would a social planner, concerned with maximizing overall welfare, coordinate inventory levels and customer participation rates?

Because the analysis now considers overall (social) performance, individual customers' joining strategies are not modeled directly. Instead, the fraction of arrivals of type i that actually join is represented by the effective arrival rate λ_i . Hence, λ_i replaces $\Lambda_i q_i$ and becomes the decision variable indicating how many potential arrivals the planner decides to serve. The planner also chooses the target inventory levels (S_1, S_2) .

6.1 Social Welfare Function

The social welfare function is:

$$SW(\lambda_1, \lambda_2, S_1, S_2) = \lambda_1 R_1 + \lambda_2 R_2 - C(\lambda_1, \lambda_2, S_1, S_2),$$

where $\lambda_i R_i$ is the total reward obtained from type- i customers and the corresponding total cost function $C(\lambda_1, \lambda_2, S_1, S_2)$ represents the overall costs incurred by both products:

$$C(\lambda_1, \lambda_2, S_1, S_2) = \sum_{i=1}^2 (h_i \mathbb{E}[I_i(\lambda_1, \lambda_2)] + c_i \lambda_i \mathbb{E}[W_i(\lambda_1, \lambda_2)]).$$

In the expression above, the first term $h_i \mathbb{E}[I_i(\lambda_1, \lambda_2)]$ represents the total holding cost for product i , calculated by multiplying the per-unit holding cost h_i by the expected inventory level derived in Section 3.3. The second term $c_i \lambda_i \mathbb{E}[W_i(\lambda_1, \lambda_2)]$ captures the total waiting cost incurred by type- i customers, combining the per-customer waiting cost rate c_i with the effective arrival rate λ_i and the expected waiting time from Proposition 3.1.

When these components are combined for both products, we obtain the complete cost function:

$$C(\lambda_1, \lambda_2, S_1, S_2) = \sum_{i=1}^2 \left[h_i S_i - h_i \frac{\lambda_i}{\mu - \lambda_1 - \lambda_2} \left(1 - \left(\frac{\lambda_i}{\mu - \lambda_j} \right)^{S_i} \right) + c_i \frac{\lambda_i}{\mu - \lambda_1 - \lambda_2} \left(\frac{\lambda_i}{\mu - \lambda_j} \right)^{S_i} \right], \quad (6.1)$$

and the social welfare function:

$$SW(\lambda_1, \lambda_2, S_1, S_2) = \sum_{i=1}^2 \left[\lambda_i R_i - h_i S_i + h_i \frac{\lambda_i}{\mu - \lambda_1 - \lambda_2} \left(1 - \left(\frac{\lambda_i}{\mu - \lambda_j} \right)^{S_i} \right) - c_i \frac{\lambda_i}{\mu - \lambda_1 - \lambda_2} \left(\frac{\lambda_i}{\mu - \lambda_j} \right)^{S_i} \right]. \quad (6.2)$$

The social welfare function captures economic efficiency by measuring the total value generated in the system rather than just monetary transfers. While prices appear in the profit function,

they cancel out in the welfare calculation since they represent transfers between customers and the producer. Instead, social welfare accounts for the full customer reward (R_i), holding costs, and waiting costs — regardless of which party experiences them. Consequently, the welfare-maximizing solution may allocate capacity differently than what emerges under pure profit maximization.

The optimization of $\text{SW}(\lambda_1, \lambda_2, S_1, S_2)$ follows a hierarchical approach. First, we derive optimal inventory levels $S_1^*(\lambda_1, \lambda_2)$ and $S_2^*(\lambda_1, \lambda_2)$ for any given arrival rates, establishing upper bounds \bar{S}_1 and \bar{S}_2 . Since these optimal inventory levels change discretely with arrival rates, they partition the feasible region into subdomains with constant inventory values. We then maximize welfare within each subdomain with respect to λ_1 and λ_2 , and identify the global optimum by comparing these local maxima.

6.2 Optimal Target Inventory Levels

From a social planner's perspective, the ideal inventory level for each product balances three factors: holding costs, customer waiting costs, and the probability of immediate service. This tradeoff has an elegant mathematical characterization.

Proposition 6.1. *For any positive fixed λ_1, λ_2 the optimal target inventory levels (S_1^*, S_2^*) minimizing the total cost (6.1) are given by*

$$S_i^*(\lambda_1, \lambda_2) = \left\lceil \frac{\log\left(\frac{h_i}{h_i+c_i}\right)}{\log\left(\frac{\lambda_i}{\mu-\lambda_j}\right)} \right\rceil - 1 \quad \text{for } i = 1, 2.$$

Proof sketch. The total cost can be decomposed as $C(S_1, S_2) = C_1(S_1) + C_2(S_2)$, allowing separate optimization for each product. Examining the cost difference $\Delta C_i(S_i) = C_i(S_i + 1) - C_i(S_i)$, we identify the threshold where increasing S_i no longer reduces cost. The complete derivation appears in Appendix D.1. \square

The formula's structure shows several properties of optimal inventory management. The ratio $\frac{h_i}{h_i+c_i}$ in the logarithm term creates a natural balance point between holding and waiting costs. As this ratio approaches zero (when $c_i \gg h_i$), optimal inventory increases to reduce waiting time. The dependence on $\frac{\lambda_i}{\mu-\lambda_j}$ reflects how congestion affects inventory decisions — as the effective service capacity $\mu - \lambda_j$ decreases due to the other product's demand, higher inventory becomes necessary to maintain service levels. The ceiling function ensures we obtain a practical integer solution.

Finally, recall that $\Lambda_1 + \Lambda_2 < \mu$. This implies

$$S_i < \left\lceil \frac{\log\left(\frac{h_i}{h_i+c_i}\right)}{\log\left(\frac{\Lambda_i}{\mu}\right)} \right\rceil \quad \text{for } i = 1, 2 \tag{6.3}$$

for any feasible λ_1, λ_2 .

6.3 Welfare Optimization Approach

Having established the optimal inventory levels for each product, we now need to determine the effective arrival rates λ_1 and λ_2 that maximize social welfare. This optimization is challenging for two reasons: $S_i^*(\lambda_1, \lambda_2)$ changes discretely across the feasible region, creating discontinuities in

the objective function, and even within regions of constant inventory levels, the welfare function's complexity prevents analytical solutions.

We approach this problem by partitioning the feasible region

$$\mathcal{D} = \{(\lambda_1, \lambda_2) : 0 \leq \lambda_i \leq \Lambda_i, \lambda_1 + \lambda_2 < \mu\}$$

into subdomains where the optimal inventory levels remain constant. From Proposition 6.1, we know that $(S_i^* = s_i)$ occurs when:

$$\left(\frac{\lambda_i}{\mu - \lambda_j}\right)^{s_i+1} \leq \frac{h_i}{h_i + c_i} < \left(\frac{\lambda_i}{\mu - \lambda_j}\right)^{s_i}$$

Rearranging these inequalities yields boundary curves in the λ_1 - λ_2 plane. For $s_1, s_2 > 0$, these boundaries define subdomains:

$$\mathcal{D}_{s_1, s_2} = \left\{ (\lambda_1, \lambda_2) \in \mathcal{D} : \mu - \frac{\lambda_1}{\beta_1^{1/s_1}} < \lambda_2 \leq \mu - \frac{\lambda_1}{\beta_1^{1/(s_1+1)}}, \right. \\ \left. \mu - \frac{\lambda_2}{\beta_2^{1/s_2}} < \lambda_1 \leq \mu - \frac{\lambda_2}{\beta_2^{1/(s_2+1)}} \right\},$$

where $\beta_i = \frac{h_i}{h_i + c_i}$. For $s_i = 0$, the conditions simplify to $\lambda_j \leq \mu - \frac{\lambda_i}{\beta_i}$.

Within each subdomain, the social welfare function is smooth but still analytically complex. We identify critical points using numerical methods to solve the first-order conditions $\partial \text{SW} / \partial \lambda_1 = 0$ and $\partial \text{SW} / \partial \lambda_2 = 0$, while also examining boundary solutions. The global optimum is determined by comparing these local maxima across all subdomains.

This approach transforms a discontinuous optimization problem into a collection of smooth subproblems with well-defined boundaries. The computational complexity remains manageable because the upper bounds on inventory levels are typically modest in practical settings. Appendix D.2 provides further mathematical details on optimization techniques.

6.4 Welfare-Maximizing Policy

The social planner's optimization yields a coordinated policy $(\lambda_1^*, \lambda_2^*, S_1^*, S_2^*)$ that maximizes overall welfare rather than individual objectives. Unlike the decentralized approach where the producer sets inventory levels and customers independently determine joining probabilities, the welfare-maximizing policy directly controls both aspects of the system.

The solution procedure involves:

1. Establishing upper bounds \bar{S}_1 and \bar{S}_2 on inventory levels based on cost ratios $\frac{h_i}{h_i + c_i}$ and system parameters.
2. For each candidate inventory pair (s_1, s_2) within these bounds:
 - (a) Identifying the subdomain \mathcal{D}_{s_1, s_2} where $(S_1^*, S_2^*) = (s_1, s_2)$;
 - (b) Optimizing effective arrival rates (λ_1, λ_2) within this subdomain;
 - (c) Computing the resulting social welfare.
3. Selecting the inventory-arrival rate combination that yields the highest welfare.

This centralized approach can generate different outcomes than the decentralized Stackelberg equilibrium. While a profit-maximizing producer might restrict service to maintain high prices, the social planner typically admits more customers and maintains different inventory levels to balance holding costs against waiting costs.

6.5 Bridging Decentralized and Centralized Solutions

The decentralized Stackelberg outcome from Section 5 generally differs from the welfare optimum: both the effective arrival rates λ_i and the inventory levels S_i may be higher or lower than their socially optimal counterparts, depending on parameters (cf. Figure 14 in our numerical experiments, illustrating that the deviation can go in either direction; see also Öz and Karaesmen [26] for the single-product case). We now show that, for any fixed target inventory levels S_1, S_2 , a simple correction scheme can implement the welfare-maximizing arrival rates.

Fix a target inventory pair (S_1, S_2) and let $(\lambda_1^*, \lambda_2^*)$ maximize $\text{SW}(\lambda_1, \lambda_2, S_1, S_2)$ over feasible (λ_1, λ_2) , with $q_i^* := \lambda_i^*/\Lambda_i$. Suppose a regulator applies a type- i admission correction τ_i (a toll if $\tau_i > 0$, a subsidy if $\tau_i < 0$), so the utility from joining becomes $U_i(q_1, q_2) - \tau_i$. Since these transfers are redistributed, the welfare function remains unchanged. Choosing

$$\tau_i = R_i - p_i - c_i \mathbb{E}[W_i(\lambda_1^*, \lambda_2^*)], \quad i = 1, 2,$$

supports (q_1^*, q_2^*) as a Nash equilibrium of the customer game at inventory (S_1, S_2) , implementing the planner's target effective arrival rates.

Implementing the full welfare optimum $(\lambda_1^*, \lambda_2^*, S_1^*, S_2^*)$ would additionally require inducing the producer to choose (S_1^*, S_2^*) ; the interdependence between inventory and customer joining behavior, combined with the discrete nature of inventory decisions, makes characterizing such a joint alignment scheme a nontrivial problem that we leave for future work.

7 Numerical Experiment: Waiting-Cost Asymmetry

This section examines system behavior when customer types differ in how much waiting they can tolerate. Examples of such asymmetry include business versus leisure travelers in transportation services, emergency versus elective patients in healthcare, and real-time versus batch processing workloads in computing resources. We compare the decentralized solution (profit-maximizing producer anticipating equilibrium behavior) with the centralized solution (welfare-maximizing planner), examining how profit, welfare, inventory decisions, and joining behavior vary across a range of asymmetry levels and potential utilization rates.

7.1 Measuring Asymmetry

A type- i customer joins when the expected wait satisfies $\mathbb{E}[W_i(\cdot)] \leq (R_i - p_i)/c_i$. Multiplying by the service rate μ gives a dimensionless quantity

$$\nu_i := \frac{\mu(R_i - p_i)}{c_i},$$

representing the maximum tolerable wait in units of mean service time $1/\mu$; larger ν_i means greater delay tolerance.

To isolate asymmetry between customer types, we track the ratio

$$\kappa := \frac{\nu_1}{\nu_2}.$$

Here $\kappa = 1$ means both types tolerate delay equally relative to their surplus; $\kappa > 1$ means type 2 is more delay-sensitive. In our symmetric setup ($R_1 = R_2, p_1 = p_2$), this simplifies to $\kappa = c_2/c_1$.

7.2 Experimental Setup

We normalize $\mu = 1$ and impose symmetry in all parameters except type-2 waiting cost: $R_1 = R_2 = 10, p_1 = p_2 = 5, h_1 = h_2 = 0.4$, and $c_1 = 3$ (Appendix E.2 reports results for an alternative configuration with $c_1 = 1$ and $h_1 = 0.05$).

We vary $\kappa \in [1, 20]$, from equal waiting tolerance ($\kappa = 1$) to type-2 tolerating only 1/20th as much waiting ($\kappa = 20$), implemented by setting $\nu_2 = \nu_1/\kappa$; under $(R_1, p_1) = (R_2, p_2)$ this simplifies to $c_2 = \kappa c_1$. The second axis is the potential utilization $\rho := (\Lambda_1 + \Lambda_2)/\mu \in [0.65, 0.90]$, with $\Lambda_1 = \Lambda_2 = \rho\mu/2$. Because customers may balk, realized utilization is typically below ρ (see Figure 10 in Appendix E.1).

For each (κ, ρ) we compute: (i) the *decentralized* Stackelberg outcome $(S_i^{\text{DEC}}, q_i^{\text{DEC}})$, where the producer maximizes profit anticipating Nash equilibrium joining rates; and (ii) the *centralized* outcome $(S_i^{\text{CEN}}, \lambda_i^{\text{CEN}})$, where a social planner maximizes welfare. For comparability we define $q_i^{\text{CEN}} := \lambda_i^{\text{CEN}}/\Lambda_i$ and refer to both q_i^{DEC} and q_i^{CEN} as joining rates.

Results are displayed as heatmaps over the (κ, ρ) plane, computed on a grid with step 0.01 in κ and 0.001 in ρ . Unless stated otherwise, holding costs are symmetric ($h_2/h_1 = 1$). Section 7.5 plots cross-sections at $\rho = 0.9$ for $h_2/h_1 \in \{0.9, 1.0, 1.1\}$, both to examine sensitivity to holding-cost asymmetry and to provide a clearer view of how outcomes vary with κ at fixed potential utilization.

7.3 Profit and Social Welfare

Figures 3 and 4 display the producer's profit under the decentralized solution (Π^{DEC}) and the social welfare under the centralized solution (SW^{CEN}) across the (κ, ρ) plane. Both metrics increase in ρ : although higher ρ implies greater potential congestion, it also means a larger pool of potential customers ($\Lambda_1 + \Lambda_2 = \rho\mu$), and this demand effect dominates.

In contrast, both metrics decrease in κ . As κ rises, type-2 customers tolerate less waiting, forcing the system to either hold more inventory (increasing costs) or accept lower type-2 participation (reducing revenue and rewards). Although both producer and planner adjust S_2 to partially compensate (see Section 7.4), this is insufficient to fully offset the decline.

The social welfare achieved under the decentralized solution, SW^{DEC} (Figure 11 in Appendix E.1), lies below SW^{CEN} throughout the parameter space. To quantify this welfare loss when all parties optimize individually rather than a planner coordinating for social welfare, we compute the ratio

$$\frac{\text{SW}^{\text{DEC}}(\kappa, \rho)}{\text{SW}^{\text{CEN}}(\kappa, \rho)} \in (0, 1].$$

Figure 5 reveals that this ratio does not vary monotonically in either parameter. Plateau near 0.92 appears in the upper-right region, where both solutions exclude type-2 entirely ($S_2 = 0, q_2 = 0$). Once type-2 is excluded, varying κ no longer affects the system; both solutions reduce to a single-type problem with $S_1^{\text{DEC}} = 1, S_1^{\text{CEN}} = 2$, and $q_1 = 1$.

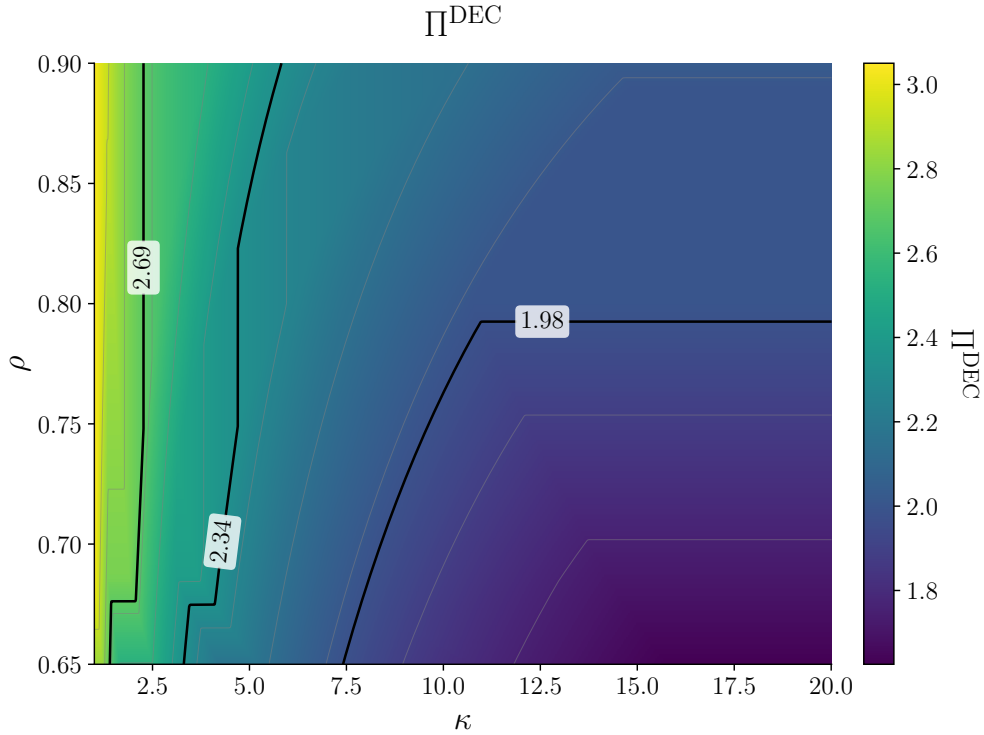


Figure 3: Producer's profit Π^{DEC} under decentralization over the (κ, ρ) plane. Thick black contours mark 1.98, 2.34, 2.69 (25%, 50%, 75% of range); thin gray contours provide detail.

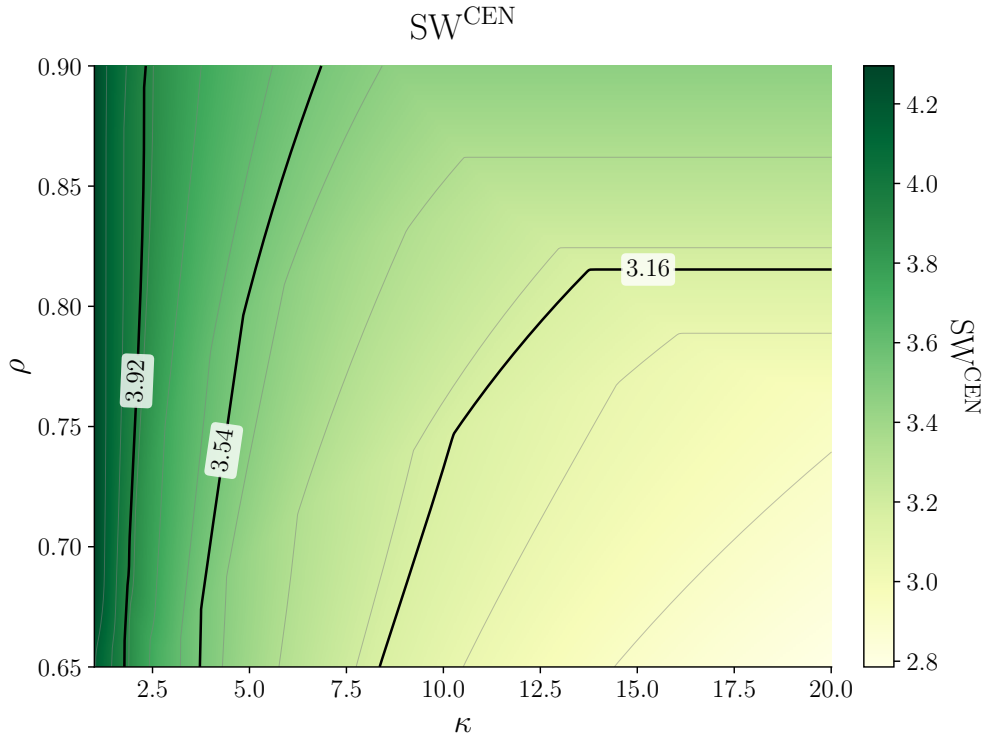


Figure 4: Social welfare SW^{CEN} under centralization over the (κ, ρ) plane. Thick black contours mark 3.16, 3.54, 3.92 (25%, 50%, 75% of range); thin gray contours provide detail.

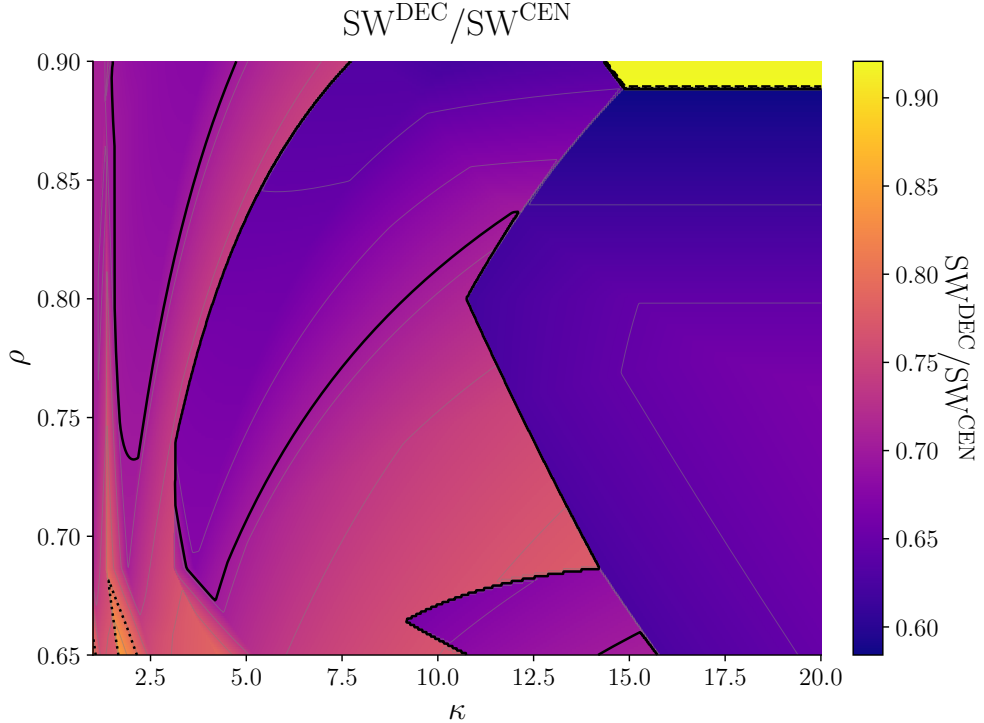


Figure 5: Ratio of decentralized to centralized welfare, SW^{DEC}/SW^{CEN} over the (κ, ρ) plane. Contours mark 0.70 (solid), 0.80 (dotted), and 0.90 (dashed); thin gray contours provide detail.

7.4 Target Inventories and Joining Behavior

Figure 6 shows type-2 target inventory levels and joining rates. Both the producer and the planner respond to rising κ by increasing S_2 , holding more inventory to reduce expected waiting. Eventually, however, holding cost outweighs the benefit and the system gives up on type-2: inventory drops to zero. This compensate-then-drop pattern is the dominant feature of the heatmaps, though the boundary where exclusion occurs differs between producer and planner. At low ρ , the decentralized solution exhibits exclusion within our κ range, while the centralized solution's exclusion threshold lies beyond $\kappa = 20$.

Type-1 joining rates stay close to 1 throughout most of the parameter space, with S_1 adjusting modestly (Figure 12 in Appendix E.1). However, high q_1 does not guarantee type-1 dominance. Figure 7 plots the type-1 share of total joining. The centralized solution always has type-1 at or above half, but the decentralized equilibrium exhibits a region at low κ where $q_1^{DEC} < q_2^{DEC}$ — the type with lower waiting cost participates less. This inversion disappears as κ grows.

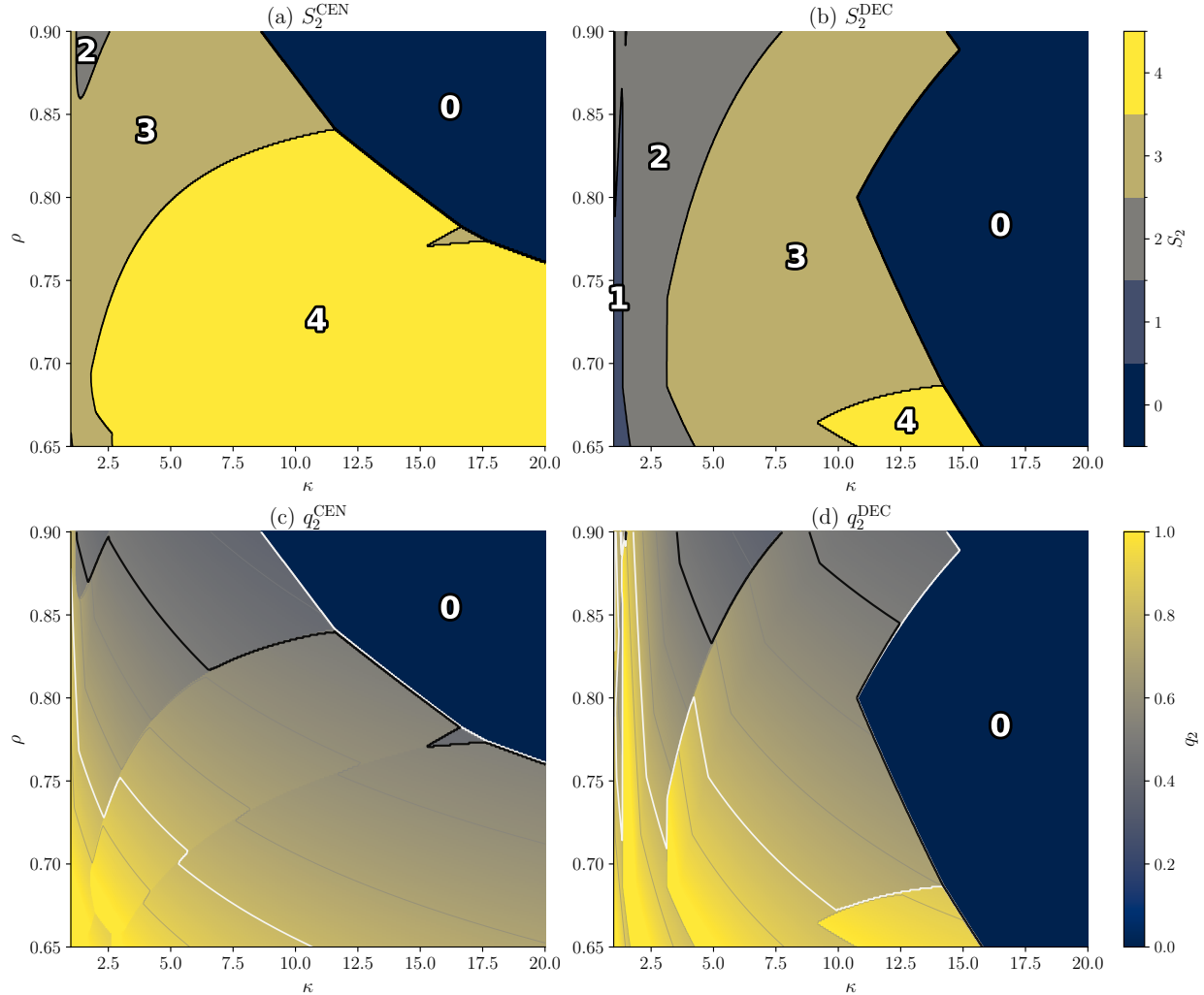


Figure 6: Type-2 decisions over the (κ, ρ) plane. Top row: inventory S_2 ; contours mark integer transitions. Bottom row: joining probability q_2 ; contours at 0.2, 0.8 (thick white) and 0.5 (thick black); thin gray contours provide detail.

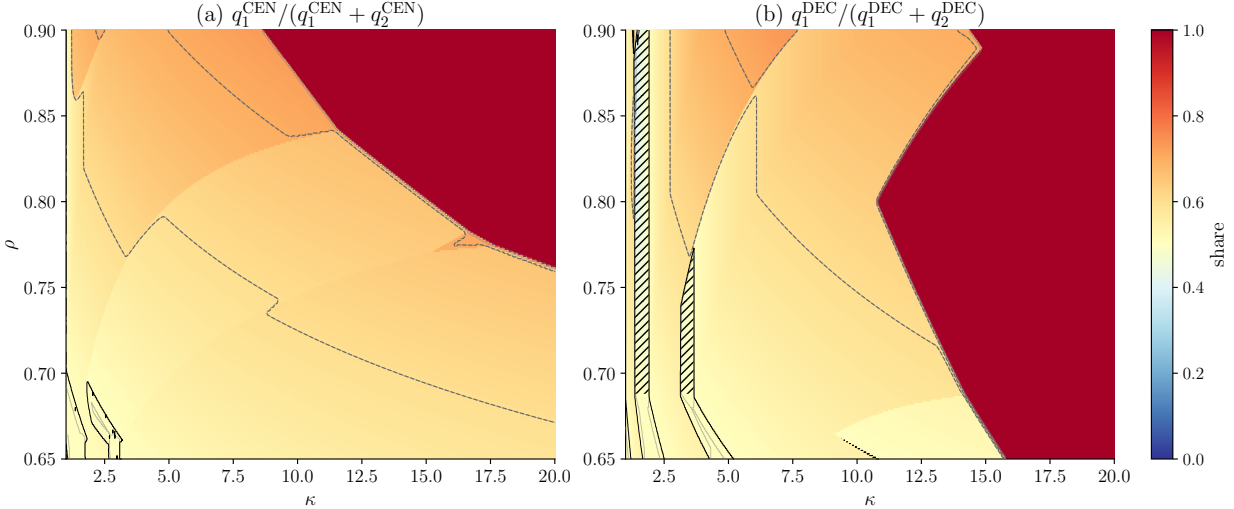


Figure 7: Type-1 share $q_1/(q_1 + q_2)$ over the (κ, ρ) plane. Contours at 0.5 (thin solid), 0.6 and 0.7 (dashed). Hatching indicates type-2 majority (share < 0.5).

7.5 Holding-Cost Sensitivity

The baseline experiment fixes symmetric holding costs ($h_2/h_1 = 1$). We now vary this ratio with h_1 fixed and h_2 varying. Higher h_2/h_1 makes type-2 inventory more expensive to hold, limiting the system’s ability to buffer type-2 waiting times as κ rises. Conversely, lower h_2/h_1 makes inventory a cheaper tool for accommodating high- c_2 customers, extending the range of κ over which type-2 remains viable. Figure 8 reports outcome metrics as functions of κ at $\rho = 0.9$; Figure 9 reports the associated type-2 decisions.

Changing h_2/h_1 primarily shifts the regime boundaries at which type-2 becomes unattractive to serve. Higher h_2/h_1 pushes the exclusion cutoff to lower κ ; lower h_2/h_1 expands the region where type-2 is served. The stepwise changes in S_2 produce corresponding kinks and jumps in joining rates and welfare, reflecting transitions between integer inventory regimes. The welfare ratio SW^{DEC}/SW^{CEN} is most sensitive to h_2/h_1 near these transitions, where producer and planner cutoffs diverge; away from the boundaries, both solutions react similarly and the ratio is comparatively stable.

Additional results — including effective utilization, expected waiting times, and component-wise comparisons between centralized and decentralized solutions — are reported in Appendix E.1.

7.6 Implications

Our numerical analysis yields several insights:

- When one customer type becomes more delay-sensitive, holding additional inventory for that type reduces expected waiting and sustains participation. However, holding costs eventually outweigh the benefit, making it optimal to stop serving the delay-sensitive type entirely. The transition is abrupt: small parameter changes near the boundary can shift the system from serving both types to serving only one.
- At low asymmetry, decentralized equilibria exhibit a counterintuitive pattern: the customer type with lower waiting cost participates less. This inversion arises because individual joining

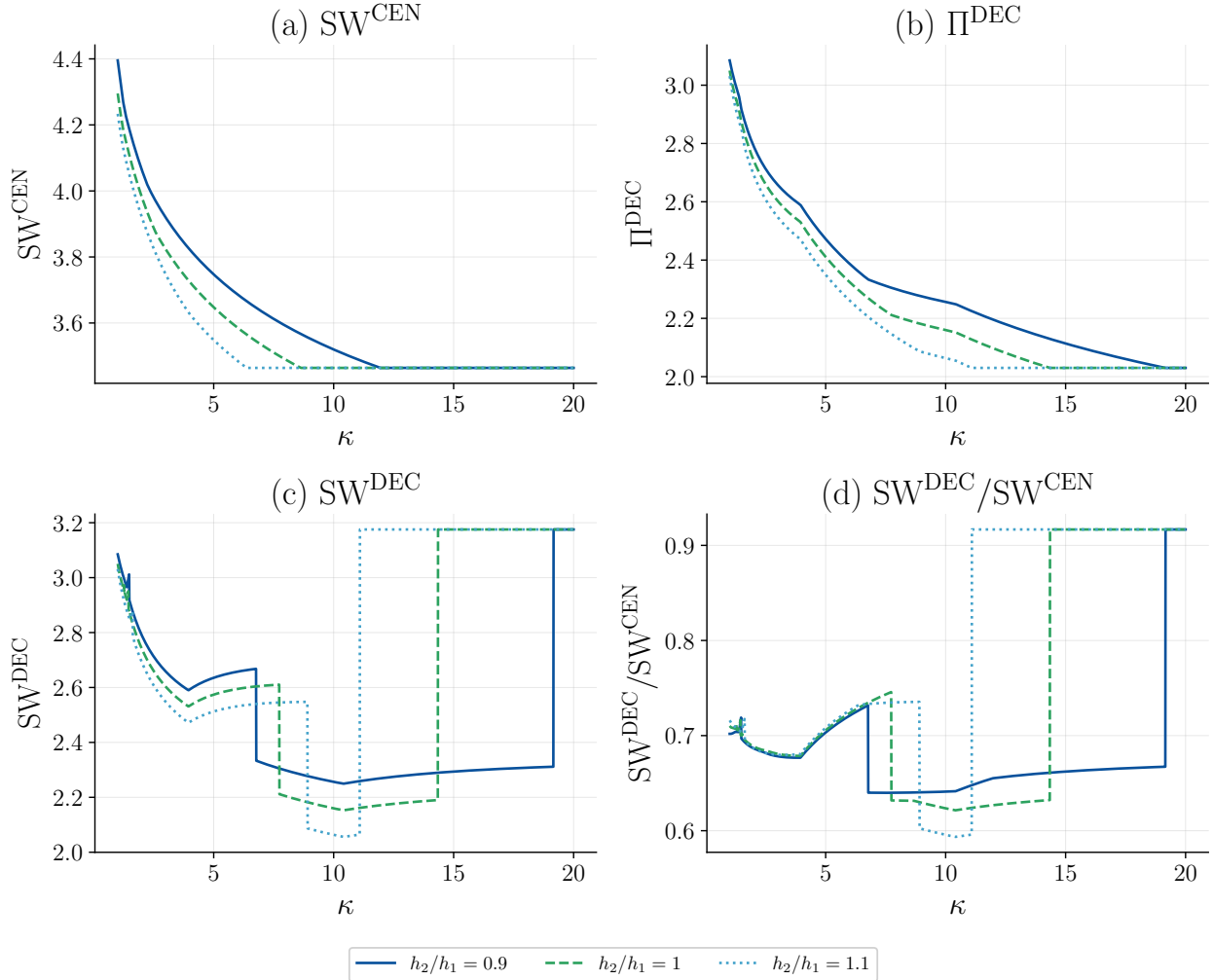


Figure 8: Cross-section at $\rho = 0.9$ as functions of κ for different h_2/h_1 ratios. Top row: SW^{CEN} (left) and Π^{DEC} (right). Bottom row: SW^{DEC} (left) and SW^{DEC}/SW^{CEN} (right).

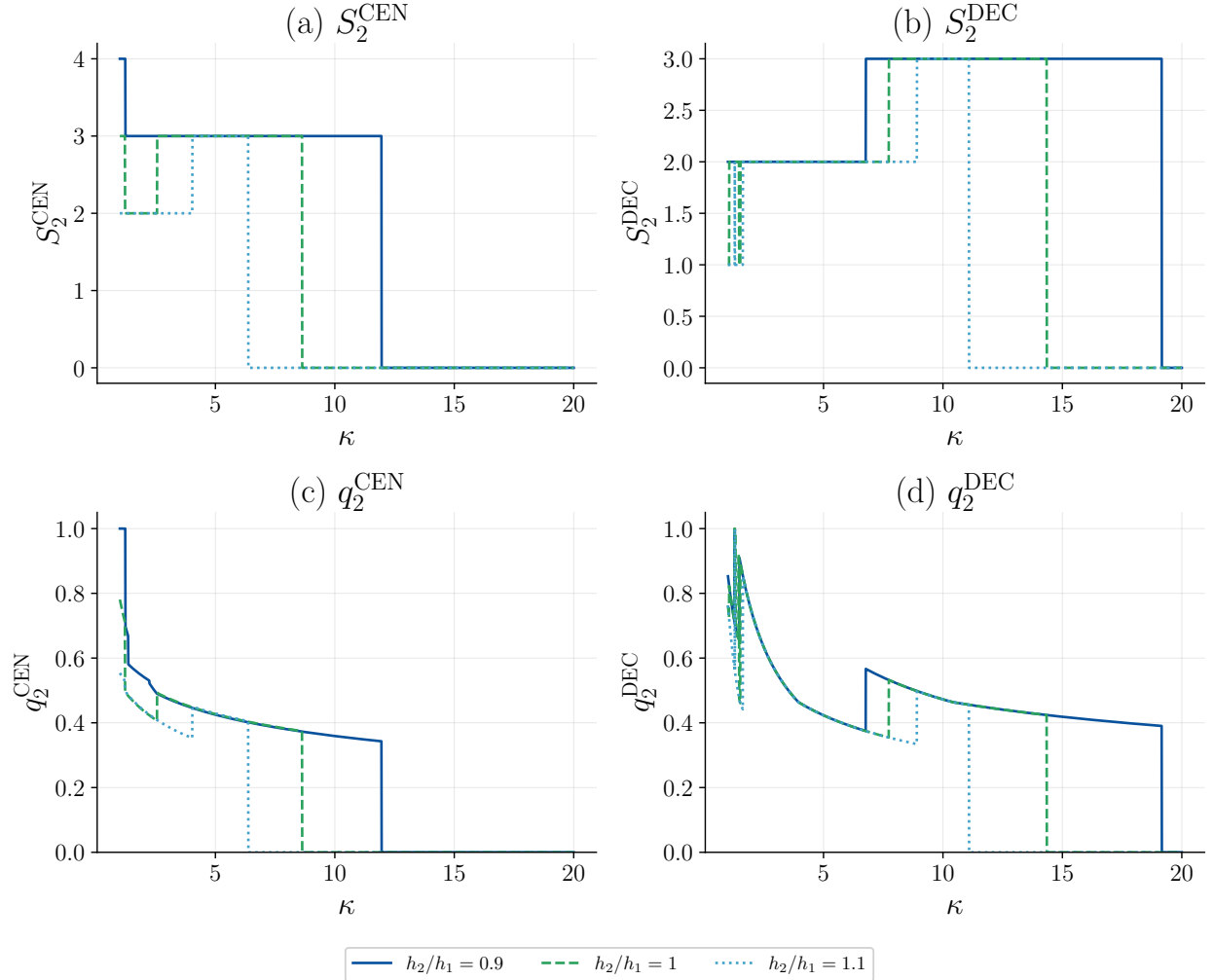


Figure 9: Cross-section at $\rho = 0.9$: type-2 decisions as functions of κ for different h_2/h_1 ratios. Top row: inventory S_2 . Bottom row: joining probability q_2 .

decisions do not account for system-wide effects. The phenomenon disappears as asymmetry grows.

- The parameter regions where a profit-maximizing firm stops serving the delay-sensitive type differ from those where a welfare-maximizing planner would do so. This disagreement about exclusion boundaries — rather than differences in inventory levels or joining rates — is the primary driver of welfare loss from decentralized decision-making.
- Because welfare loss concentrates where profit-maximizing and welfare-maximizing policies make different serve-or-exclude decisions, tolls or subsidies would be most effective when the system is near the margin of abandoning a customer type.

8 Conclusion

This paper analyzed strategic customer behavior in a two-product make-to-stock queueing system where products share production capacity. We established several key results:

First, we derived closed-form expressions for expected waiting times, inventory levels, and backlogs, showing how these measures respond to inventory levels and customer joining strategies. We then proved that Nash equilibria exist and are unique when at least one product has positive inventory, while a continuum of equilibria can arise in special zero-inventory cases.

For the producer, we demonstrated that profit-maximizing inventory levels have finite upper bounds, eliminating the need to search an unbounded parameter space. Similarly, the social planner's optimal inventory policy follows a clear structure based on the ratio of holding to waiting costs, even as effective arrival rates vary.

Our numerical experiments illustrated how inventory buffers waiting-cost asymmetry — up to a point — and how profit-maximizing and welfare-maximizing policies can disagree on when to exclude delay-sensitive customers.

The optimization methods described in this paper are implemented in Python and available at github.com/ksrvskj/make-to-stock-2product.

References

- [1] Vineet Abhishek, Ian Kash, and Peter Key. Fixed and market pricing for cloud services. (1): 157–162, 2012.
- [2] Hossein Abouee-Mehrizi, Ahmet Bora Balcioğlu, and Opher Baron. Strategies for a centralized single product multiclass $M/G/1$ make-to-stock queue. *Operations Research*, 60(4):803–812, 2012.
- [3] Kenneth J. Arrow, Theodore Harris, and Jacob Marschak. Optimal inventory policy. *Econometrica*, 19(3):250–272, 1951.
- [4] Baris Ata and Sergey Shneorson. Dynamic control of an $m/m/1$ service system with adjustable arrival and service rates. *Management Science*, 52(11):1778–1791, 2006.
- [5] Saif Benjaafar and Mounir ElHafsi. Production and inventory control of a single product assemble-to-order system with multiple customer classes. *Management Science*, 52(12):1896–1912, 2006.
- [6] Apostolos N. Burnetas and Alexandros Economou. Equilibrium customer strategies in a single-server Markovian queue with setup times. *Queueing Systems*, 56(3–4):213–228, 2007.
- [7] John A. Buzacott and J. George Shanthikumar. *Stochastic Models of Manufacturing Systems*. Prentice Hall, Englewood Cliffs, NJ, 1993.
- [8] Gerard P. Cachon and Robert Swinney. Purchasing, pricing, and quick response in the presence of strategic consumers. *Management Science*, 55(3):497–511, 2009.
- [9] Xiaolan Cai, Jian Li, Shenglin Chen, and Xiangtong Tang. Joint pricing and inventory control in a make-to-stock queue with delay-sensitive customers. *Journal of the Operational Research Society*, 72(8):1841–1856, 2020.
- [10] René Caldentey and Lawrence M. Wein. Revenue management of a make-to-stock queue. *Operations Research*, 54(5):859–875, October 2006.
- [11] Francis de Véricourt, Fikri Karaesmen, and Yves Dallery. Optimal stock allocation for a capacitated supply system. *Management Science*, 48(11):1486–1501, 2002.
- [12] Noel M. Edelson and David K. Hilderbrand. Congestion tolls for Poisson queuing processes. *Econometrica*, 43(1):81–92, 1975.
- [13] Awi Federgruen and Zvi Katalan. The stochastic economic lot scheduling problem: Cyclical base-stock policies with idle times. *Management Science*, 42(6):783–796, 1996.
- [14] Stephen C. Graves, A. H. G. Rinnooy Kan, and Paul H. Zipkin, editors. *Logistics of Production and Inventory*, volume 4 of *Handbooks in Operations Research and Management Science*. North-Holland, Amsterdam, 1993.
- [15] Albert Y. Ha. Inventory rationing in a make-to-stock production system with several demand classes and lost sales. *Management Science*, 43(8):1093–1103, 1997.
- [16] Ford W. Harris. How many parts to make at once. *Factory, The Magazine of Management*, 10(2):135–136, 1913.
- [17] Refael Hassin. On the optimality of first-come last-served queues. *Econometrica*, 53(1):201–202, 1985.

- [18] Refael Hassin. *Rational Queueing*. CRC Press, Boca Raton, FL, 2016.
- [19] Refael Hassin and Moshe Haviv. *To Queue or Not to Queue: Equilibrium Behavior in Queueing Systems*. Springer, Boston, 2003.
- [20] Refael Hassin and Ricky Roet-Green. The impact of inspection cost on equilibrium, revenue, and social welfare in a single-server queue. *Operations Research*, 65(3):804–820, 2017.
- [21] Samuel Karlin. Optimal policy for dynamic inventory process with stochastic demands subject to seasonal variations. *Journal of the Society for Industrial and Applied Mathematics*, 8(4):611–629, 1960.
- [22] Qiang Li, Peng Guo, C. L. Li, and J. Song. Equilibrium joining strategies and optimal control of a make-to-stock queue. *Production and Operations Management*, 25(9):1513–1527, 2016.
- [23] Fuhong Lin, Xianwei Zhou, Daochao Huang, Wei Song, and Dongsheng Han. Service scheduling in cloud computing based on queuing game model. *KSII Transactions on Internet and Information Systems*, 8(5):1554–1566, 2014.
- [24] Haim Mendelson. Pricing computer services: Queueing effects. *Communications of the ACM*, 28(3):312–321, 1985.
- [25] P. Naor. The regulation of queue size by levying tolls. *Econometrica*, 37(1):15–24, 1969.
- [26] Can Öz and Fikri Karaesmen. On a production/inventory system with strategic customers and unobservable inventory levels. In *SMMOS 2015: 10th Conference on Stochastic Models of Manufacturing and Service Operations*, pages 161–168, Volos, Greece, 2015. University of Thessaly Press.
- [27] Herbert Scarf. The optimality of (S, s) policies in the dynamic inventory problem. *Mathematical Methods in the Social Sciences*, pages 196–202, 1960.
- [28] Edward A. Silver, David F. Pyke, and Rein Peterson. *Inventory Management and Production Planning and Scheduling*. Wiley, New York, 3rd edition, 1998.
- [29] Michael H. Veatch and Lawrence M. Wein. Optimal control of a two-station tandem production/inventory system. *Operations Research*, 42(2):337–350, 1996.
- [30] Arthur F. Veinott. Optimal policy for a multi-product, dynamic, nonstationary inventory problem. *Management Science*, 12(3):206–222, 1965.
- [31] Yimin Wang and Chen Cai. Strategic behavior and optimal inventory level in a make-to-stock queueing system with retrial customers. *Axioms*, 12(5):319, 2023.
- [32] Amir G. Zare, Hossein Abouee-Mehrizi, and Oded Berman. Two-echelon production inventory systems with strategic customers. *Probability in the Engineering and Informational Sciences*, 35(2):258–275, 2021.
- [33] Xuelu Zhang and Jinting Wang. Optimal inventory threshold for a dynamic service make-to-stock system with strategic customers. *Applied Stochastic Models in Business and Industry*, 35:1103–1123, May 2019.
- [34] Ning Zhao and Zhe Lian. A queueing-inventory system with two classes of customers. *International Journal of Production Economics*, 129(1):225–231, 2011.
- [35] Paul Zipkin. *Foundations of Inventory Management*. McGraw-Hill, New York, 2000.

Appendix A System Performance Proofs

A.1 Queue Position Distribution

Proof of (3.4). Without loss of generality, we consider the case where $i = 1$; the argument for $i = 2$ follows analogously by symmetry.

When a newly arriving type-1 customer finds product 1 out of stock, the system ensures there are exactly S_1 type-1 jobs in the production queue designated for replenishment. If a customer joins, they become the newest type-1 backorder. Their unit is supplied by the completion of the oldest replenishment type-1 job currently in the queue (after any earlier backorders). The join decision also triggers a new type-1 job appended at the tail, which becomes the newest replenishment job to maintain the inventory position at S_1 .

The existing jobs in queue came from independent Poisson arrival streams with rates λ_1 and λ_2 . Each of the current $N(t) = n$ jobs in queue is type-1 with probability $\lambda_1/(\lambda_1 + \lambda_2)$ or type-2 with probability $\lambda_2/(\lambda_1 + \lambda_2)$, subject to the condition that at least S_1 are type-1. This is the binomial thinning property. Without additional constraints, the probability of exactly k type-1 jobs among m is

$$\binom{m}{k} \left(\frac{\lambda_1}{\lambda_1 + \lambda_2} \right)^k \left(\frac{\lambda_2}{\lambda_1 + \lambda_2} \right)^{m-k}.$$

Once $N(t) = n$ is given, suppose $N_1^a(t) = n^a$ and $N_1^b(t) = n^b$, so $n^a + n^b = n$. Because the system is out of stock for product 1 and a potential customer is considering this position in queue, there must be exactly S_1 type-1 replenishment jobs in total. The last job in the n^a group must be the first of these replenishment jobs, and exactly $S_1 - 1$ type-1 replenishment jobs must be among the n^b jobs that would be behind the potential customer's position.

Hence, the conditional probability of $\{N_1^a = n^a, N_1^b = n^b\}$, given that $N(t) = n$, involves choosing $(S_1 - 1)$ among (n^b) positions to be type 1. This selection yields a binomial coefficient $\binom{n^b}{S_1 - 1}$, multiplied by the usual powers of $\frac{\lambda_1}{\lambda_1 + \lambda_2}$ and $\frac{\lambda_2}{\lambda_1 + \lambda_2}$ for type-1 vs. type-2 classification:

$$\mathbb{P}\left\{N_1^a = n^a, N_1^b = n^b \mid N = n\right\} = \binom{n^b}{S_1 - 1} \left(\frac{\lambda_1}{\lambda_1 + \lambda_2} \right)^{S_1} \left(\frac{\lambda_2}{\lambda_1 + \lambda_2} \right)^{n^b - S_1 + 1}$$

if $n^a + n^b = n$ and zero otherwise.

Combining **(i)** the M/M/1 stationary distribution of $N(t)$ (see (3.1)), **(ii)** the binomial-thinning argument, and **(iii)** the backlog-replacement constraint yields the unconditional joint distribution of $(N_1^a(t), N_1^b(t))$:

$$\mathbb{P}\{N_1^a = n^a, N_1^b = n^b\} = \binom{n^b}{S_1 - 1} \frac{(\lambda_1 + \lambda_2)^{n^a - 1} \lambda_1^{S_1} \lambda_2^{n^b - S_1 + 1} (\mu - \lambda_1 - \lambda_2)}{\mu^{n^a + n^b + 1}},$$

valid for $n^a \geq 1$ and $n^b \geq S_1 - 1$, and zero otherwise. Intuitively, the total queue length is $n^a + n^b$, with n^a tasks up to (and including) the target job, and n^b jobs strictly behind. Among those n^b trailing jobs, $S_1 - 1$ are forced to be type 1 tasks, and the rest type 2. \square

A.2 Waiting Time Derivation

Proof of Proposition 3.1. Step 1: Expressing $\mathbb{E}[N_1^a]$. From Section 3.1.2, the joint distribution of (N_1^a, N_1^b) for a type-1 backlog arrival is

$$\mathbb{P}\{N_1^a = n^a, N_1^b = n^b\} = \binom{n^b}{S_1 - 1} \frac{(\lambda_1 + \lambda_2)^{n^a-1} \lambda_1^{S_1} \lambda_2^{n^b-S_1+1} (\mu - \lambda_1 - \lambda_2)}{\mu^{n^a+n^b+1}},$$

valid for $n^a \geq 1$ and $n^b \geq S_1 - 1$, and zero otherwise. Hence,

$$\mathbb{E}[N_1^a] = \sum_{n^b=S_1-1}^{\infty} \sum_{n^a=1}^{\infty} n^a \mathbb{P}\{N_1^a = n^a, N_1^b = n^b\}.$$

Substitute the expression for $\mathbb{P}\{N_1^a = n^a, N_1^b = n^b\}$ and group factors accordingly.

Step 2: Separating the Double Sum. Note that

$$\mathbb{E}[N_1^a] = (\mu - \lambda_1 - \lambda_2) \lambda_1^{S_1} \left[\sum_{n^a=1}^{\infty} n^a \frac{(\lambda_1 + \lambda_2)^{n^a-1}}{\mu^{n^a}} \right] \left[\sum_{n^b=S_1-1}^{\infty} \binom{n^b}{S_1 - 1} \frac{\lambda_2^{n^b-(S_1-1)}}{\mu^{n^b+1}} \right].$$

This follows by rewriting $\mu^{-(n^a+n^b+1)}$ as $\mu^{-n^a} \mu^{-n^b-1}$ and factoring out terms that do not depend on n^a or n^b .

Step 3: Summation Over n^a . The sum over n^a is

$$\sum_{n^a=1}^{\infty} n^a \frac{(\lambda_1 + \lambda_2)^{n^a-1}}{\mu^{n^a}} = \frac{1}{\mu} \sum_{n^a=1}^{\infty} n^a \left(\frac{\lambda_1 + \lambda_2}{\mu} \right)^{n^a-1} = \frac{1}{\mu} \cdot \frac{1}{\left(1 - \frac{\lambda_1 + \lambda_2}{\mu} \right)^2} = \frac{\mu}{(\mu - \lambda_1 - \lambda_2)^2}.$$

(The identity $\sum_{k=1}^{\infty} kx^k = \frac{x}{(1-x)^2}$ for $|x| < 1$ applies.)

Step 4: Summation Over n^b . Let $k = n^b - (S_1 - 1)$. Then k runs from 0 to ∞ , and

$$\sum_{n^b=S_1-1}^{\infty} \binom{n^b}{S_1 - 1} \frac{\lambda_2^{n^b-(S_1-1)}}{\mu^{n^b+1}} = \frac{1}{\mu^{S_1}} \sum_{k=0}^{\infty} \binom{k + S_1 - 1}{S_1 - 1} \left(\frac{\lambda_2}{\mu} \right)^k.$$

By the binomial identity $\sum_{k=0}^{\infty} \binom{k+n}{n} x^k = \frac{1}{(1-x)^{n+1}}$ (for $|x| < 1$), one obtains

$$\frac{1}{\mu^{S_1}} \left(\frac{\mu}{\mu - \lambda_2} \right)^{S_1} = \left(\frac{1}{\mu - \lambda_2} \right)^{S_1}.$$

Step 5: Final Computation. Combining the two sums gives

$$\mathbb{E}[N_1^a] = (\mu - \lambda_1 - \lambda_2) \lambda_1^{S_1} \frac{\mu}{(\mu - \lambda_1 - \lambda_2)^2} \left(\frac{1}{\mu - \lambda_2} \right)^{S_1}.$$

After simplifying,

$$\mathbb{E}[N_1^a] = \frac{\mu \lambda_1^{S_1}}{(\mu - \lambda_2)^{S_1} (\mu - \lambda_1 - \lambda_2)}.$$

Since $\mathbb{E}[W_1(\lambda_1, \lambda_2)] = \frac{1}{\mu} \mathbb{E}[N_1^a]$, the result in (3.5) follows immediately.

Symmetry for Product 2. An entirely similar argument applies when a newly arriving type-2 customer finds product 2 out of stock, enforcing exactly S_2 replenishment jobs for product 2. Interchanging the roles of λ_1 , λ_2 , and S_1 , S_2 yields

$$\mathbb{E}[W_2(\lambda_1, \lambda_2)] = \frac{\lambda_2^{S_2}}{(\mu - \lambda_1)^{S_2} (\mu - \lambda_1 - \lambda_2)}. \quad (\text{A.1})$$

□

Appendix B Strategic Behavior Proofs

B.1 Utility and Monotonicity Properties

Proof of Lemma 4.1. Continuity follows because U_1 is a composition of continuous functions on a compact domain. Monotonicity is shown by examining partial derivatives under the two scenarios $S_1 = 0$ and $S_1 > 0$:

Scenario $S_1 = 0$. In this scenario, the utility simplifies to:

$$U_1(q_1, q_2) = R_1 - p_1 - c_1 \cdot \frac{1}{\mu - q_1 \Lambda_1 - q_2 \Lambda_2}.$$

Its derivative with respect to q_1 is:

$$\frac{\partial U_1}{\partial q_1} = -\frac{c_1 \Lambda_1}{(\mu - q_1 \Lambda_1 - q_2 \Lambda_2)^2} < 0,$$

and similarly,

$$\frac{\partial U_1}{\partial q_2} = -\frac{c_1 \Lambda_2}{(\mu - q_1 \Lambda_1 - q_2 \Lambda_2)^2} < 0.$$

Scenario $S_1 > 0$. Here, we have:

$$U_1(q_1, q_2) = R_1 - p_1 - c_1 \cdot \frac{(q_1 \Lambda_1)^{S_1}}{(\mu - q_2 \Lambda_2)^{S_1} (\mu - q_1 \Lambda_1 - q_2 \Lambda_2)}.$$

A direct calculation shows:

$$\frac{\partial U_1}{\partial q_1} = -\frac{c_1 (q_1 \Lambda_1)^{S_1} [S_1(\mu - q_1 \Lambda_1 - q_2 \Lambda_2) + q_1 \Lambda_1]}{q_1 (\mu - q_1 \Lambda_1 - q_2 \Lambda_2)^2 (\mu - q_2 \Lambda_2)^{S_1}} < 0,$$

and

$$\frac{\partial U_1}{\partial q_2} = -\frac{c_1 \Lambda_2 (q_1 \Lambda_1)^{S_1} [S_1(\mu - q_1 \Lambda_1 - q_2 \Lambda_2) + q_2 \Lambda_2]}{(\mu - q_1 \Lambda_1 - q_2 \Lambda_2)^2 (\mu - q_2 \Lambda_2)^{S_1}} < 0.$$

Thus, $U_1(q_1, q_2)$ is strictly decreasing in both q_1 and q_2 . □

B.2 Unique Fixed Points

Proof of Lemma 4.2. Fix any $q_2 \in [0, 1]$. By Lemma 4.1, the utility function $U_1(q_1, q_2)$ is strictly decreasing in q_1 for every fixed q_2 . This property ensures that the mapping $q_1 \mapsto \text{BR}_1(q_1, q_2)$ has a unique fixed point, as detailed below.

1. If $U_1(0, q_2) \leq 0$, then for every $q_1 \in [0, 1]$ the inequality

$$U_1(q_1, q_2) \leq U_1(0, q_2) \leq 0$$

holds. Consequently, the best response is always $\{0\}$; that is, $\text{BR}_1(q_1, q_2) = \{0\}$ for all q_1 . In this situation, the fixed point is $q_1 = 0$ if and only if $U_1(0, q_2) \leq 0$.

2. If $U_1(1, q_2) \geq 0$, then for every $q_1 \in [0, 1]$ one has

$$U_1(q_1, q_2) \geq U_1(1, q_2) \geq 0.$$

Therefore, the best response is always $\{1\}$ (i.e., $\text{BR}_1(q_1, q_2) = \{1\}$ for all q_1), and the unique fixed point is $q_1 = 1$ if and only if $U_1(1, q_2) \geq 0$.

3. Otherwise, suppose that

$$U_1(0, q_2) > 0 \quad \text{and} \quad U_1(1, q_2) < 0.$$

Then, by continuity and strict monotonicity of $U_1(q_1, q_2)$, the Intermediate Value Theorem guarantees the existence of a unique $q_1^* \in (0, 1)$ such that

$$U_1(q_1^*, q_2) = 0.$$

For $q_1 < q_1^*$, the strict decrease implies $U_1(q_1, q_2) > 0$ so that $\text{BR}_1(q_1, q_2) = \{1\}$; for $q_1 > q_1^*$, one obtains $U_1(q_1, q_2) < 0$ and hence $\text{BR}_1(q_1, q_2) = \{0\}$. At $q_1 = q_1^*$, since $U_1(q_1^*, q_2) = 0$, it holds that $\text{BR}_1(q_1^*, q_2) = [0, 1]$. Thus the only self-consistent fixed point in $[0, 1]$ is q_1^* , which is the unique solution of $U_1(q_1, q_2) = 0$.

A symmetric argument applies for type 2 by fixing q_1 . □

B.3 Detailed Classification of Nash Equilibria

Proof of Proposition 4.1. Step 1: Possible Coordinates via Lemma 4.2. Applying Lemma 4.2 to each type shows that, for any $q_2 \in [0, 1]$, $\text{BR}_1(q_1, q_2)$ has exactly one fixed point in q_1 . This unique fixed point is either 0, 1, or the fraction in $(0, 1)$ where $U_1(q_1^*, q_2) = 0$. Similarly for q_2 at any fixed q_1 . Hence each q_i must lie in $\{0\} \cup (0, 1) \cup \{1\}$. Combining both coordinates yields the 9 cases of Table 1.

Step 2: Verifying Each Cell's Inequalities.

Corner Cells: - **(0, 0)**. Equilibrium if and only if $(0, 0) = (\text{BR}_1(0, 0), \text{BR}_2(0, 0))$, which happens precisely when

$$U_1(0, 0) \leq 0 \quad \text{and} \quad U_2(0, 0) \leq 0.$$

All type-1 and type-2 customers balk.

- **(0, 1)**. Equilibrium if and only if $(0, 1) = (\text{BR}_1(0, 1), \text{BR}_2(0, 1))$, which happens exactly when

$$U_1(0, 1) \leq 0 \quad \text{and} \quad U_2(0, 1) \geq 0.$$

Type-1 balks, type-2 joins.

- **(1, 0)**. Equilibrium if and only if $(1, 0) = (\text{BR}_1(1, 0), \text{BR}_2(1, 0))$, which happens if and only if

$$U_1(1, 0) \geq 0 \quad \text{and} \quad U_2(1, 0) \leq 0.$$

Type-1 joins, type-2 balks.

- **(1, 1)**. Equilibrium if and only if $(1, 1) = (\text{BR}_1(1, 1), \text{BR}_2(1, 1))$, which occurs precisely when

$$U_1(1, 1) \geq 0 \quad \text{and} \quad U_2(1, 1) \geq 0.$$

Both types join.

Partial-Corner Cases: - **(0, q_2^*)** with $q_2^* \in (0, 1)$. Equilibrium if and only if

$$(0, q_2^*) = (\text{BR}_1(0, q_2^*), \text{BR}_2(0, q_2^*)) ,$$

which requires

$$U_1(0, q_2^*) \leq 0, \quad U_2(0, 0) > 0, U_2(0, 1) < 0, U_2(0, q_2^*) = 0.$$

Strict monotonicity ensures that if $U_2(0, q_2^*) = 0$ has a unique solution $q_2^* \in (0, 1)$, the inequalities $U_2(0, 0) > 0$ and $U_2(0, 1) < 0$ automatically hold. Hence they do not appear explicitly in Table 1. Similar inequalities are likewise omitted in other cells of the table where a unique interior solution exists - the strict monotonicity of the utility functions ensures that the appropriate boundary conditions are satisfied whenever there is a solution in $(0, 1)$.

Type-1 balks, type-2 mixes in $(0, 1)$.

- **(q_1^* , 0)** with $q_1^* \in (0, 1)$. Equilibrium if and only if

$$(q_1^*, 0) = (\text{BR}_1(q_1^*, 0), \text{BR}_2(q_1^*, 0)) ,$$

which is equivalent to

$$U_1(0, 0) > 0, \quad U_1(1, 0) < 0, \quad U_1(q_1^*, 0) = 0, \quad U_2(q_1^*, 0) \leq 0.$$

Type-1 is partial in $(0, 1)$, type-2 balks.

- **(q_1^* , 1)** with $q_1^* \in (0, 1)$. Equilibrium if and only if

$$(q_1^*, 1) = (\text{BR}_1(q_1^*, 1), \text{BR}_2(q_1^*, 1)) ,$$

which necessitates

$$U_1(0, 1) > 0, \quad U_1(1, 1) < 0, \quad U_1(q_1^*, 1) = 0, \quad U_2(q_1^*, 1) \geq 0.$$

Type-1 is partial, type-2 joins.

- **(1, q_2^*)** with $q_2^* \in (0, 1)$. Equilibrium if and only if

$$(1, q_2^*) = (\text{BR}_1(1, q_2^*), \text{BR}_2(1, q_2^*)) ,$$

which implies

$$U_1(1, q_2^*) \geq 0, \quad U_2(1, 0) > 0, U_2(1, 1) < 0, U_2(1, q_2^*) = 0.$$

Type-1 joins, type-2 is partial in $(0, 1)$.

Interior Case: - (q_1^*, q_2^*) with $q_1^*, q_2^* \in (0, 1)$. Equilibrium if and only if

$$(q_1^*, q_2^*) = (\text{BR}_1(q_1^*, q_2^*), \text{BR}_2(q_1^*, q_2^*)) ,$$

which holds precisely when

$$\begin{aligned} U_1(0, q_2^*) &> 0, & U_1(1, q_2^*) &< 0, & U_1(q_1^*, q_2^*) &= 0, \\ U_2(q_1^*, 0) &> 0, & U_2(q_1^*, 1) &< 0, & U_2(q_1^*, q_2^*) &= 0. \end{aligned}$$

Both types are partial (interior) joiners.

Conclusion: These nine cases completely characterize the possible Nash equilibria, with each equilibrium lying in exactly one of the cells of Table 1. □

B.4 Complete Nash Equilibrium Existence Proof

Proof of Proposition 4.2. The proof uses Brouwer's Fixed Point Theorem, which states that any continuous function mapping a compact, convex set into itself has a fixed point. Although BR_1 and BR_2 are set-valued correspondences, a continuous single-valued function can be constructed from them via Lemma 4.2.

Step 1: Constructing a Continuous Function from the Best-Response Correspondences.

For each fixed $q_2 \in [0, 1]$, Lemma 4.2 guarantees a unique fixed point in q_1 for $\text{BR}_1(q_1, q_2)$. Denote this point by $f_1(q_2)$. Likewise, for each fixed q_1 , let $f_2(q_1)$ be the unique fixed point in q_2 for $\text{BR}_2(q_1, q_2)$. Define

$$f : [0, 1]^2 \rightarrow [0, 1]^2 \quad \text{by} \quad f(q_1, q_2) = (f_1(q_2), f_2(q_1)) .$$

Step 2: Continuity of f_1 and f_2 .

Focus on f_1 . Fix a point q_2^0 in $[0, 1]$, and let $\{q_2^n\}$ be a sequence converging to q_2^0 . By Lemma 4.2, each $f_1(q_2^n)$ is determined by one of the following:

1. $f_1(q_2^n) = 0$ if $U_1(0, q_2^n) \leq 0$,
2. $f_1(q_2^n) = 1$ if $U_1(1, q_2^n) \geq 0$,
3. $f_1(q_2^n) = q_1^n \in (0, 1)$ if $U_1(q_1^n, q_2^n) = 0$ otherwise.

Consider any convergent subsequence $\{f_1(q_2^{n_k})\} \rightarrow y$. By the continuity of U_1 (Lemma 4.1), the limit y must satisfy the same case at q_2^0 , i.e. $f_1(q_2^0) = y$. Since every convergent subsequence converges to $f_1(q_2^0)$, it follows that $f_1(q_2^n) \rightarrow f_1(q_2^0)$. Thus f_1 is continuous. By symmetry, f_2 is also continuous.

Step 3: Applying Brouwer's Fixed Point Theorem.

Because f is a continuous map from the compact, convex set $[0, 1]^2$ to itself, Brouwer's theorem guarantees a fixed point (q_1^*, q_2^*) such that

$$f(q_1^*, q_2^*) = (q_1^*, q_2^*) .$$

Step 4: Showing the Fixed Point is a Nash Equilibrium.

At this fixed point, $q_1^* = f_1(q_2^*)$ and $q_2^* = f_2(q_1^*)$. By construction of f_1 and f_2 , it follows that $q_1^* \in \text{BR}_1(q_1^*, q_2^*)$ and $q_2^* \in \text{BR}_2(q_1^*, q_2^*)$. Hence (q_1^*, q_2^*) is indeed a Nash equilibrium. □

B.5 Analysis for Zero Inventory Scenario

Proof of Proposition 4.3. Step 1: Detailed Classification of Equilibrium Cases.

When $S_1 = 0$ and $S_2 = 0$, the utility functions reduce to:

$$U_1(q_1, q_2) = R_1 - p_1 - c_1 \frac{1}{\mu - q_1 \Lambda_1 - q_2 \Lambda_2}, \quad U_2(q_1, q_2) = R_2 - p_2 - c_2 \frac{1}{\mu - q_1 \Lambda_1 - q_2 \Lambda_2}.$$

In this simplified setting, they allow explicit solutions for one type's joining probability if the other type's probability is fixed. Consequently, the general equilibrium conditions from Table 1 break down into the specific cases shown in Table 3.

Table 3: Equilibrium Outcomes for $S_1 = 0, S_2 = 0$

$(0,0):$ $\mu \leq \frac{c_1}{R_1 - p_1}$ $\mu \leq \frac{c_2}{R_2 - p_2}$	$(0, q_2^*):$ $q_2^* = \frac{1}{\Lambda_2} (\mu - \frac{c_2}{R_2 - p_2})$: $\mu > \frac{c_2}{R_2 - p_2}$ $\mu < \frac{c_2}{R_2 - p_2} + \Lambda_2$ $\frac{c_1}{R_1 - p_1} \geq \frac{c_2}{R_2 - p_2}$	$(0,1):$ $\mu \geq \frac{c_2}{R_2 - p_2} + \Lambda_2$ $\mu \leq \frac{c_1}{R_1 - p_1} + \Lambda_2$
$(q_1^*, 0),$ $q_1^* = \frac{1}{\Lambda_1} (\mu - \frac{c_1}{R_1 - p_1})$: $\mu > \frac{c_1}{R_1 - p_1}$ $\mu < \frac{c_1}{R_1 - p_1} + \Lambda_1$ $\frac{c_1}{R_1 - p_1} \leq \frac{c_2}{R_2 - p_2}$	$(q_1^*, q_2^*),$ $q_1^* \Lambda_1 + q_2^* \Lambda_2 = \mu - \frac{c_1}{R_1 - p_1},$ $0 < q_1^*, q_2^* < 1:$ $\mu > \frac{c_1}{R_1 - p_1}$ $\mu < \frac{c_1}{R_1 - p_1} + \Lambda_1 + \Lambda_2$ $\frac{c_1}{R_1 - p_1} = \frac{c_2}{R_2 - p_2}$	$(q_1^*, 1),$ $q_1^* = \frac{1}{\Lambda_1} (\mu - \Lambda_2 - \frac{c_1}{R_1 - p_1})$: $\mu > \frac{c_1}{R_1 - p_1} + \Lambda_2$ $\mu < \frac{c_1}{R_1 - p_1} + \Lambda_1 + \Lambda_2$ $\frac{c_1}{R_1 - p_1} \geq \frac{c_2}{R_2 - p_2}$
$(1,0):$ $\mu \geq \frac{c_1}{R_1 - p_1} + \Lambda_1$ $\mu \leq \frac{c_2}{R_2 - p_2} + \Lambda_1$	$(1, q_2^*),$ $q_2^* = \frac{1}{\Lambda_2} (\mu - \Lambda_1 - \frac{c_2}{R_2 - p_2})$: $\mu > \frac{c_2}{R_2 - p_2} + \Lambda_1$ $\mu < \frac{c_2}{R_2 - p_2} + \Lambda_1 + \Lambda_2$ $\frac{c_1}{R_1 - p_1} \leq \frac{c_2}{R_2 - p_2}$	$(1,1):$ $\mu \geq \frac{c_1}{R_1 - p_1} + \Lambda_1 + \Lambda_2$ $\mu \geq \frac{c_2}{R_2 - p_2} + \Lambda_1 + \Lambda_2$

To clarify how the cells in Table 3 arise, consider the following points.

- An interior equilibrium $(q_1^*, q_2^*) \in (0, 1)^2$ must satisfy

$$U_1(q_1^*, q_2^*) = 0 \quad \text{and} \quad U_2(q_1^*, q_2^*) = 0.$$

Subtracting these two equations implies

$$\frac{c_1}{R_1 - p_1} = \frac{c_2}{R_2 - p_2}.$$

Under this condition, substituting back into $U_1 = 0$ (or $U_2 = 0$) yields a line:

$$q_1^* \Lambda_1 + q_2^* \Lambda_2 = \mu - \frac{c_1}{R_1 - p_1}.$$

To ensure at least one point of this line lies in $(0, 1)^2$, it must satisfy:

$$q_2^*(0) > 0 \quad \text{and} \quad q_2^*(1) < 1.$$

Plugging in $q_1^* = 0$ and $q_1^* = 1$ gives:

$$\frac{1}{\Lambda_2} \left(\mu - \frac{c_1}{R_1 - p_1} \right) > 0, \quad \frac{1}{\Lambda_2} \left(\mu - \frac{c_1}{R_1 - p_1} - \Lambda_1 \right) < 1,$$

which is equivalent to

$$\frac{c_1}{R_1 - p_1} < \mu < \frac{c_1}{R_1 - p_1} + \Lambda_1 + \Lambda_2.$$

- To see how other cells arise, consider $(q_1^*, 1)$. For it to be an equilibrium,

$$U_1(q_1^*, 1) = 0 \quad \text{and} \quad U_2(q_1^*, 1) \geq 0,$$

which translates into

$$R_1 - p_1 - c_1 \frac{1}{\mu - q_1^* \Lambda_1 - \Lambda_2} = 0 \quad \text{and} \quad R_2 - p_2 - c_2 \frac{1}{\mu - q_1^* \Lambda_1 - \Lambda_2} \geq 0.$$

Hence,

$$q_1^* = \frac{1}{\Lambda_1} \left(\mu - \Lambda_2 - \frac{c_1}{R_1 - p_1} \right) \quad \text{and} \quad \frac{c_1}{R_1 - p_1} \geq \frac{c_2}{R_2 - p_2}.$$

Since q_1^* must lie in $(0, 1)$,

$$\frac{c_1}{R_1 - p_1} + \Lambda_2 < \mu < \frac{c_1}{R_1 - p_1} + \Lambda_1 + \Lambda_2.$$

- Similar computations under other assumptions on (q_1^*, q_2^*) yield the remaining cells in Table 3.

Step 2: Equilibrium Coexistence Analysis. Equilibria may or may not coexist, depending on how $\frac{c_1}{R_1 - p_1}$ compares to $\frac{c_2}{R_2 - p_2}$. Three cases arise:

$$(1) \frac{c_1}{R_1 - p_1} > \frac{c_2}{R_2 - p_2}, \quad (2) \frac{c_1}{R_1 - p_1} < \frac{c_2}{R_2 - p_2}, \quad \text{or} \quad (3) \frac{c_1}{R_1 - p_1} = \frac{c_2}{R_2 - p_2}.$$

Cases (1) and (2) are symmetric by exchanging the roles of products 1 and 2, so the details below focus on (1) and (3).

Case 1: $\frac{c_1}{R_1 - p_1} > \frac{c_2}{R_2 - p_2}$. Because the conditions in other cells conflict with this inequality, only $(0, 0)$, $(0, q_2^*)$, $(0, 1)$, $(q_1^*, 1)$, and $(1, 1)$ remain feasible. Intuitively, type-1 has a higher cost ratio and is therefore less inclined to join, so $q_1^* \leq q_2^*$. In this setting:

- $(0, 0)$ requires $\mu \leq \frac{c_1}{R_1 - p_1}$ and $\mu \leq \frac{c_2}{R_2 - p_2}$. Since $\frac{c_1}{R_1 - p_1} > \frac{c_2}{R_2 - p_2}$, the binding constraint is $\mu \leq \frac{c_2}{R_2 - p_2}$. All other cells in this case require μ to be strictly above $\frac{c_2}{R_2 - p_2}$ (either to exceed it or to exceed $\frac{c_1}{R_1 - p_1}$ or to add Λ_i), so $(0, 0)$ cannot coincide with any of them.
- $(1, 1)$ requires $\mu \geq \frac{c_1}{R_1 - p_1} + \Lambda_1 + \Lambda_2$ and $\mu \geq \frac{c_2}{R_2 - p_2} + \Lambda_1 + \Lambda_2$. Because $\frac{c_1}{R_1 - p_1} > \frac{c_2}{R_2 - p_2}$, the first condition is stricter, so $\mu \geq \frac{c_1}{R_1 - p_1} + \Lambda_1 + \Lambda_2$. All other cells in this case require μ to be below that threshold (or within a smaller range), so $(1, 1)$ also cannot coexist with any other cell.
- $(0, q_2^*)$ and $(0, 1)$ cannot coexist because by Lemma 4.2, for fixed $q_1 = 0$, there is exactly one fixed point of $\text{BR}_2(0, q_2)$ in q_2 .
- $(0, 1)$ and $(q_1^*, 1)$ cannot coexist because by Lemma 4.2, for fixed $q_2 = 1$, there is exactly one fixed point of $\text{BR}_1(q_1, 1)$ in q_1 .

- $(0, q_2^*)$ and $(q_1^*, 1)$ have mutually exclusive μ -ranges, since

$$(0, q_2^*) : \frac{c_2}{R_2 - p_2} < \mu < \frac{c_2}{R_2 - p_2} + \Lambda_2,$$

while

$$(q_1^*, 1) : \frac{c_1}{R_1 - p_1} + \Lambda_2 < \mu < \frac{c_1}{R_1 - p_1} + \Lambda_1 + \Lambda_2.$$

Because $\frac{c_1}{R_1 - p_1} > \frac{c_2}{R_2 - p_2}$, we have $\frac{c_1}{R_1 - p_1} + \Lambda_2 > \frac{c_2}{R_2 - p_2} + \Lambda_2$. Thus, these intervals do not overlap, so $(0, q_2^*)$ and $(q_1^*, 1)$ also cannot coexist.

Moreover, whenever one strategy is fixed at 0 or 1, the other type's best response must be unique (Lemma 4.2). Hence, we cannot have two different equilibria of the form $(1, q_2)$ and $(1, q'_2)$, or $(0, q_2)$ and $(0, q'_2)$. Consequently, no two equilibria can coexist on the same boundary cell, ensuring uniqueness in this case.

Case 3: $\frac{c_1}{R_1 - p_1} = \frac{c_2}{R_2 - p_2}$. If

$$\mu \leq \frac{c_1}{R_1 - p_1} \quad \text{or} \quad \mu \geq \frac{c_1}{R_1 - p_1} + \Lambda_1 + \Lambda_2,$$

the equilibrium is either $(0, 0)$ or $(1, 1)$, and it is unique.

On the other hand, if

$$\frac{c_1}{R_1 - p_1} < \mu < \frac{c_1}{R_1 - p_1} + \Lambda_1 + \Lambda_2,$$

the interior cell conditions hold. In this case, the entire line segment

$$(q_1^*, q_2^*) \quad \text{where} \quad q_1^* \Lambda_1 + q_2^* \Lambda_2 = \mu - \frac{c_1}{R_1 - p_1}, \quad 0 \leq q_1^*, q_2^* \leq 1$$

forms a continuum of equilibria. In particular, points on that line with q_i^* at 0 or 1 lie on boundary cells in Table 3 and thus connect the interior segment to two of the border equilibria.

□

B.6 Analysis for Positive Inventory Scenario

Proof of Proposition 4.4. Step 1: $S_i > 0$ implies $q_i > 0$ in any equilibrium.

If $S_i > 0$ and $q_i = 0$, then

$$U_i(0, q_j) = R_i - p_i - c_i \frac{(0)^{S_i}}{(\mu - q_j \Lambda_j)^{S_i} (\mu - q_j \Lambda_j)} = R_i - p_i > 0$$

(since $R_i > p_i$). Hence type i would strictly prefer to join, making $q_i = 0$ impossible in equilibrium.

Step 2: *Uniqueness when both $S_1, S_2 > 0$.*

Step 2.1: Detailed Classification of Equilibrium Cases. To illustrate the possible equilibrium scenarios when $S_1 > 0$ and $S_2 > 0$, first note that Table 1 includes cells where $q_i = 0$. However, under $S_i > 0$, we have shown that $q_i = 0$ cannot arise in equilibrium. Consequently, only cells with $q_1, q_2 \in (0, 1]$ remain relevant. These lead to the equilibrium configurations summarized in Table 4:

We next show that only one of these cases can actually occur, and when it does, the equilibrium is unique. The argument proceeds in two steps.

Table 4: General Forms of Equilibrium Conditions for $S_1 > 0, S_2 > 0$

(q_1^*, q_2^*) , $q_1^*, q_2^* \in (0, 1)$ — NE: $q_1^* = \text{BR}_1(q_1^*, q_2^*), q_2^* = \text{BR}_2(q_1^*, q_2^*)$ $U_1(q_1^*, q_2^*) = 0, U_2(q_1^*, q_2^*) = 0$	$(q_1^*, 1)$, $q_1^* \in (0, 1)$ — NE: $q_1^* = \text{BR}_1(q_1^*, 1), 1 = \text{BR}_2(q_1^*, 1)$ $U_1(q_1^*, 1) = 0, U_2(q_1^*, 1) \geq 0$
$(1, q_2^*)$, $q_2^* \in (0, 1)$ — NE: $1 = \text{BR}_1(1, q_2^*), q_2^* = \text{BR}_2(1, q_2^*)$ $U_1(1, q_2^*) \geq 0, U_2(1, q_2^*) = 0$	$(1, 1)$ — NE: $1 = \text{BR}_1(1, 1), 1 = \text{BR}_2(1, 1)$ $U_1(1, 1) \geq 0, U_2(1, 1) \geq 0$

Step 2.2: Interior Analysis. Consider the case where (q_1^*, q_2^*) has both $q_1^*, q_2^* \in (0, 1)$ and satisfies

$$U_1(q_1^*, q_2^*) = 0 \quad \text{and} \quad U_2(q_1^*, q_2^*) = 0.$$

Here, the goal is to show that any such interior equilibrium must be unique within $(0, 1)^2$.

To handle interior solutions $(q_1, q_2) \in (0, 1)^2$, define two functions:

$$\begin{aligned} g_1(q_2) &: \text{the unique } q_1 \text{ satisfying } U_1(q_1, q_2) = 0, \\ g_2(q_1) &: \text{the unique } q_2 \text{ satisfying } U_2(q_1, q_2) = 0. \end{aligned} \quad (\text{B.1})$$

These functions are well-defined by monotonicity of U_1 and U_2 (Lemma 4.1). Then consider the composition

$$\varphi(q_1) = g_1(g_2(q_1)).$$

If multiple equilibria existed in $(0, 1)^2$, there would be multiple fixed points of φ , i.e. multiple solutions to $\varphi(q_1) = q_1$.

Using the Implicit Function Theorem, one obtains:

$$\varphi'(q_1) = \frac{\partial g_1}{\partial q_2} \cdot \frac{\partial g_2}{\partial q_1} = \left(-\frac{\frac{\partial U_1}{\partial q_2}}{\frac{\partial U_1}{\partial q_1}} \right) \cdot \left(-\frac{\frac{\partial U_2}{\partial q_1}}{\frac{\partial U_2}{\partial q_2}} \right).$$

For $S_i > 0$, the partial derivatives are:

$$\frac{\partial U_1}{\partial q_1} = -\frac{c_1 (q_1 \Lambda_1)^{S_1} [S_1 (\mu - q_1 \Lambda_1 - q_2 \Lambda_2) + q_1 \Lambda_1] (\mu - q_2 \Lambda_2)^{-S_1}}{q_1 (q_1 \Lambda_1 + q_2 \Lambda_2 - \mu)^2},$$

$$\frac{\partial U_1}{\partial q_2} = -\frac{c_1 \Lambda_2 (q_1 \Lambda_1)^{S_1} [S_1 (\mu - q_1 \Lambda_1 - q_2 \Lambda_2) + q_2 \Lambda_2] (\mu - q_2 \Lambda_2)^{-S_1}}{(q_1 \Lambda_1 + q_2 \Lambda_2 - \mu)^2}.$$

Similar expressions hold for $\frac{\partial U_2}{\partial q_1}$ and $\frac{\partial U_2}{\partial q_2}$. Substituting these into $\varphi'(q_1)$ and simplifying yields

$$\varphi'(q_1) = \frac{q_1 \Lambda_1 q_2 \Lambda_2 (S_1 (\mu - q_1 \Lambda_1 - q_2 \Lambda_2) + \mu - q_2 \Lambda_2) (S_2 (\mu - q_1 \Lambda_1 - q_2 \Lambda_2) + \mu - q_1 \Lambda_1)}{(q_1 \Lambda_1 - \mu) (\mu - q_2 \Lambda_2) (S_1 (\mu - q_1 \Lambda_1 - q_2 \Lambda_2) + q_1 \Lambda_1) (S_2 (\mu - q_1 \Lambda_1 - q_2 \Lambda_2) + q_2 \Lambda_2)}.$$

Recall from Section 2 that $\mu > \Lambda_1 + \Lambda_2$. Hence, for $q_1, q_2 \leq 1$, $\mu > q_1\Lambda_1 + q_2\Lambda_2$ ensures all factors in the fraction remain positive, implying $\varphi'(q_1) > 0$. What remains is to show that $\varphi'(q_1) < 1$.

Let

$$A = \mu - q_1\Lambda_1 - q_2\Lambda_2, \quad B_1 = \mu - q_1\Lambda_1, \quad B_2 = \mu - q_2\Lambda_2.$$

Then

$$\varphi'(q_1) = \frac{(B_1 - A)(B_2 - A)(S_1A + B_2)(S_2A + B_1)}{B_1B_2(S_1A + B_2 - A)(S_2A + B_1 - A)}.$$

Dividing the numerator and denominator by $(B_1B_2(S_1A + B_2)(S_2A + B_1))$ simplifies the expression to:

$$\varphi'(q_1) = \frac{\left(1 - \frac{A}{B_1}\right)\left(1 - \frac{A}{B_2}\right)}{\left(1 - \frac{A}{S_2A + B_1}\right)\left(1 - \frac{A}{S_1A + B_2}\right)},$$

and since $\frac{A}{S_iA + B_j} < \frac{A}{B_j}$, each factor in the denominator is smaller than its counterpart in the numerator, implying $\varphi'(q_1) < 1$.

Thus, φ is a strictly increasing function with derivative less than 1, indicating that its slope is always below that of the line $y = x$. Consequently, φ can cross $y = x$ at most once, so $\varphi(q_1) = q_1$ has at most one solution. In other words, there is at most a single fixed point, which is the unique interior Nash equilibrium (q_1^*, q_2^*) .

Step 2.3: Boundary Analysis. Suppose there is already an equilibrium $(q_1^*, 1)$ with $q_1^* \in (0, 1]$. Another equilibrium of the same form $(\tilde{q}_1^*, 1)$ cannot arise, because by Lemma 4.2, for fixed $q_2 = 1$, there is exactly one fixed point of $\text{BR}_1(q_1, 1)$ in q_1 . It remains to show that no second equilibrium of the form (\tilde{q}_1^*, q_2^*) can exist with $\tilde{q}_1^* \in (0, 1]$ and $q_2^* \in (0, 1)$.

Assume by contradiction that such a second equilibrium (\tilde{q}_1^*, q_2^*) does exist. By Lemma 4.2, for any fixed q_2 , let $f_1(q_2)$ denote the unique fixed point of $\text{BR}_1(q_1, q_2)$ in q_1 , and similarly for any fixed q_1 , let $f_2(q_1)$ denote the unique fixed point of $\text{BR}_2(q_1, q_2)$ in q_2 . Define

$$\psi(q_1) = f_1(f_2(q_1)).$$

Since any Nash equilibrium (q_1^*, q_2^*) must satisfy $q_2^* = f_2(q_1^*)$ and $q_1^* = f_1(q_2^*)$ (as these are fixed points of the respective best responses), having two equilibria would imply two distinct solutions to $\psi(q_1) = q_1$.

Next, observe that $(q_1^*, 1)$ being an equilibrium means $f_2(q_1^*) = 1$, while the other equilibrium (\tilde{q}_1^*, q_2^*) has $f_2(\tilde{q}_1^*) < 1$. By monotonicity of U_2 (Lemma 4.1), there must be a threshold $q'_1 \in [q_1^*, 1]$ such that

$$f_2(q_1) = \begin{cases} 1, & 0 \leq q_1 \leq q'_1, \\ g_2(q_1), & q_1 > q'_1, \end{cases}$$

where $g_2(q_1)$ is the interior solution defined earlier (i.e., the value making $U_2 = 0$).

Hence,

$$\psi(q_1) = f_1(f_2(q_1)) = \begin{cases} f_1(1), & 0 \leq q_1 \leq q'_1, \\ f_1(g_2(q_1)), & q_1 > q'_1. \end{cases}$$

On $[0, q'_1]$, ψ is constant at the value $f_1(1)$, giving it slope 0. For $q_1 > q'_1$, $\psi(q_1)$ is either identically 1 or given by $g_1(g_2(q_1))$, which is strictly increasing with derivative less than 1 (Step 2's argument). Moreover, ψ is continuous at q'_1 . Hence, across $[0, 1]$, ψ is piecewise constant and piecewise strictly increasing with slope < 1 . Therefore, it can intersect the line $y = x$ at most once.

Since $q_1 = q_1^*$ is already one intersection (the known equilibrium $(q_1^*, 1)$), a second intersection would contradict the above argument that ψ crosses $y = x$ only once. Thus, no second solution is possible, completing the contradiction.

The same reasoning applies if the boundary equilibrium is $(1, q_2^*)$. Therefore, if $(q_1^*, 1)$ (or $(1, q_2^*)$) exists, no other equilibrium is possible, completing the uniqueness proof.

Step 3: Uniqueness with asymmetric inventory.

Assume without loss of generality that $S_1 = 0$ and $S_2 > 0$.

Step 3.1: Detailed Classification of Equilibrium Cases. All possible forms of equilibrium conditions appear in Table 5, which is analogous to Table 4 from the $S_1 > 0, S_2 > 0$ scenario. The only difference here is that q_1 may be zero, introducing an extra boundary row.

Table 5: Possible Equilibria for $S_1 = 0, S_2 > 0$

$(\mathbf{0}, q_2^*)$, $q_2^* \in (0, 1)$ — NE: $0 = \text{BR}_1(0, q_2^*), q_2^* = \text{BR}_2(0, q_2^*)$ $U_1(0, q_2^*) \leq 0, U_2(0, q_2^*) = 0$	$(\mathbf{0}, \mathbf{1})$ — NE: $0 = \text{BR}_1(0, 1), 1 = \text{BR}_2(0, 1)$ $U_1(0, 1) \leq 0, U_2(0, 1) \geq 0$
(q_1^*, q_2^*) , $q_1^*, q_2^* \in (0, 1)$ — NE: $q_1^* = \text{BR}_1(q_1^*, q_2^*), q_2^* = \text{BR}_2(q_1^*, q_2^*)$ $U_1(q_1^*, q_2^*) = 0, U_2(q_1^*, q_2^*) = 0$	$(q_1^*, \mathbf{1})$, $q_1^* \in (0, 1)$ — NE: $q_1^* = \text{BR}_1(q_1^*, 1), 1 = \text{BR}_2(q_1^*, 1)$ $U_1(q_1^*, 1) = 0, U_2(q_1^*, 1) \geq 0$
$(\mathbf{1}, q_2^*)$, $q_2^* \in (0, 1)$ — NE: $1 = \text{BR}_1(1, q_2^*), q_2^* = \text{BR}_2(1, q_2^*)$ $U_1(1, q_2^*) \geq 0, U_2(1, q_2^*) = 0$	$(\mathbf{1}, \mathbf{1})$ — NE: $1 = \text{BR}_1(1, 1), 1 = \text{BR}_2(1, 1)$ $U_1(1, 1) \geq 0, U_2(1, 1) \geq 0$

Four main equilibrium categories remain from the strictly positive scenario: (q_1^*, q_2^*) , $(q_1^*, 1)$, $(1, q_2^*)$, and $(1, 1)$. In addition, two new boundary cells arise here: $(0, q_2^*)$ and $(0, 1)$. The argument proceeds in two steps.

Step 3.2: Interior Analysis. When $q_1 > 0$ and $q_2 < 1$, consider points where U_1 and U_2 are zero. To handle these interior solutions $(q_1, q_2) \in (0, 1)^2$, define as before:

$$\begin{aligned} g_1(q_2) &: \text{the unique } q_1 \text{ satisfying } U_1(q_1, q_2) = 0, \\ g_2(q_1) &: \text{the unique } q_2 \text{ satisfying } U_2(q_1, q_2) = 0. \end{aligned} \tag{B.2}$$

The partial derivative calculations are nearly identical to those in Step 2, except $\frac{\partial U_1}{\partial q_1}$ and $\frac{\partial U_1}{\partial q_2}$ simplify because $S_1 = 0$. Specifically,

$$\frac{\partial U_1}{\partial q_1} = -\frac{c_1 \Lambda_1}{(\mu - q_1 \Lambda_1 - q_2 \Lambda_2)^2}, \quad \frac{\partial U_1}{\partial q_2} = -\frac{c_1 \Lambda_2}{(\mu - q_1 \Lambda_1 - q_2 \Lambda_2)^2}.$$

This yields a similar expression for $\varphi'(q_1)$ in the composition $\varphi(q_1) = g_1(g_2(q_1))$. One obtains

$$\varphi'(q_1) = \frac{(B_1 - A)(S_2 A + B_1)}{B_1(S_2 A + B_1 - A)},$$

where $A = \mu - q_1 \Lambda_1 - q_2 \Lambda_2$ and $B_1 = \mu - q_1 \Lambda_1$. By the same ratio argument as before, $0 < \varphi'(q_1) < 1$, so at most one interior equilibrium exists.

Step 3.3: Boundary Analysis. By Lemma 4.2, for any fixed q_2 , let $f_1(q_2)$ denote the unique fixed point of $\text{BR}_1(q_1, q_2)$ in q_1 , and similarly for any fixed q_1 , let $f_2(q_1)$ denote the unique fixed point of $\text{BR}_2(q_1, q_2)$ in q_2 .

Any equilibria from $(q_1^*, 1)$, $(1, q_2^*)$ or $(1, 1)$ cannot coexist by the argument as in Step 2.3.

Two equilibria of the form $(0, q_2^*)$ with $q_2^* \in (0, 1]$ cannot coexist since by Lemma 4.2, for fixed $q_1 = 0$, there is exactly one fixed point of $\text{BR}_2(0, q_2)$ in q_2 . It remains to prove that $(0, q_2^*)$ with $q_2^* \in (0, 1]$ cannot coexist with any of $(q_1^*, 1)$, $(1, q_2^*)$, $(1, 1)$.

Indeed, suppose $(0, q_2^*)$ where $q_2^* \in (0, 1]$ and (q_1^*, \tilde{q}_2^*) where $q_1^*, \tilde{q}_2^* \in (0, 1]$ coexist. Define

$$\psi(q_1) = f_1(f_2(q_1)).$$

By the same argument as before, ψ is continuous and consists of (1) a constant piece $f_1(f_2(0))$ for small q_1 ; (2) a strictly increasing segment with slope less than 1 for larger q_1 . This contradicts the existence of two fixed points of ψ .

Hence, there is a unique Nash equilibrium overall for $S_1 = 0$ and $S_2 > 0$. \square

Appendix C Profit Optimization Proofs

C.1 Inventory Threshold Derivation

Proof of Proposition 5.1. Step 1: Positivity of the utility functions. Let $U_i^{S_i}(1, 1)$ be the utility of a type- i customer when the target inventory level is S_i and all customers join. Concretely,

$$U_1^{S_1}(1, 1) = R_1 - p_1 - c_1 \frac{\Lambda_1^{S_1}}{(\mu - \Lambda_2)^{S_1} (\mu - \Lambda_1 - \Lambda_2)},$$

$$U_2^{S_2}(1, 1) = R_2 - p_2 - c_2 \frac{\Lambda_2^{S_2}}{(\mu - \Lambda_1)^{S_2} (\mu - \Lambda_1 - \Lambda_2)}.$$

Each $U_i^{S_i}(1, 1)$ increases strictly in S_i , and

$$\lim_{S_i \rightarrow \infty} U_i^{S_i}(1, 1) = R_i - p_i > 0,$$

since $R_i > p_i$.

Step 2: Thresholds that guarantee full joining. Define

$$\bar{S}_1 = \min\{S_1 \mid U_1^{S_1}(1, 1) > 0\}, \quad \bar{S}_2 = \min\{S_2 \mid U_2^{S_2}(1, 1) > 0\}.$$

Because $U_i^{S_i}(1, 1)$ is strictly increasing and eventually positive, each \bar{S}_i is finite. If $S_i \geq \bar{S}_i$, then $U_i^{S_i}(1, 1) > 0$, so type- i customer strictly prefers to join. Hence, whenever $S_1 \geq \bar{S}_1$ and $S_2 \geq \bar{S}_2$, all customers join for both products, which is to say $q_1^{(S_1, S_2)} = q_2^{(S_1, S_2)} = 1$.

Step 3: Profit implications of large inventories. The total profit can be written as $\Pi(S_1, S_2) = \Pi_1(S_1) + \Pi_2(S_2)$, where

$$\Pi_i(S_i) = p_i \Lambda_i q_i^{(S_1, S_2)} - h_i \mathbb{E}[I_i(S_i)].$$

If $S_i \geq \bar{S}_i$, then all customers of type i join, making $p_i \Lambda_i q_i^{(S_1, S_2)} = p_i \Lambda_i$ constant. Meanwhile, the expected inventory

$$\mathbb{E}[I_i(S_i)] = S_i - \frac{\Lambda_i}{\mu - \Lambda_1 - \Lambda_2} \left(1 - \left(\frac{\Lambda_i}{\mu - \Lambda_j} \right)^{S_i} \right)$$

is an increasing function of S_i . Hence, $\Pi_i(S_i)$ decreases once $S_i > \bar{S}_i$. Consequently,

$$\Pi_i(S_i) \leq \Pi_i(\bar{S}_i) \quad \text{whenever } S_i \geq \bar{S}_i.$$

Summing over both products,

$$\Pi(S_1, S_2) = \Pi_1(S_1) + \Pi_2(S_2) \leq \Pi_1(\bar{S}_1) + \Pi_2(\bar{S}_2) = \Pi(\bar{S}_1, \bar{S}_2),$$

which completes the proof. \square

Appendix D Welfare Optimization Proofs

D.1 Optimal Target Inventory Levels Derivation

Proof of Proposition 6.1. Step 1: Separation of the Cost Function. In this proof, $C(\lambda_1, \lambda_2, S_1, S_2)$ is treated as $C(S_1, S_2)$, reflecting that λ_i are constant.

Observe that the total cost can be written as

$$C(S_1, S_2) = C_1(S_1) + C_2(S_2),$$

where

$$C_i(S_i) = h_i S_i - h_i \frac{\lambda_i}{\mu - \lambda_1 - \lambda_2} \left(1 - \left(\frac{\lambda_i}{\mu - \lambda_j} \right)^{S_i} \right) + c_i \frac{\lambda_i}{\mu - \lambda_1 - \lambda_2} \left(\frac{\lambda_i}{\mu - \lambda_j} \right)^{S_i}.$$

Since $C_1(S_1)$ is solely a function of S_1 and $C_2(S_2)$ solely of S_2 , each can be minimized separately. The argument below focuses on $C_1(S_1)$; the same reasoning applies to $C_2(S_2)$.

Step 2: Cost Difference and Monotonicity.

$$C_1(S_1) = h_1 S_1 - h_1 \frac{\lambda_1}{\mu - \lambda_1 - \lambda_2} \left(1 - \left(\frac{\lambda_1}{\mu - \lambda_2} \right)^{S_1} \right) + c_1 \frac{\lambda_1}{\mu - \lambda_1 - \lambda_2} \left(\frac{\lambda_1}{\mu - \lambda_2} \right)^{S_1}.$$

Define the cost difference

$$\Delta C_1(S_1) = C_1(S_1 + 1) - C_1(S_1).$$

A direct computation shows

$$\begin{aligned}
\Delta C_1(S_1) &= h_1 - \frac{\lambda_1}{\mu - \lambda_1 - \lambda_2} \left[h_1 \left(\left(1 - \left(\frac{\lambda_1}{\mu - \lambda_2} \right)^{S_1+1} \right) - \left(1 - \left(\frac{\lambda_1}{\mu - \lambda_2} \right)^{S_1} \right) \right) \right. \\
&\quad \left. - c_1 \left(\left(1 - \left(\frac{\lambda_1}{\mu - \lambda_2} \right)^{S_1+1} \right) - \left(1 - \left(\frac{\lambda_1}{\mu - \lambda_2} \right)^{S_1} \right) \right) \right] \\
&= h_1 - \frac{\lambda_1}{\mu - \lambda_1 - \lambda_2} \left(\frac{\lambda_1}{\mu - \lambda_2} \right)^{S_1} (h_1 + c_1) \frac{\mu - \lambda_1 - \lambda_2}{\mu - \lambda_2} \\
&= h_1 - (h_1 + c_1) \left(\frac{\lambda_1}{\mu - \lambda_2} \right)^{S_1+1}.
\end{aligned}$$

Moreover, $\Delta C_1(S_1)$ is strictly increasing in S_1 . Indeed,

$$\Delta C_1(S_1 + 1) - \Delta C_1(S_1) = (h_1 + c_1) \left(\frac{\lambda_1}{\mu - \lambda_2} \right)^{S_1+1} \frac{\mu - \lambda_1 - \lambda_2}{\mu - \lambda_2} > 0.$$

Step 3: Identifying the Optimal S_1^ .*

To find the cost-minimizing S_1 , examine the cost difference, $\Delta C_1(S_1)$ and choose the smallest integer S_i such that $\Delta C_i(S_i) \geq 0$. For any $S_1 < S_1^*$, $\Delta C_1(S_1) < 0$, so increasing S_1 lowers cost. Once $S_1 \geq S_1^*$ makes $\Delta C_1(S_1) \geq 0$, further increments do not reduce cost. Because $\Delta C_1(S_1)$ is strictly increasing, there is exactly one integer S_1^* satisfying

$$\Delta C_1(S_1^*) \geq 0, \quad \Delta C_1(S_1^* - 1) < 0.$$

Rewriting $\Delta C_1(S_1^*) \geq 0$ shows

$$\begin{aligned}
h_1 - (h_1 + c_1) \left(\frac{\lambda_1}{\mu - \lambda_2} \right)^{S_1^*+1} &\geq 0; \quad \left(\frac{\lambda_1}{\mu - \lambda_2} \right)^{S_1^*+1} \leq \frac{h_1}{h_1 + c_1}; \\
S_1^* &\geq \frac{\log \left(\frac{h_1}{h_1 + c_1} \right)}{\log \left(\frac{\lambda_1}{\mu - \lambda_2} \right)} - 1.
\end{aligned}$$

Hence the minimal integer solution is

$$S_1^* = \left\lceil \frac{\log \left(\frac{h_1}{h_1 + c_1} \right)}{\log \left(\frac{\lambda_1}{\mu - \lambda_2} \right)} \right\rceil - 1.$$

An identical argument applies to $C_2(S_2)$. □

D.2 Optimization Within Subdomains

In each subdomain \mathcal{D}_{s_1, s_2} , the target inventory levels remain fixed at $S_1^* = s_1$ and $S_2^* = s_2$. Substituting $S_1 = s_1$ and $S_2 = s_2$ into the social welfare function

$$\text{SW}(\lambda_1, \lambda_2) = \sum_{i=1}^2 \left[\lambda_i R_i - h_i s_i + h_i \frac{\lambda_i}{\mu - \lambda_1 - \lambda_2} \left(1 - \left(\frac{\lambda_i}{\mu - \lambda_j} \right)^{s_i} \right) - c_i \frac{\lambda_i}{\mu - \lambda_1 - \lambda_2} \left(\frac{\lambda_i}{\mu - \lambda_j} \right)^{s_i} \right]$$

produces a smooth function of λ_1, λ_2 in \mathcal{D}_{s_1, s_2} .

Although setting $\partial \text{SW} / \partial \lambda_1 = 0$ and $\partial \text{SW} / \partial \lambda_2 = 0$ may not yield a closed-form solution, standard methods (e.g. gradient-based algorithms) can find a local maximum. Explicit partial derivatives are readily computed. For instance:

$$\begin{aligned} \frac{\partial \text{SW}}{\partial \lambda_1} = R_1 + \frac{1}{(\mu - \lambda_1 - \lambda_2)^2} & [h_1(\mu - \lambda_2) + h_2\lambda_2 - (c_1 + h_1)(\mu - \lambda_2) \\ & + s_1(\mu - \lambda_1 - \lambda_2)) \left(\frac{\lambda_1}{\mu - \lambda_2} \right)^{s_1} - (c_2 + h_2)(\mu - \lambda_1 + s_2(\mu - \lambda_1 - \lambda_2)) \left(\frac{\lambda_2}{\mu - \lambda_1} \right)^{s_2+1}], \end{aligned}$$

(and similarly for $\partial \text{SW} / \partial \lambda_2$).

Appendix E Supplementary Figures

This appendix collects additional figures from the numerical experiment in Section 7. We present two parameter configurations to explore how holding cost asymmetries affect system behavior.

E.1 Baseline Configuration

The figures in this subsection use the baseline parameters from Section 7. These results complement the main text by showing additional metrics — effective utilization, expected waiting times, and component-wise comparison between centralized and decentralized solutions — across the full (κ, ρ) parameter space.

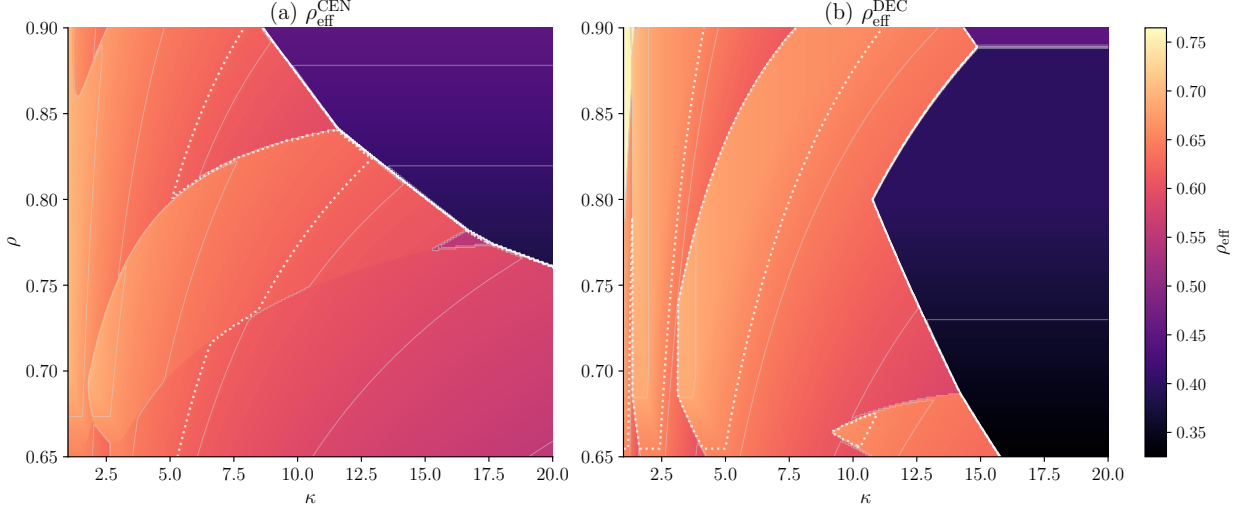


Figure 10: Effective utilization $\rho_{\text{eff}} = (q_1 \Lambda_1 + q_2 \Lambda_2) / \mu$ over the (κ, ρ) plane. White contours at 25% (solid), 50% (dashed), 75% (dotted) of range; thin gray contours provide detail.

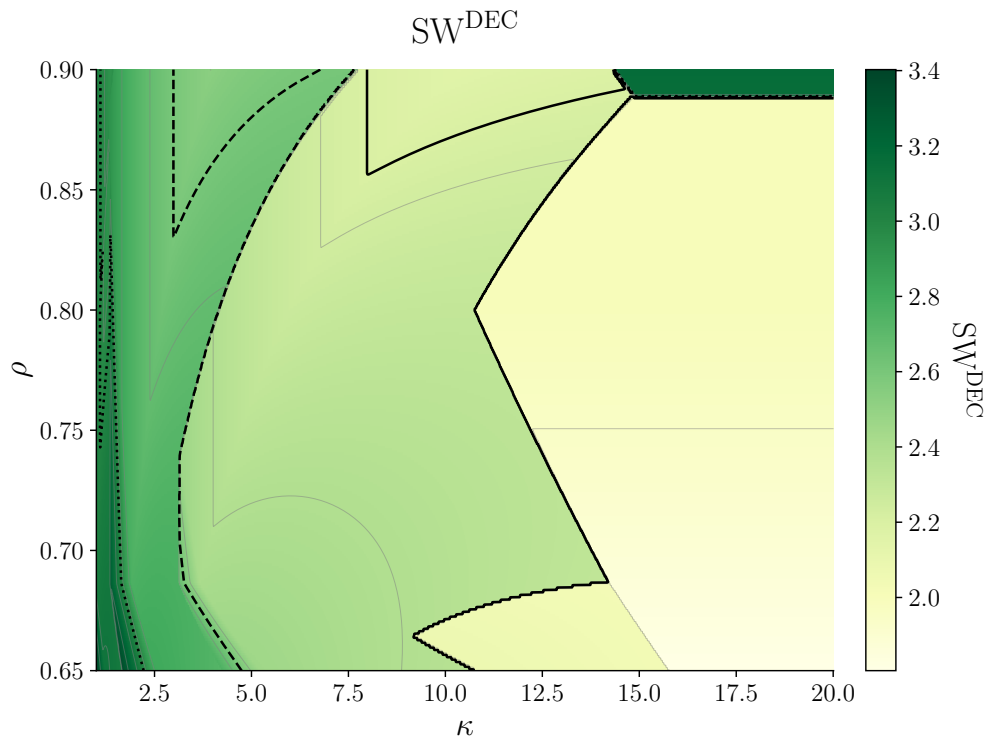


Figure 11: Social welfare SW^{DEC} under decentralization over the (κ, ρ) plane. Thick black contours mark 2.20, 2.60, 3.00 (25%, 50%, 75% of range); thin gray contours provide detail.

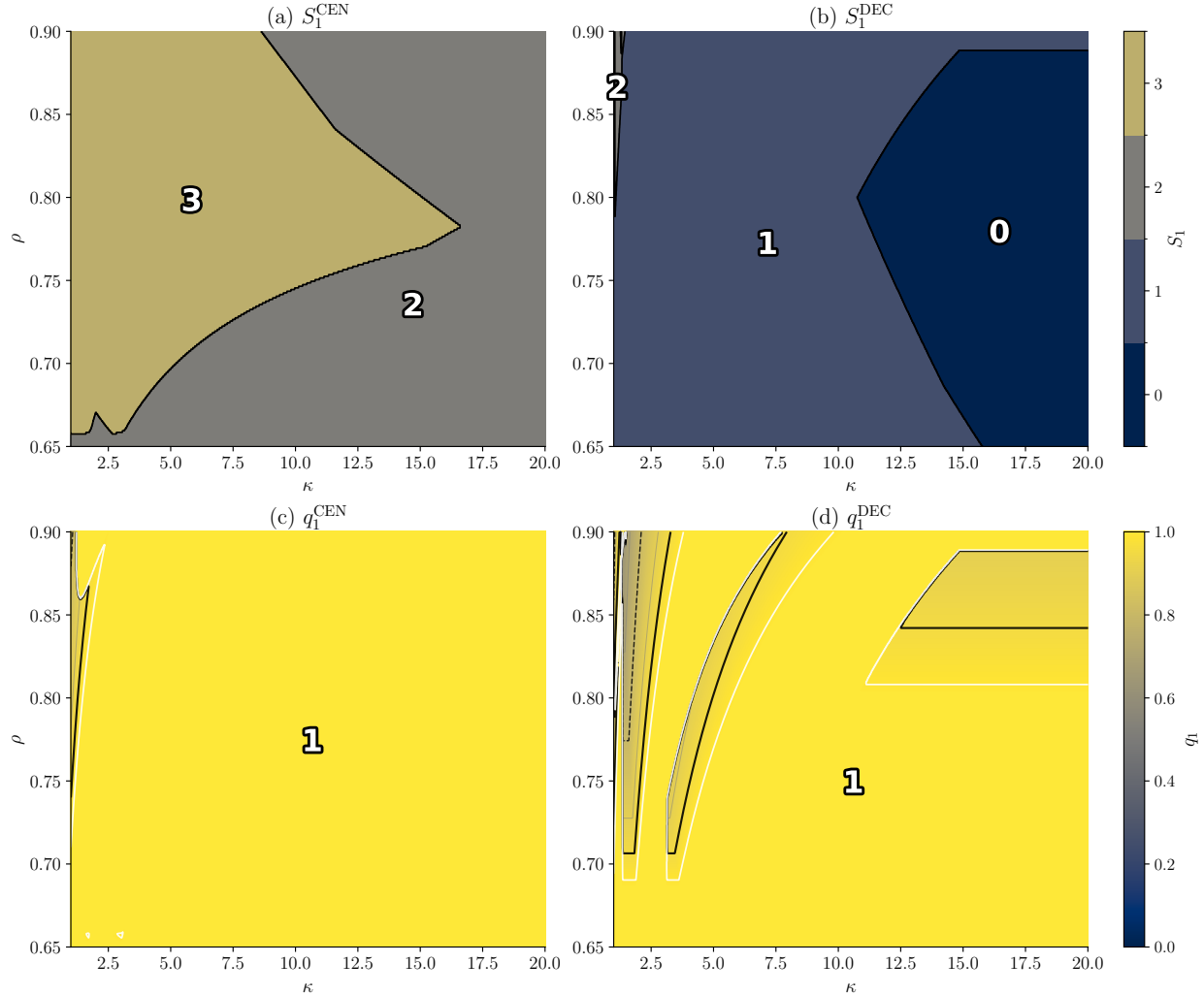


Figure 12: Type-1 decisions over the (κ, ρ) plane. Top row: inventory S_1 ; contours mark integer transitions. Bottom row: joining probability q_1 ; contours at 0.80 (dashed black), 0.95 (thick black), and 0.99 (thick white); thin gray contours provide detail.

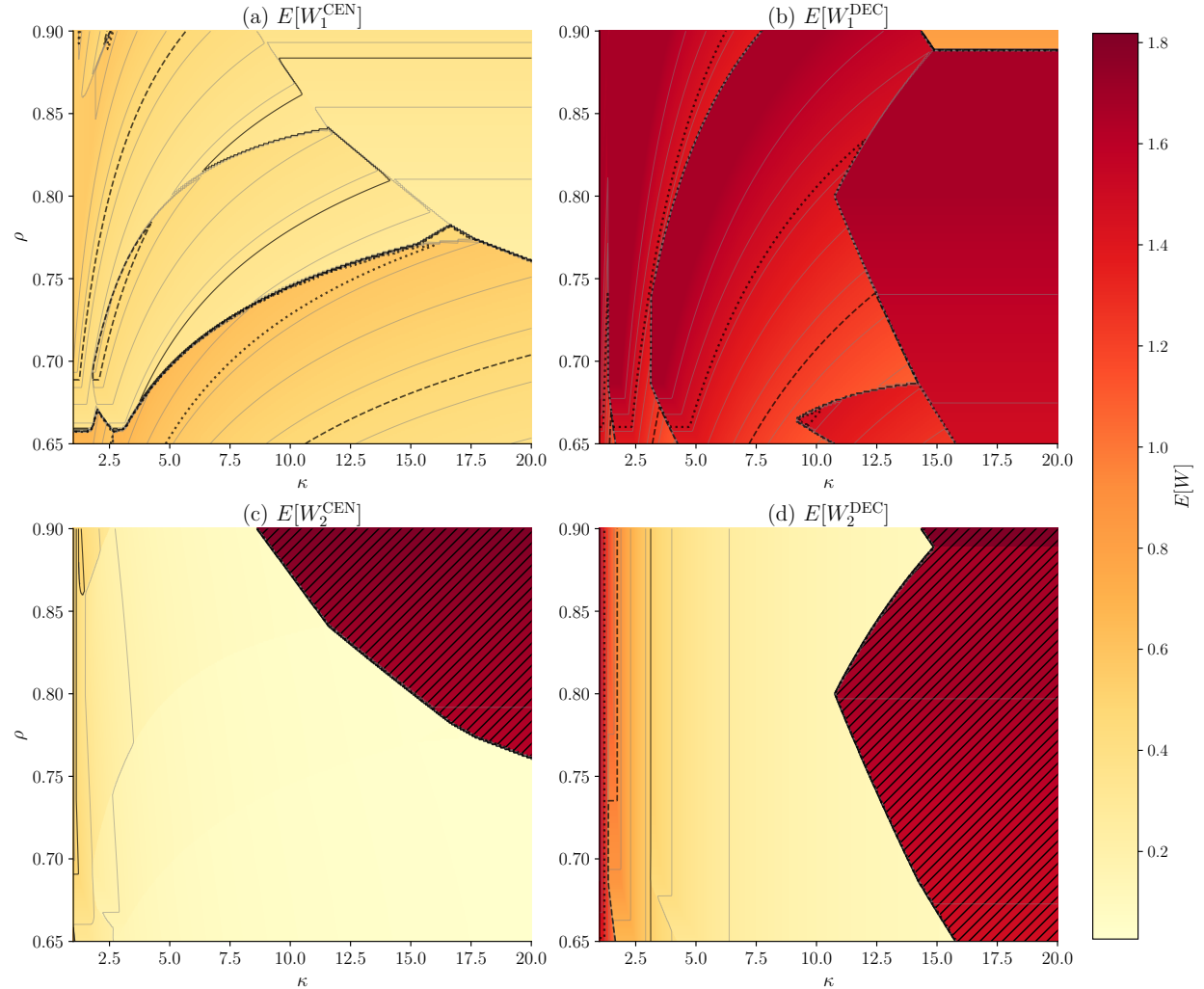


Figure 13: Expected waiting times $E[W_i]$ over the (κ, ρ) plane. Top row: type-1. Bottom row: type-2. Contours at 25% (solid), 50% (dashed), 75% (dotted) of each panel's range; thin gray contours provide detail. Hatching indicates no joining.

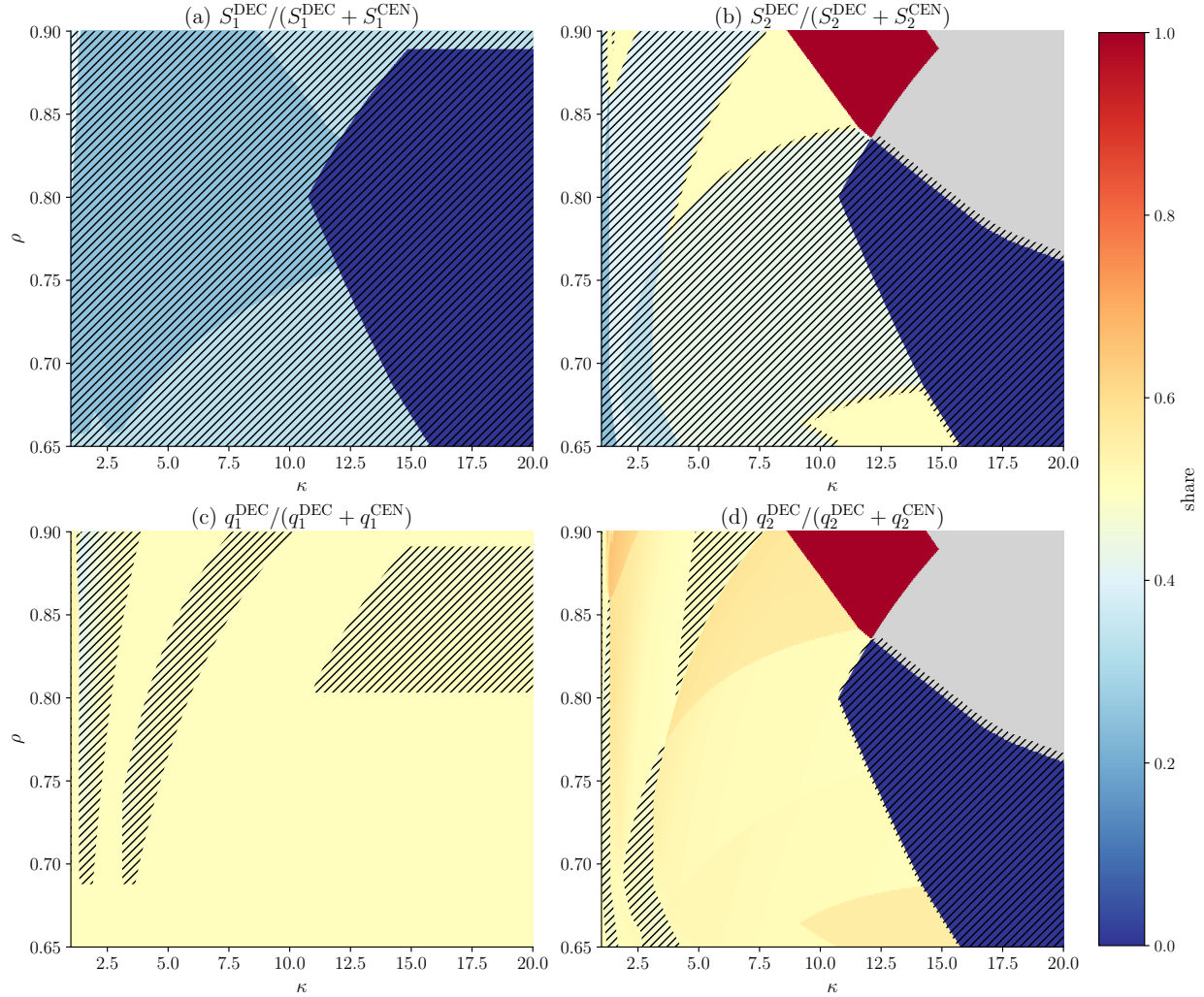


Figure 14: Decentralized shares $X^{\text{DEC}} / (X^{\text{DEC}} + X^{\text{CEN}})$ for $X \in \{S_1, S_2, q_1, q_2\}$. Top row: inventory shares. Bottom row: joining probability shares. Diverging colormap centered at 0.5: blue indicates higher under centralization, red indicates higher under decentralization. Hatching where centralization dominates (share < 0.5). Light gray regions indicate undefined shares (zero values in both settings).

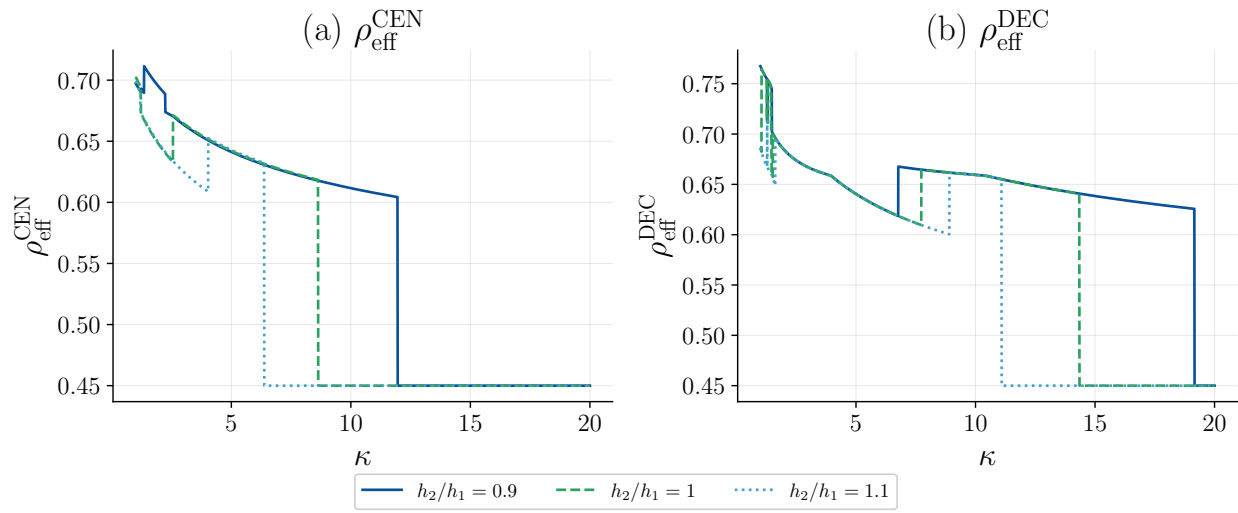


Figure 15: Cross-section at $\rho = 0.9$: effective utilization $\rho_{\text{eff}} = (q_1\Lambda_1 + q_2\Lambda_2)/\mu$ as function of κ for different h_2/h_1 ratios. Left: centralized. Right: decentralized.

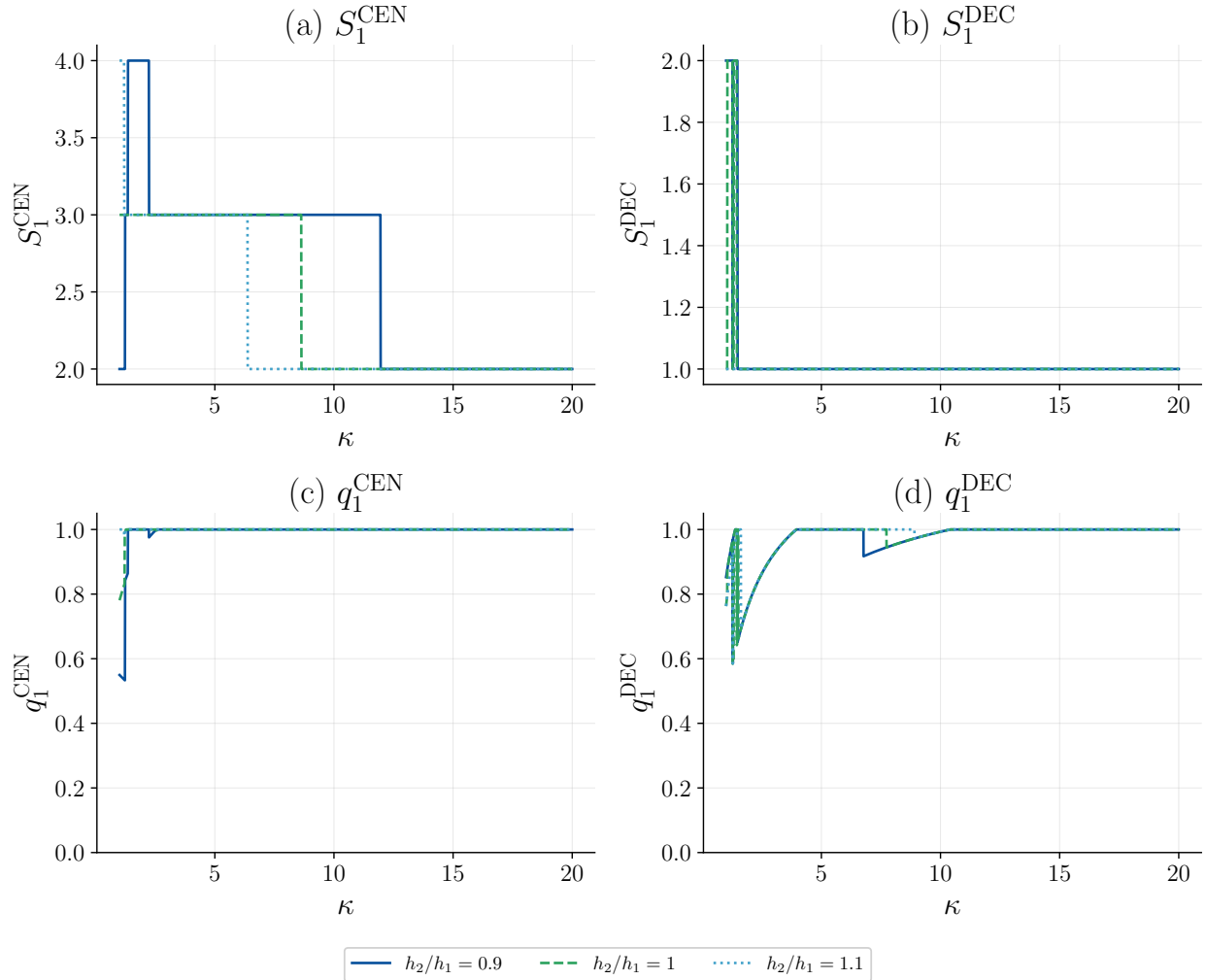


Figure 16: Cross-section at $\rho = 0.9$: type-1 decisions as functions of κ for different h_2/h_1 ratios. Top row: inventory S_1 . Bottom row: joining probability q_1 .

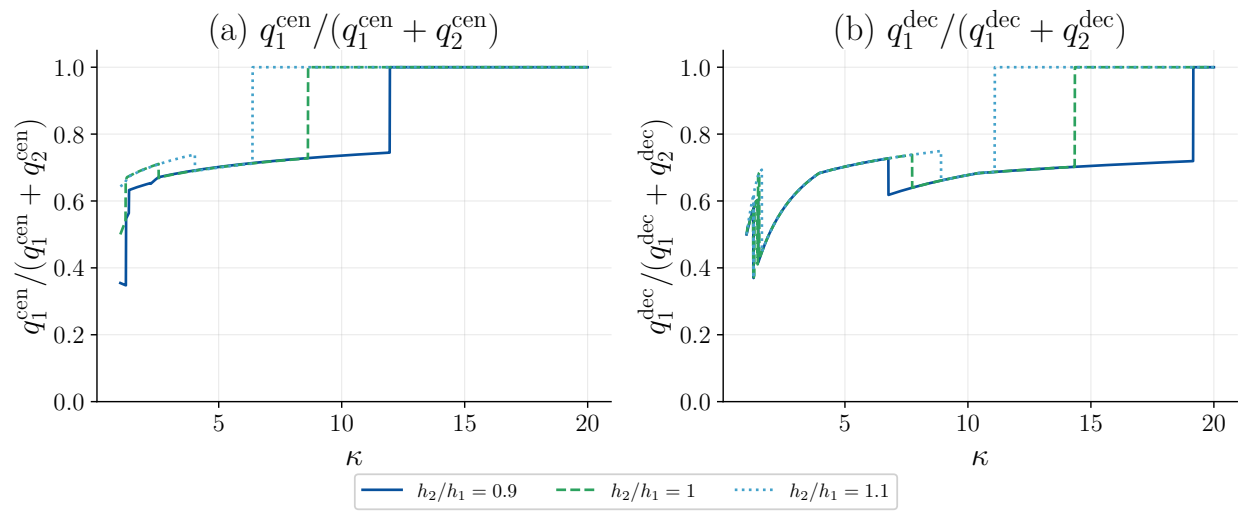


Figure 17: Cross-section at $\rho = 0.9$: type-1 share $q_1/(q_1 + q_2)$ as function of κ for different h_2/h_1 ratios. Left: centralized. Right: decentralized.

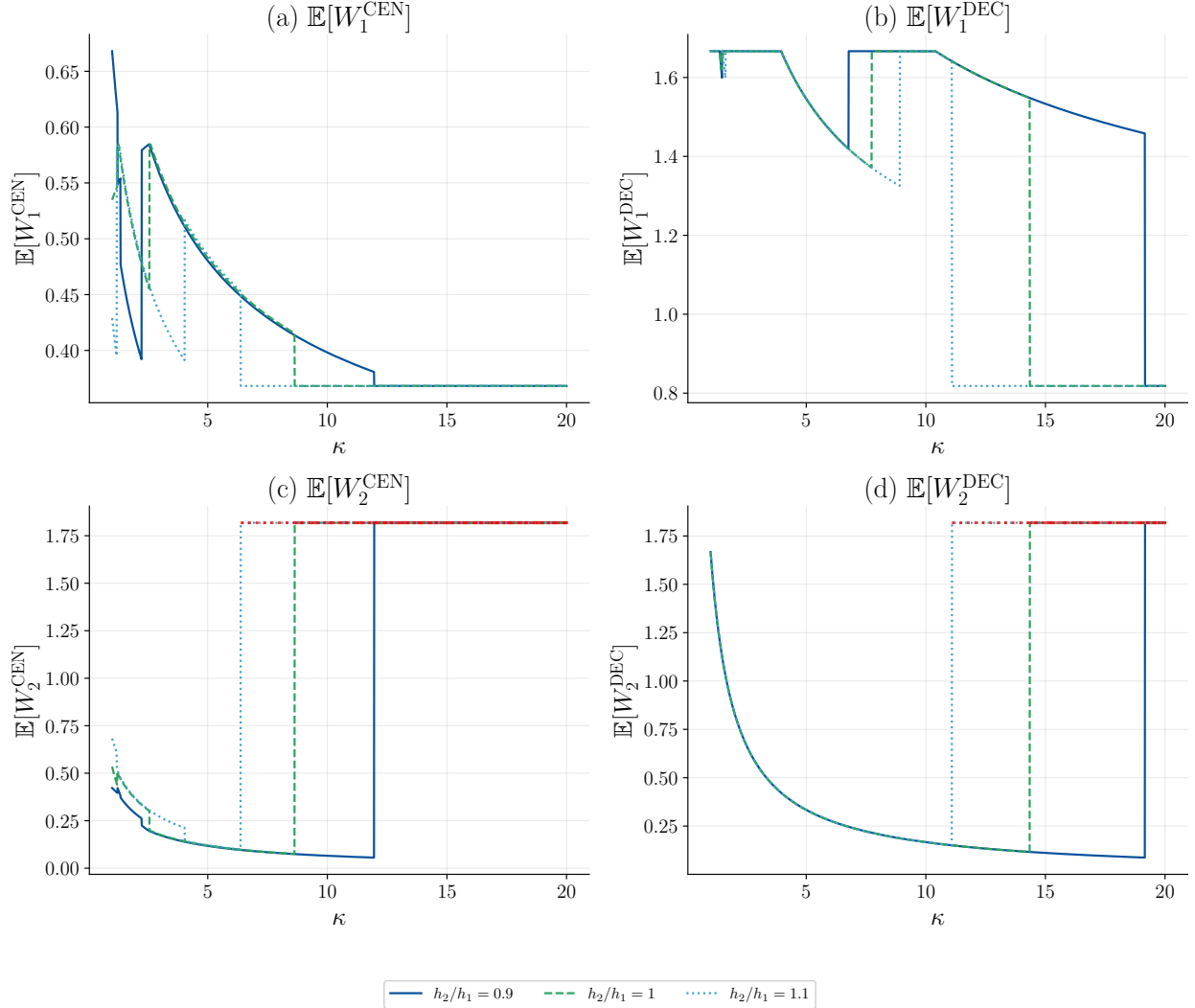


Figure 18: Cross-section at $\rho = 0.9$: expected waiting times $E[W_i]$ as functions of κ for different h_2/h_1 ratios. Red segments indicate no joining.

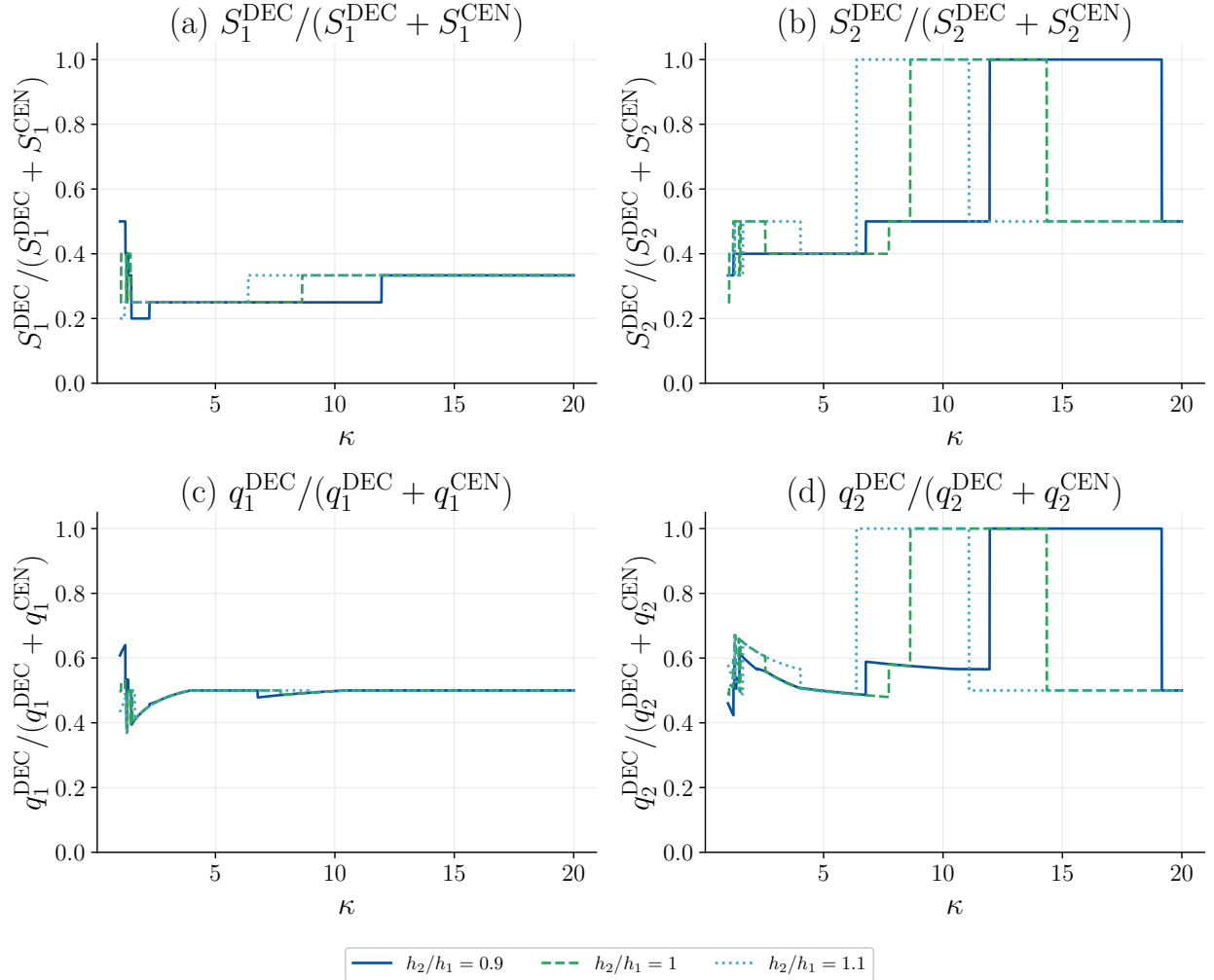


Figure 19: Cross-section at $\rho = 0.9$: decentralized shares $X^{\text{DEC}}/(X^{\text{DEC}} + X^{\text{CEN}})$ as functions of κ for different h_2/h_1 ratios. Top row: inventory shares. Bottom row: joining probability shares.

E.2 Reduced Type-1 Holding Cost

The figures below repeat the analysis with $c_1 = 1$ and $h_1 = 0.05$ (compared to the baseline $c_1 = 3$ and $h_1 = 0.4$). The lower holding cost reduces the trade-off between retaining customers and saving on inventory storage for product 1: with smaller h_i , the producer faces less pressure to limit inventory. Cross-sections are taken at $\rho = 0.8$.

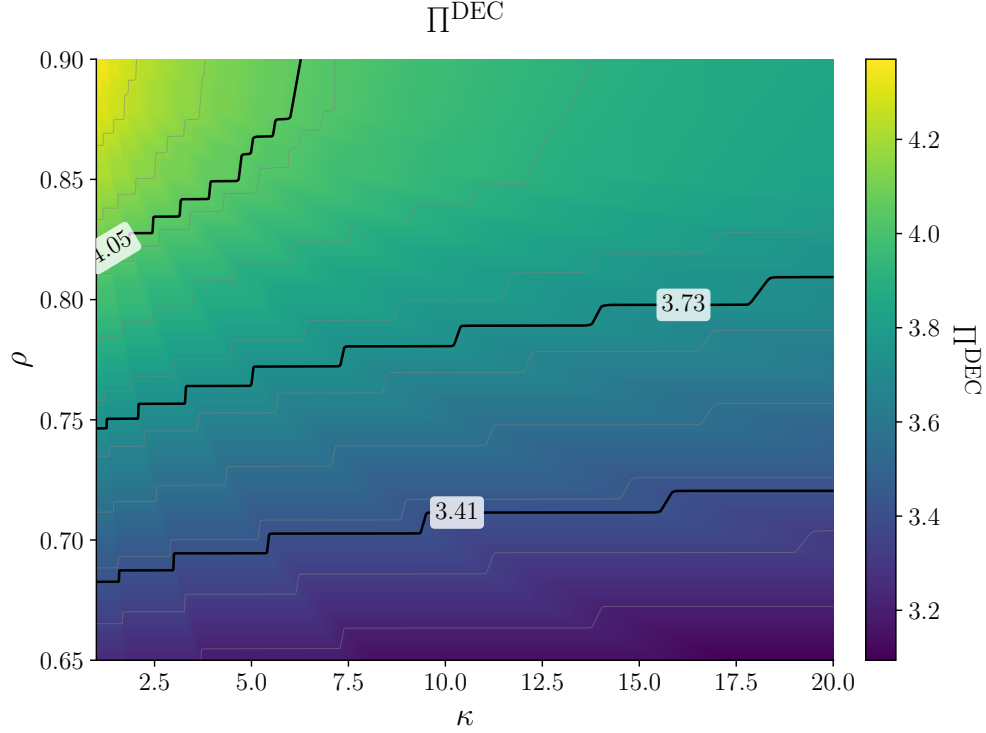


Figure 20: Producer's profit Π^{DEC} under decentralization over the (κ, ρ) plane (reduced h_1). Thick black contours mark 3.41, 3.73, 4.05 (25%, 50%, 75% of range); thin gray contours provide detail.

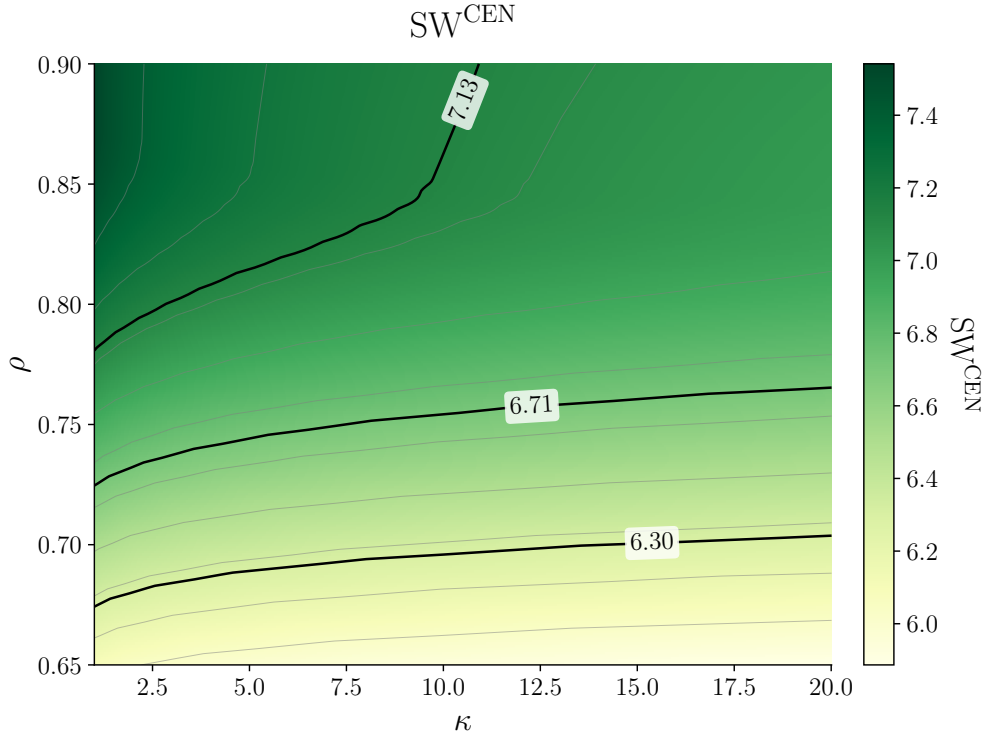


Figure 21: Social welfare SW^{CEN} under centralization over the (κ, ρ) plane (reduced h_1). Thick black contours mark 6.30, 6.71, 7.13 (25%, 50%, 75% of range); thin gray contours provide detail.

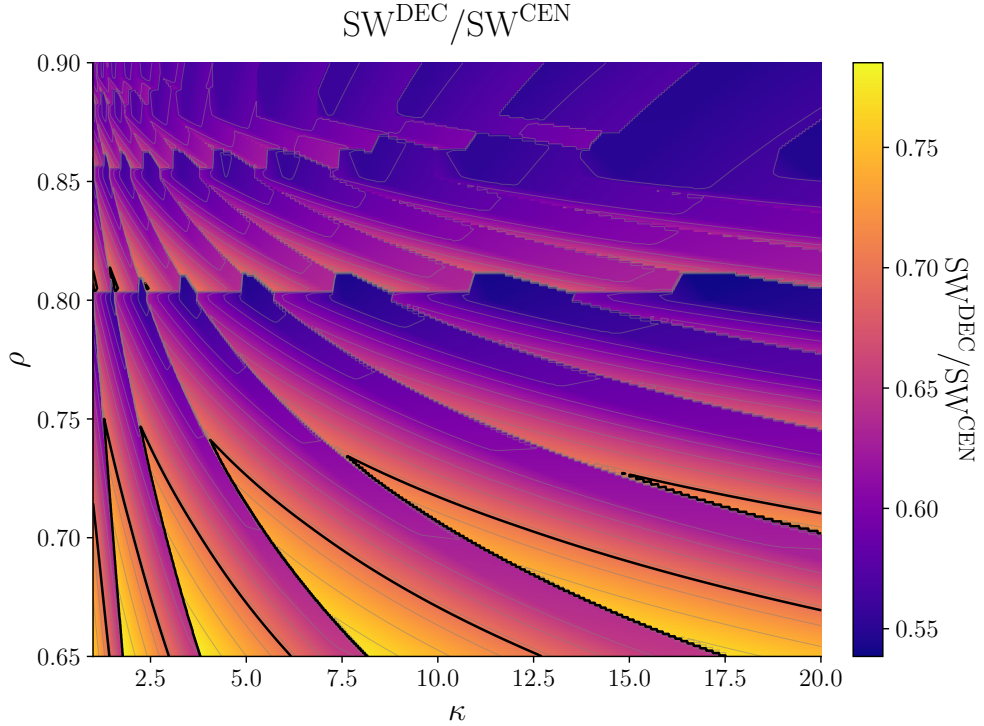


Figure 22: Efficiency SW^{DEC}/SW^{CEN} over the (κ, ρ) plane (reduced h_1). Contours mark 0.70 (solid), 0.80 (dotted), and 0.90 (dashed); thin gray contours provide detail.

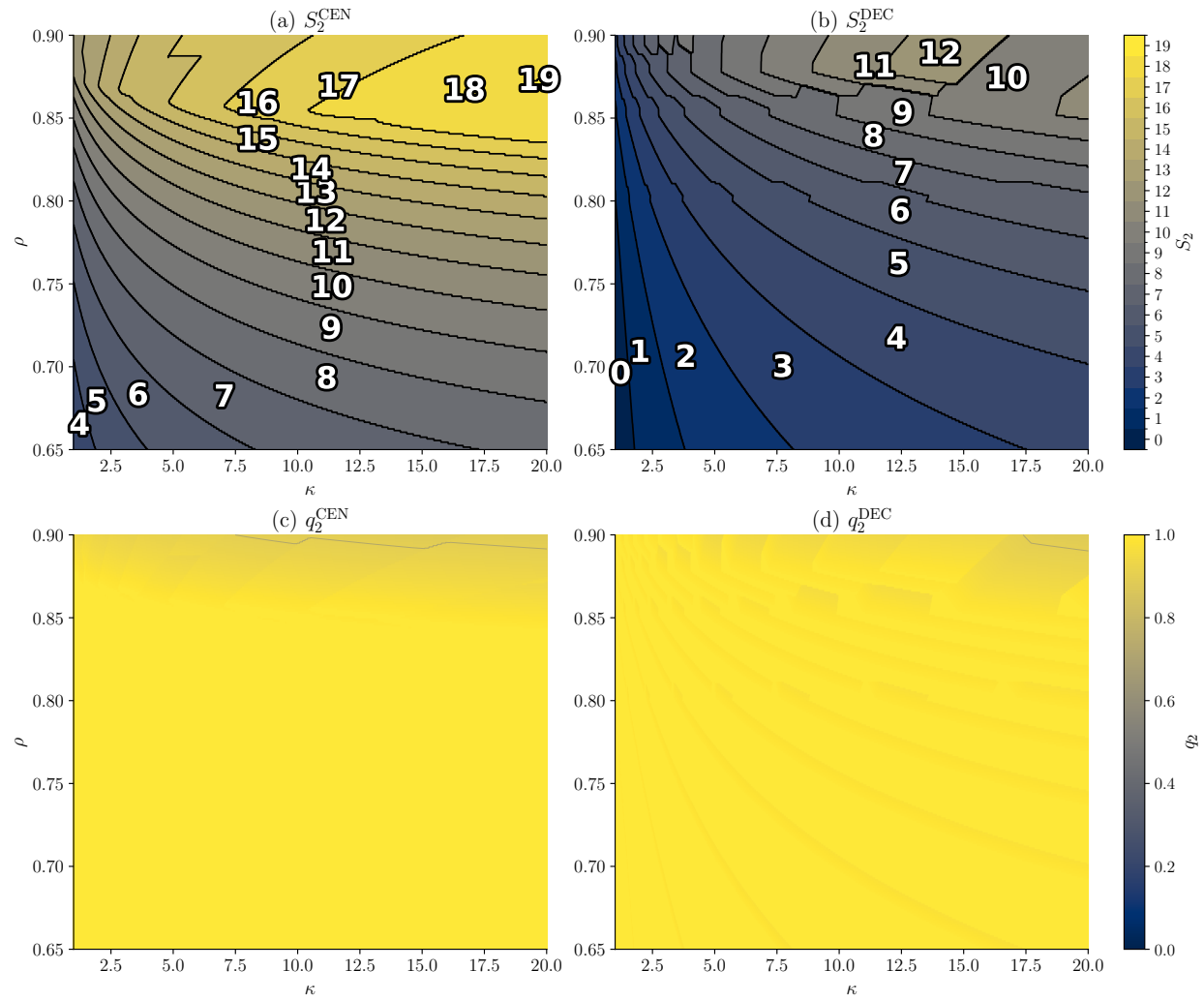


Figure 23: Type-2 decisions over the (κ, ρ) plane (reduced h_1). Top row: inventory S_2 ; contours mark integer transitions. Bottom row: joining probability q_2 .

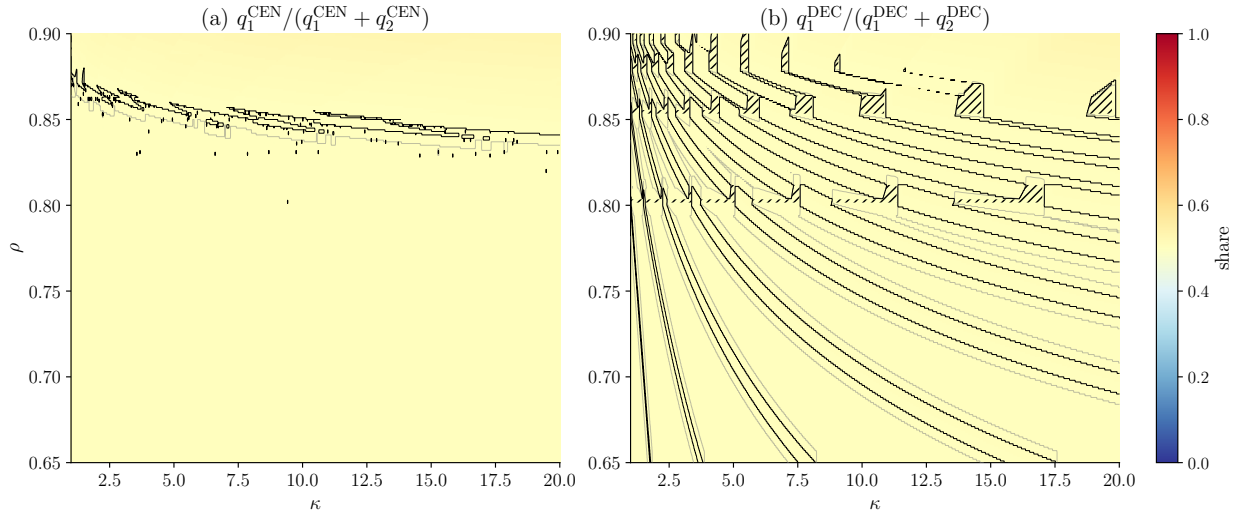


Figure 24: Type-1 share $q_1/(q_1 + q_2)$ over the (κ, ρ) plane (reduced h_1). Contours at 0.5 (thin solid), 0.6 and 0.7 (dashed). Hatching indicates type-2 majority (share < 0.5).

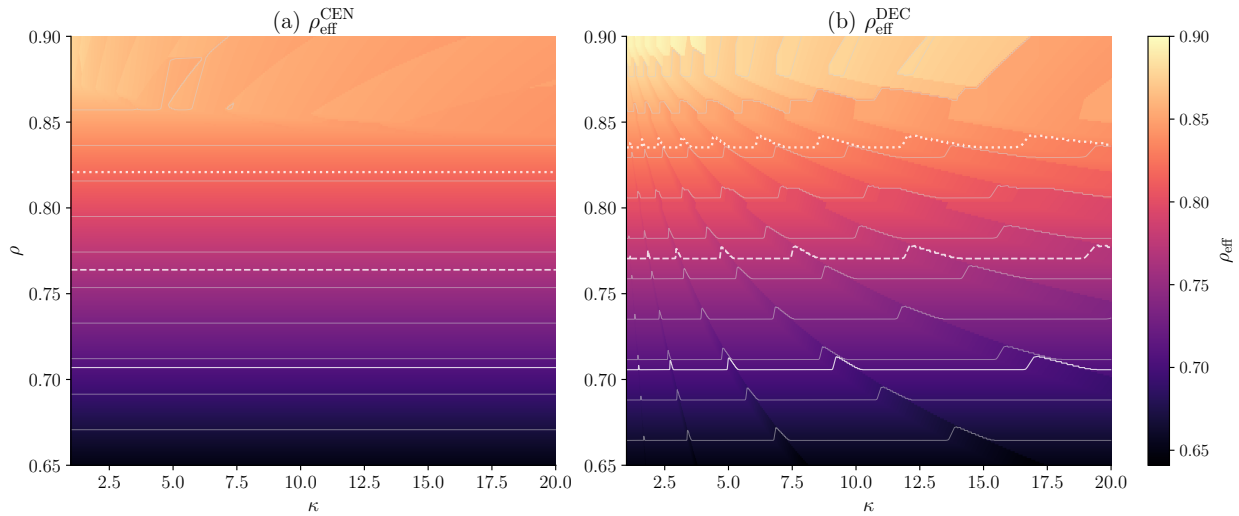


Figure 25: Effective utilization $\rho_{\text{eff}} = (q_1 \Lambda_1 + q_2 \Lambda_2)/\mu$ over the (κ, ρ) plane (reduced h_1). White contours at 25% (solid), 50% (dashed), 75% (dotted) of range; thin gray contours provide detail.

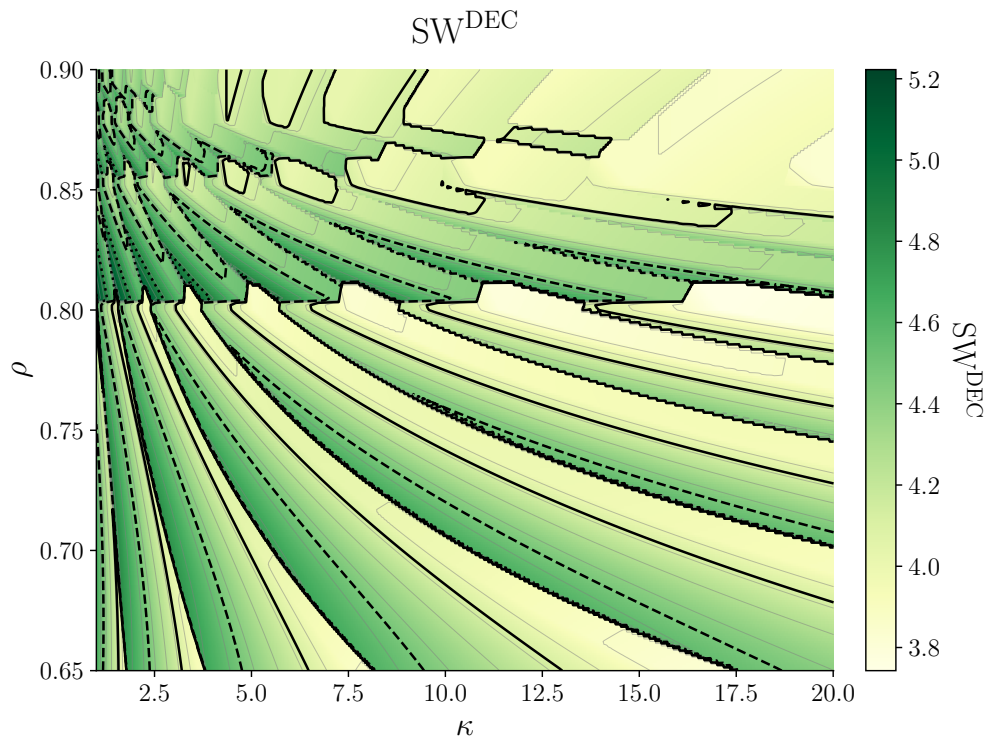


Figure 26: Social welfare SW^{DEC} under decentralization over the (κ, ρ) plane (reduced h_1). Contours mark 4.11, 4.48, 4.85 (25% solid, 50% dashed, 75% dotted); thin gray contours provide detail.

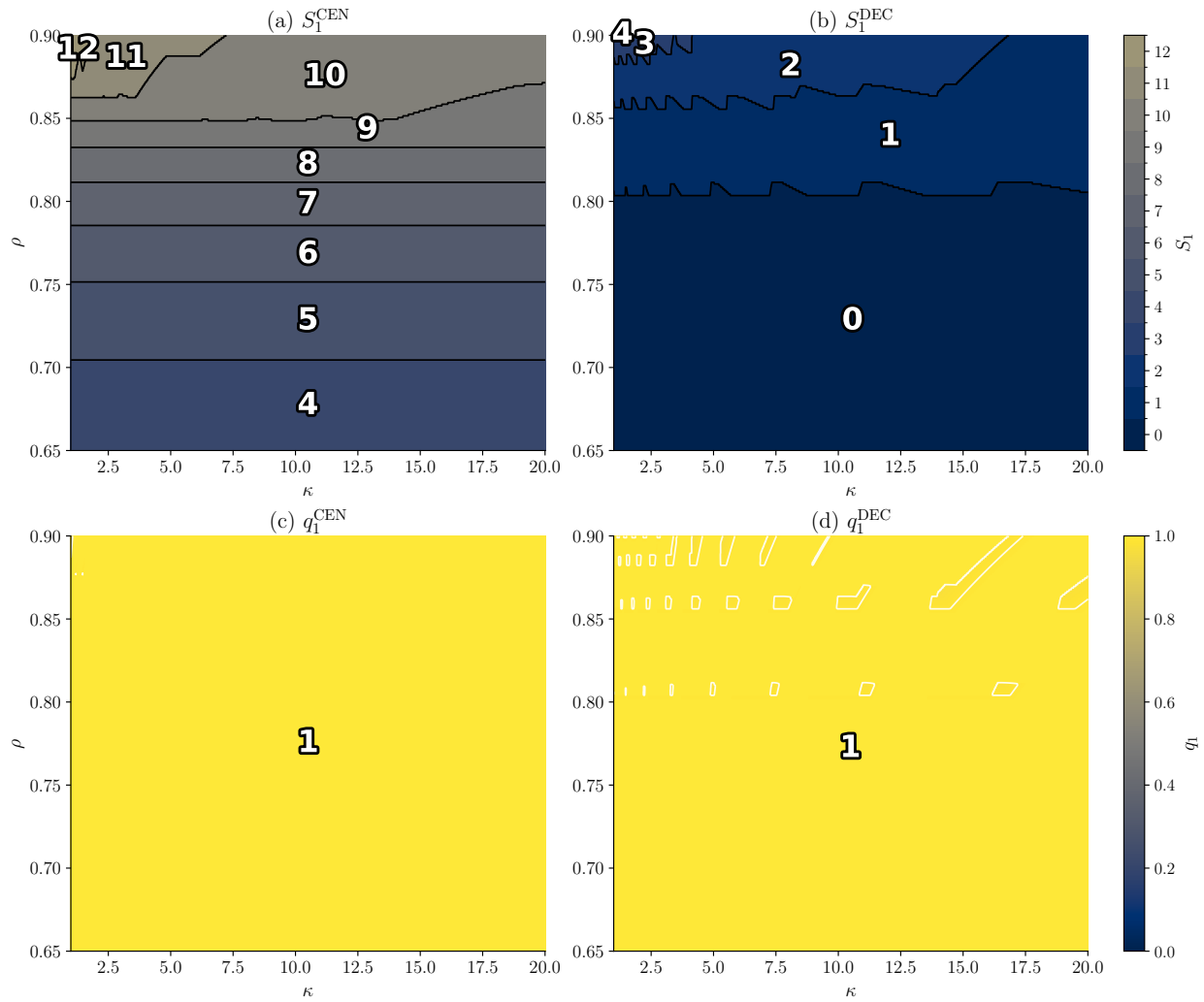


Figure 27: Type-1 decisions over the (κ, ρ) plane (reduced h_1). Top row: inventory S_1 ; contours mark integer transitions. Bottom row: joining probability q_1 ; contour at 0.99 (thick white).

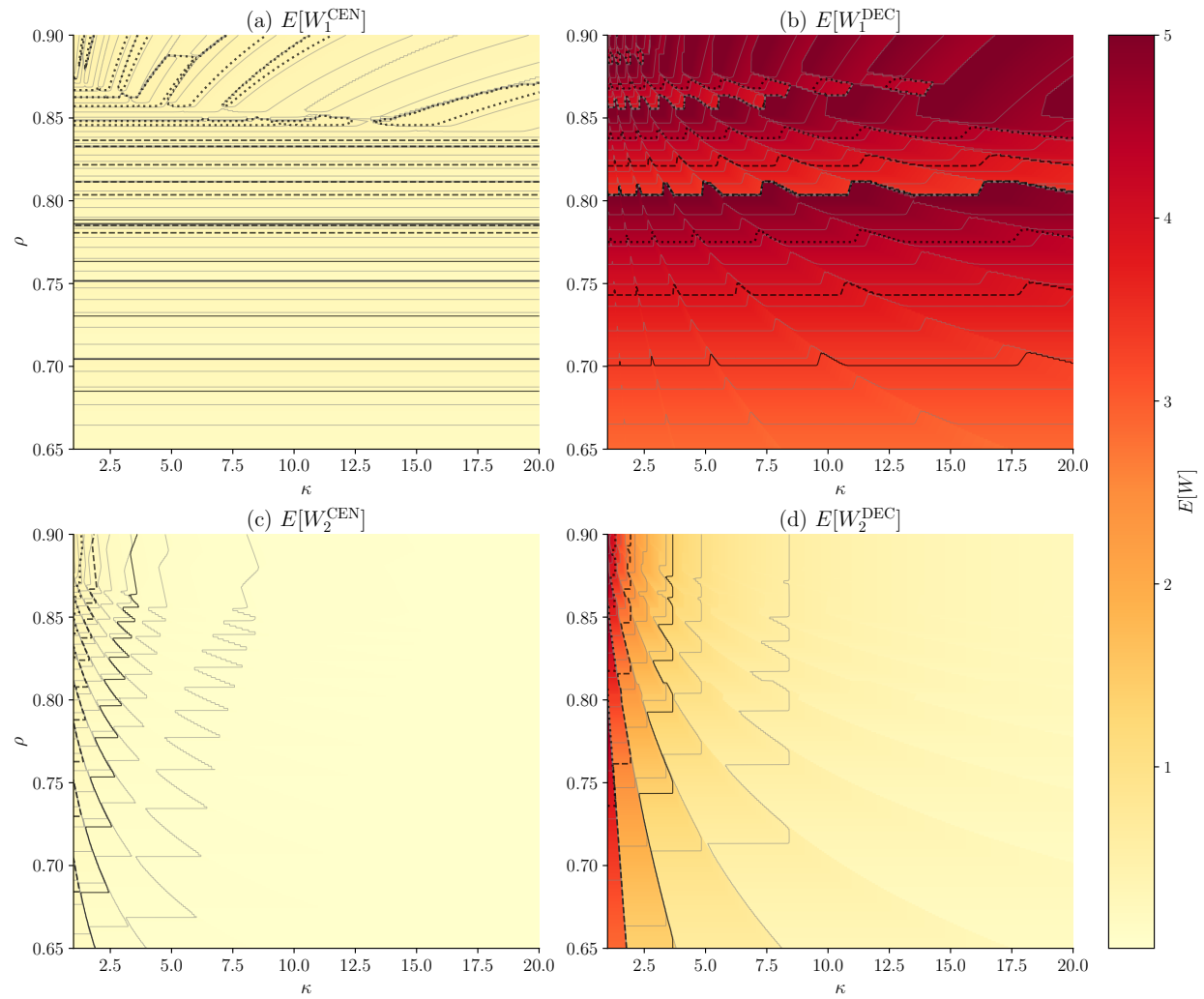


Figure 28: Expected waiting times $E[W_i]$ over the (κ, ρ) plane (reduced h_1). Top row: type-1. Bottom row: type-2. Contours at 25% (solid), 50% (dashed), 75% (dotted) of each panel's range.

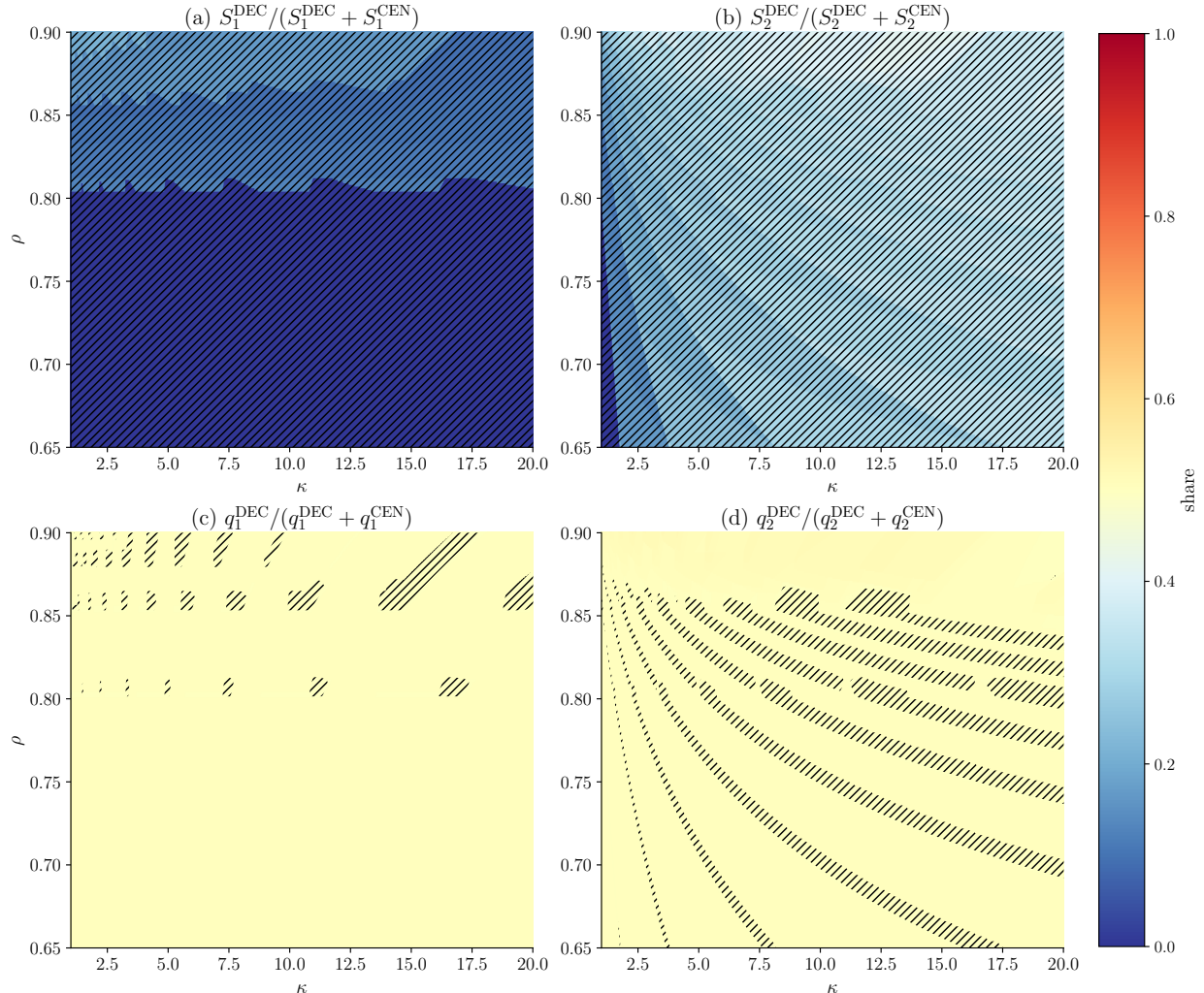


Figure 29: Decentralized shares $X^{\text{DEC}} / (X^{\text{DEC}} + X^{\text{CEN}})$ for $X \in \{S_1, S_2, q_1, q_2\}$ (reduced h_1). Top row: inventory shares. Bottom row: joining probability shares. Diverging colormap centered at 0.5: blue indicates higher under centralization, red indicates higher under decentralization (not present). Hatching where centralization strictly dominates (share < 0.5).

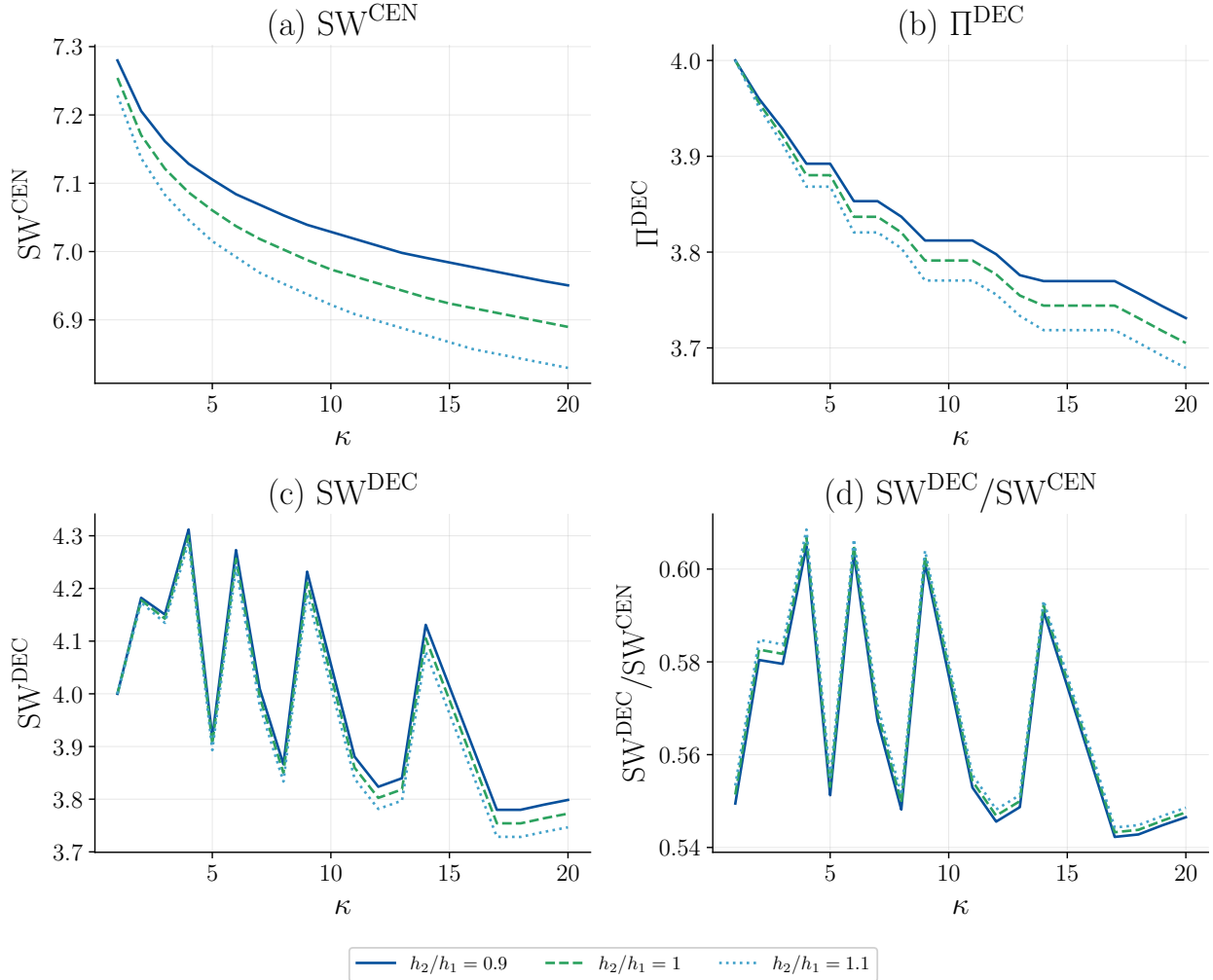


Figure 30: Cross-section at $\rho = 0.8$ as functions of κ for different h_2/h_1 ratios (reduced h_1). Top row: SW^{CEN} (left) and Π^{DEC} (right). Bottom row: SW^{DEC} (left) and efficiency ratio (right).

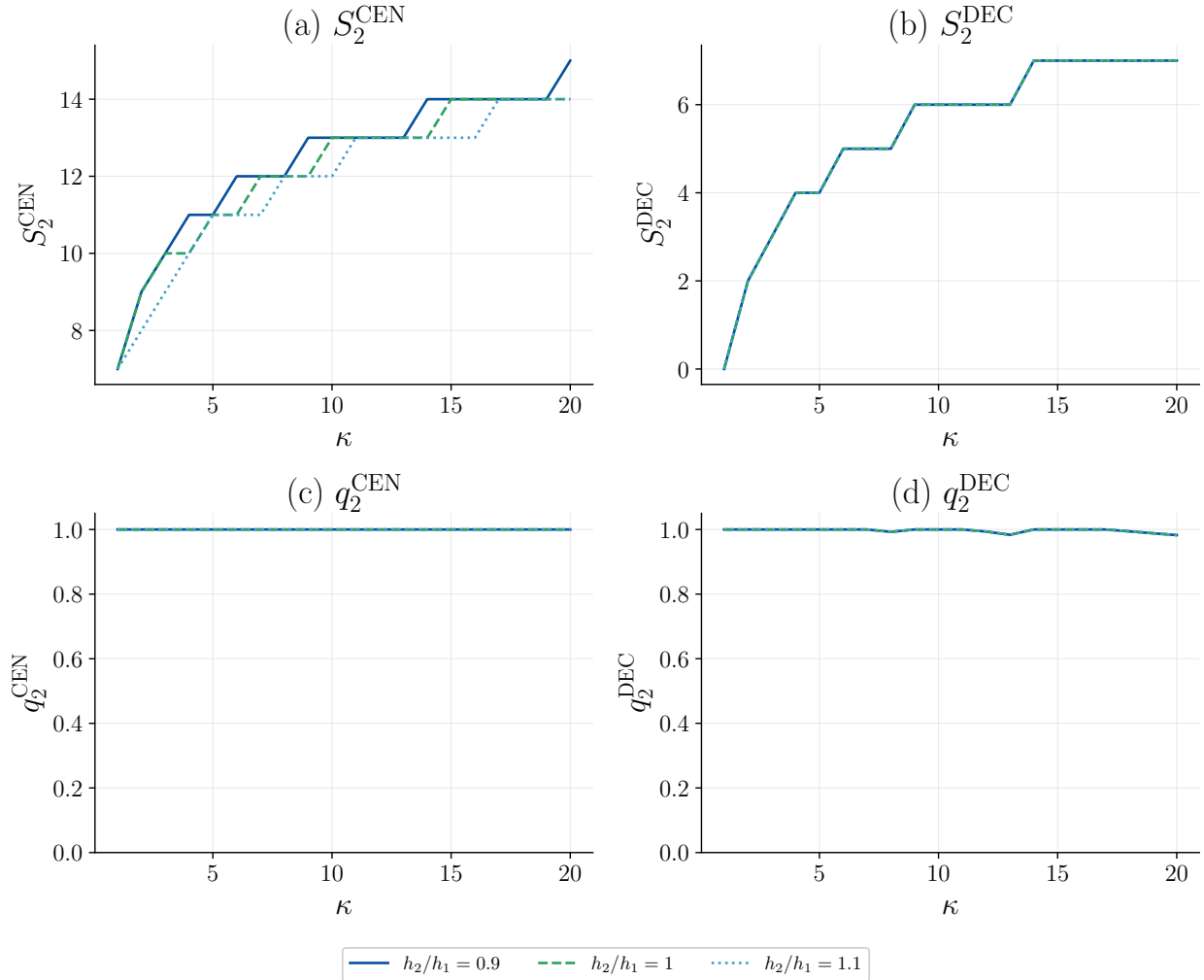


Figure 31: Cross-section at $\rho = 0.8$: type-2 decisions as functions of κ for different h_2/h_1 ratios (reduced h_1). Top row: inventory S_2 . Bottom row: joining probability q_2 .

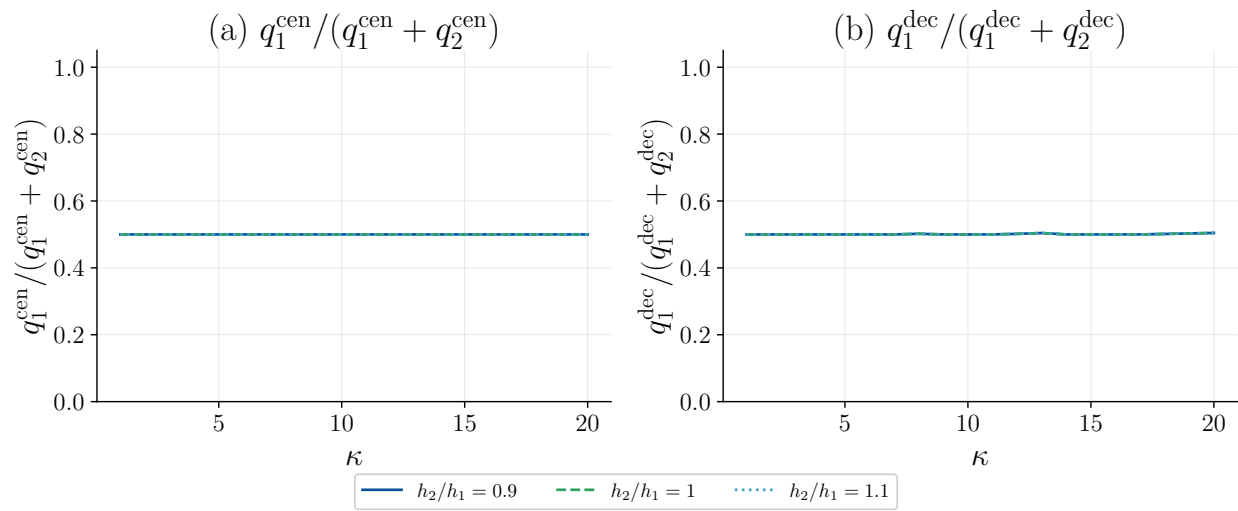


Figure 32: Cross-section at $\rho = 0.8$: type-1 share $q_1/(q_1 + q_2)$ as function of κ for different h_2/h_1 ratios (reduced h_1). Left: centralized. Right: decentralized.

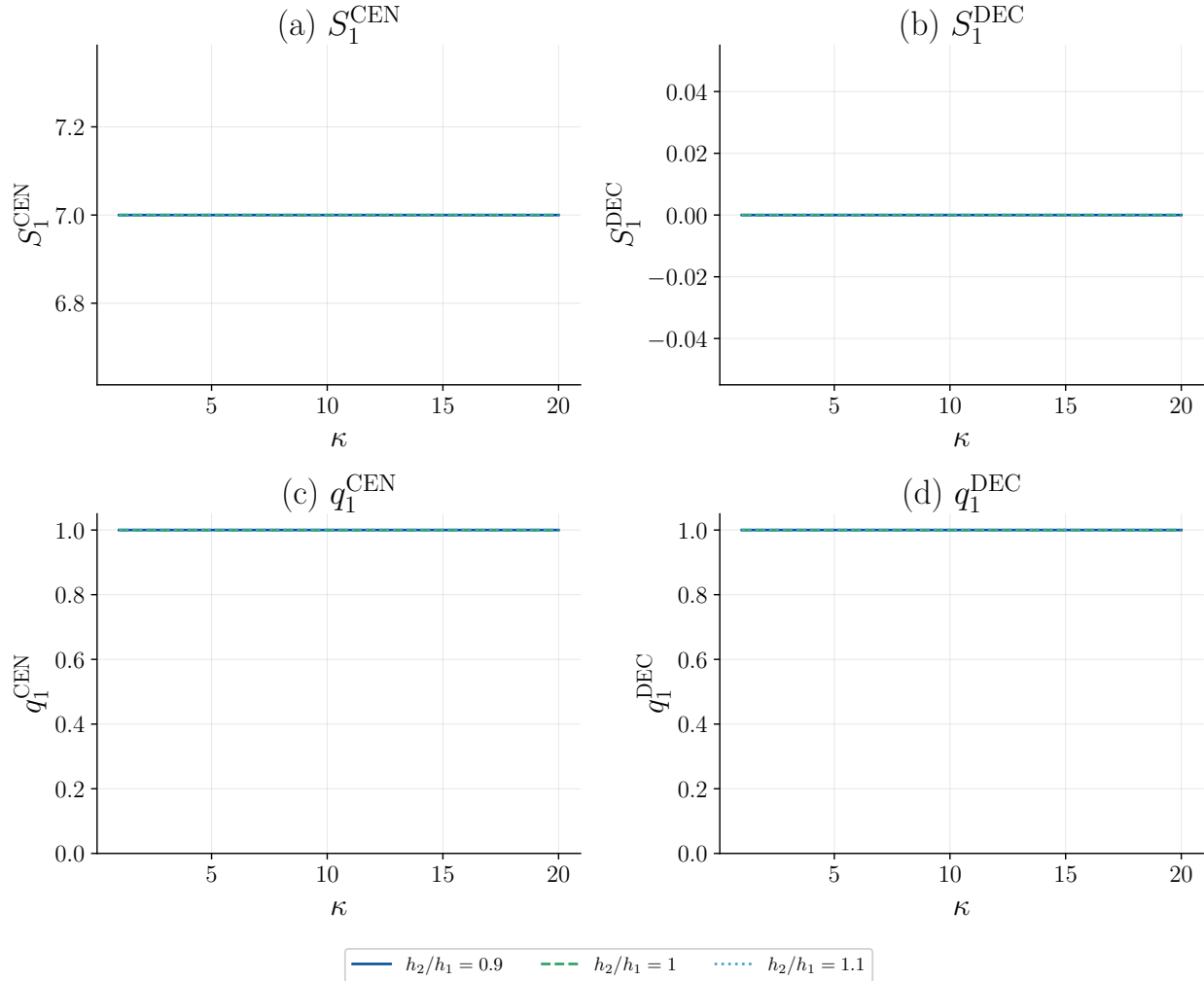


Figure 33: Cross-section at $\rho = 0.8$: type-1 decisions as functions of κ for different h_2/h_1 ratios (reduced h_1). Top row: inventory S_1 . Bottom row: joining probability q_1 .

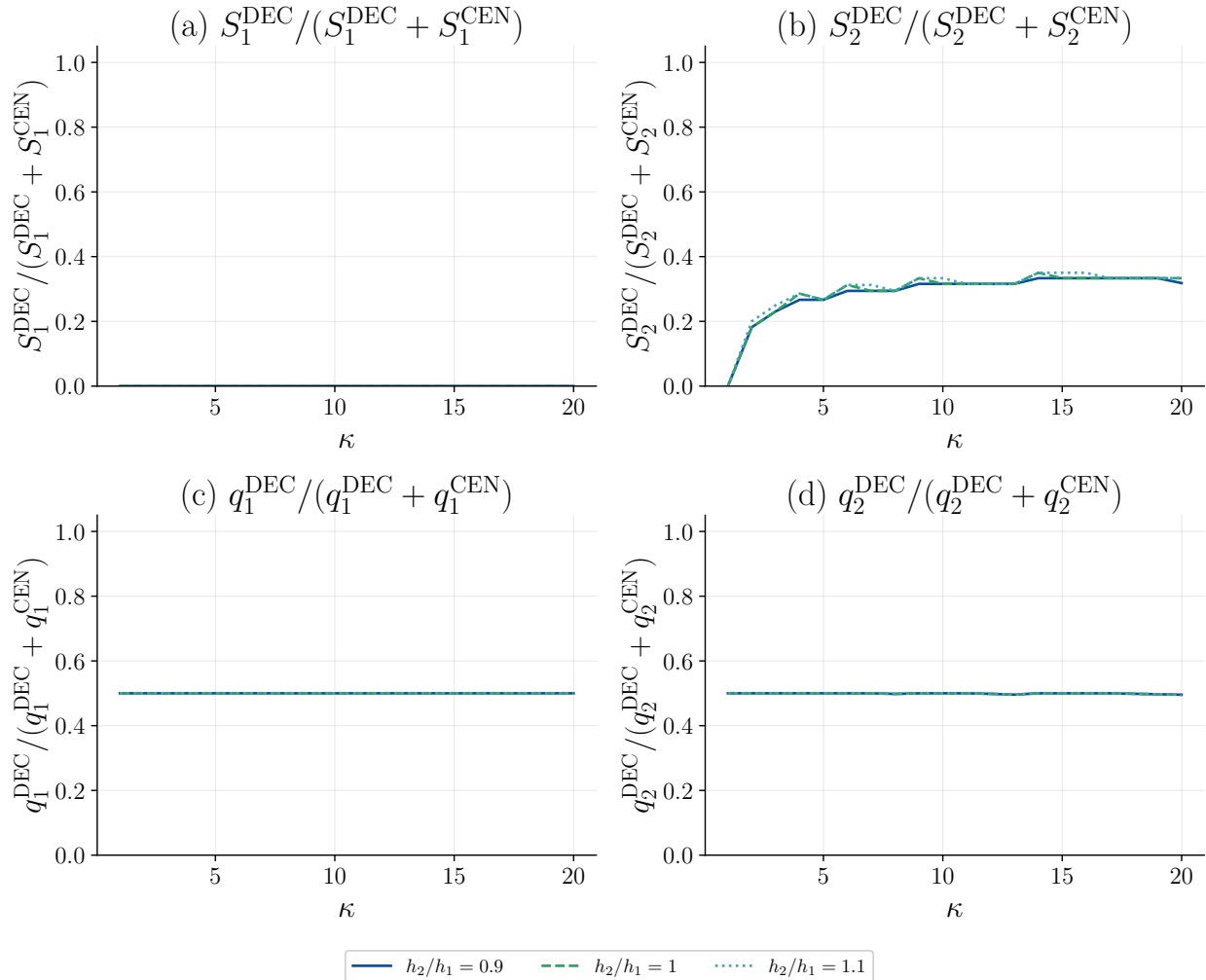


Figure 34: Cross-section at $\rho = 0.8$: decentralized shares $X^{\text{DEC}}/(X^{\text{DEC}} + X^{\text{CEN}})$ as functions of κ for different h_2/h_1 ratios (reduced h_1). Top row: inventory shares. Bottom row: joining probability shares.

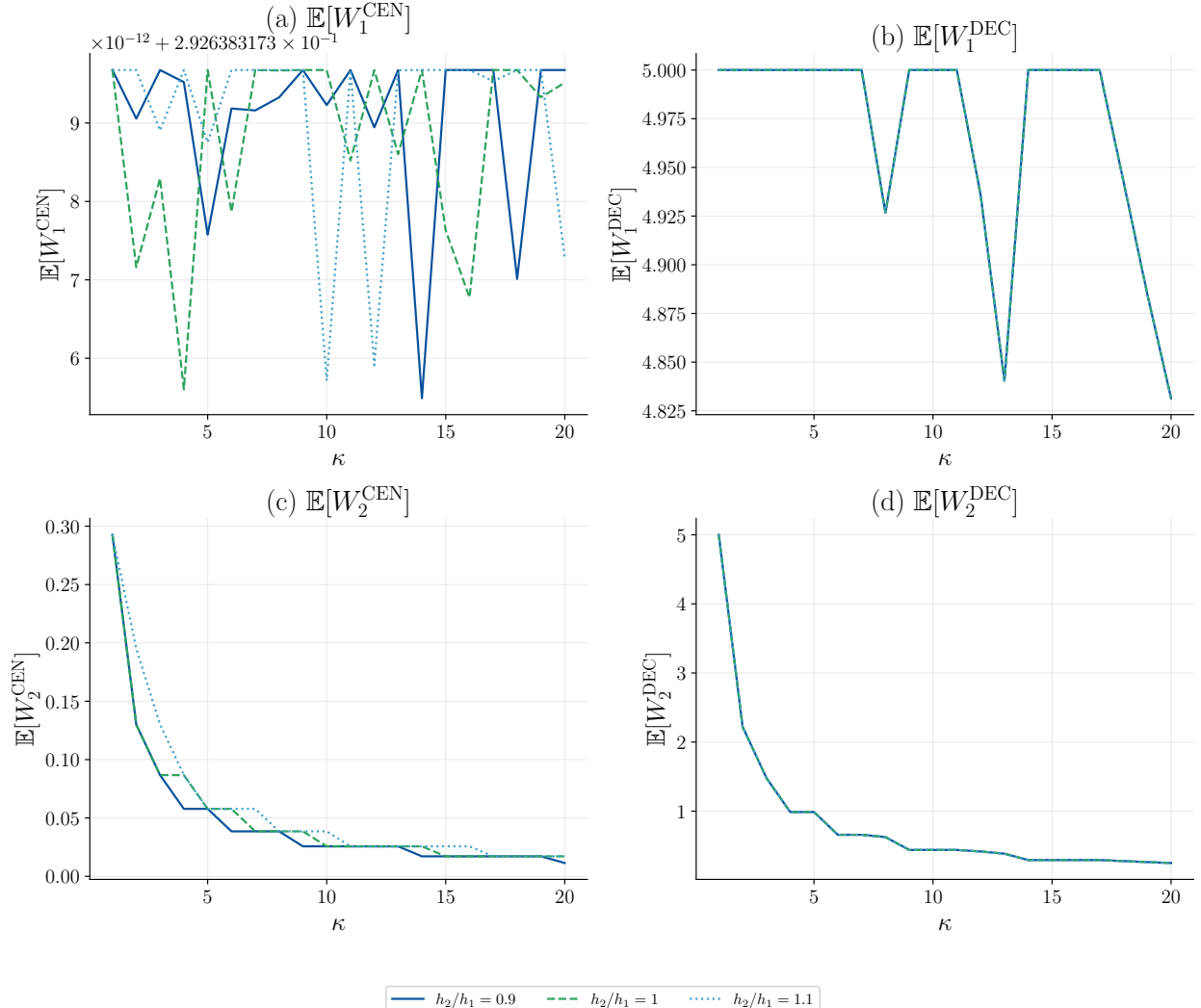


Figure 35: Cross-section at $\rho = 0.8$: expected waiting times $E[W_i]$ as functions of κ for different h_2/h_1 ratios (reduced h_1). Top row: type-1. Bottom row: type-2. Red segments indicate no joining.

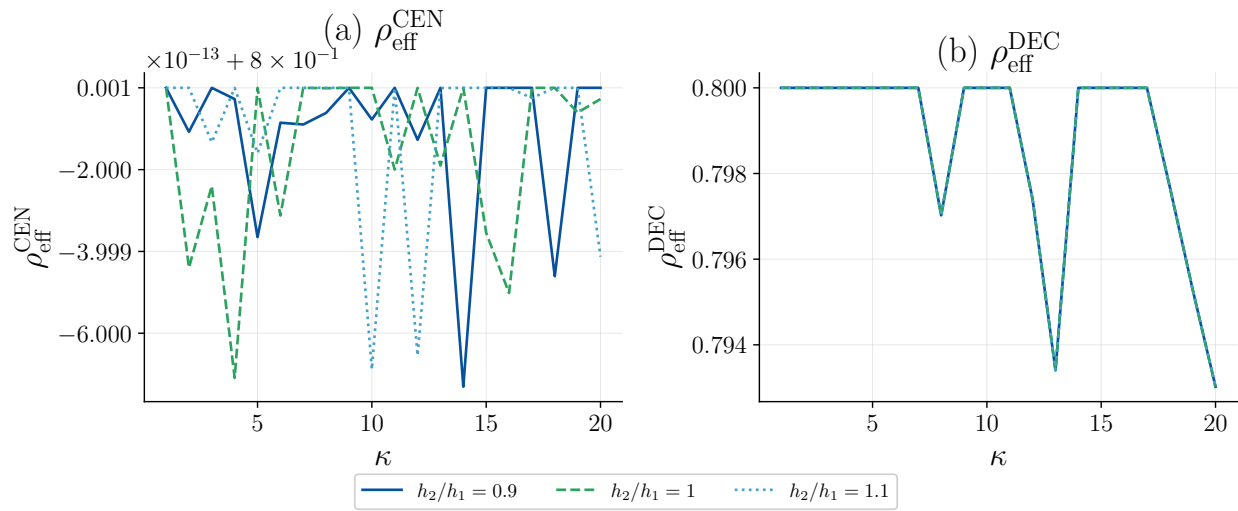


Figure 36: Cross-section at $\rho = 0.8$: effective utilization $\rho_{\text{eff}} = (q_1\Lambda_1 + q_2\Lambda_2)/\mu$ as function of κ for different h_2/h_1 ratios (reduced h_1). Left: centralized. Right: decentralized.